

CONTRIBUTIONS TO THE KINETIC MODELING OF GLYCOLYTIC
PATHWAY IN YEAST

A THESIS SUBMITTED TO
THE GRADUATE SCHOOL OF NATURAL AND APPLIED SCIENCES
OF
MIDDLE EAST TECHNICAL UNIVERSITY

BY

CEYLAN ŞAHİN

IN PARTIAL FULLFILMENT OF THE REQUIREMENTS
FOR
THE DEGREE OF DOCTOR OF PHILOSOPHY
IN
FOOD ENGINEERING

MARCH 2009

Approval of the thesis:

**CONTRIBUTIONS TO THE KINETIC MODELING OF GLYCOLYTIC
PATHWAY IN YEAST**

submitted by **CEYLAN ŞAHİN** in partial fulfillment of the requirements for the degree of **Doctor of Philosophy in Food Engineering Department, Middle East Technical University** by,

Prof. Dr. Canan Özgen
Dean, Graduate School of **Natural and Applied Sciences** _____

Prof. Dr. Zümrüt Begüm Ögel
Head of Department, **Food Engineering** _____

Prof. Dr. Haluk Hamamcı
Supervisor, **Food Engineering Dept., METU** _____

Examining Committee Members:

Prof. Dr. Zümrüt Begüm Ögel
Food Engineering Dept., METU _____

Prof. Dr. Haluk Hamamcı
Food Engineering Dept., METU _____

Prof. Dr. Pınar Çalık
Chemical Engineering Dept., METU _____

Prof. Dr. Sezai Türkel
Biological Sciences Dept., Uludağ University _____

Prof. Dr. Abdurrahman Tanyolaç
Chemical Engineering Dept., Hacettepe University _____

Date: 09.03.2009

I hereby declare that all information in this document has been obtained and presented in accordance with academic rules and ethical conduct. I also declare that, as required by these rules and conduct, I have fully cited and referenced all material and results that are not original to this work.

Name, Last name: Şahin, Ceylan

Signature :

ABSTRACT

CONTRIBUTIONS TO THE KINETIC MODELING OF GLYCOLYTIC PATHWAY IN YEAST

Şahin, Ceylan

Ph. D., Department of Food Engineering

Supervisor: Prof. Dr. Haluk Hamamcı

March 2009, 125 pages

Being at the center of most metabolic pathways and also one of the best known pathways, the glycolytic pathway has been of interest to modeling studies. This study is composed of our attempts to model ethanolic fermentation by yeast through kinetic equations of glycolytic steps and its branches. Model was based totally on experimentally measured kinetics of enzymes and transport steps, either obtained in this study or from the literature.

Effect of ethanol on enzyme activities was tested in the range of ethanol 0 to 20% (v/v) in assay mixture. All enzymes were inhibited by ethanol to some degree and these inhibitions started at different ethanol concentrations, the least affected being the pyruvate kinase and the most inhibited ones being glycerol-3-phosphate dehydrogenase, glyceraldehyde-3-phosphate dehydrogenase, phosphogluco kinase, and alcohol dehydrogenase (forward). Effect of temperature on the activities of enzymes was tested within 10-30 °C with five degrees of increments. Activation energies of enzymes were calculated using the Arrhenius equation. Activation energies of upper part of the glycolysis and the glycerol branch (glycerol-3-

phosphate dehydrogenase) were relatively higher than that of lower part enzymes as well as the ethanol branch (alcohol dehydrogenase).

Results obtained from these *in vitro* studies were incorporated into the model as mathematical relations. Model output thus obtained was compared with results of experiments conducted at several temperatures and initial ethanol concentrations. Model could estimate general trend in ethanolic fermentation that fermentation is inhibited by increasing concentrations of ethanol. Decrease in glycerol yields at lower temperatures was also estimated by the model. However, model did not fit exactly to experimental results, especially at low temperature and high ethanol concentrations. This could be attributed to stress responses of cells under these conditions, which are not considered in the model.

Keywords: Yeast, *Saccharomyces cerevisiae*, Metabolism, Kinetic Modeling, Ethanol Effect, Temperature Effect

ÖZ

MAYA GLİKOLİTİK İZYOLUNUN KİNETİK MODELLENMESİNE KATKILAR

Şahin, Ceylan

Doktora, Gıda Mühendisliği

Tez yöneticisi: Prof. Dr. Haluk Hamamcı

Mart 2009, 125 sayfa

Birçok metabolik izyolunun merkezinde olması ve en çok bilinen izyollarından biri olması nedeniyle glikolitik izyolunun modellenmesi ilgi çekmektedir. Bu çalışma, glikolitik izyolu ve dallanmalarının kinetik denklemlerini kullanarak mayanın etil alkol fermantasyonunun modellenmesi ile ilgili çalışmalarımızı içermektedir. Model, bu çalışmada veya literatürden elde edilen, deneysel olarak ölçülmüş enzim ve taşınım kinetiklerine dayanmaktadır.

Etil alkolün enzim faaliyetlerine etkisi, tepkime ortamında %0-%20 (v/v) etil alkol ile test edildi. Bütün enzimler etil alkol ile bir dereceye kadar baskılandı. Bu baskılama her enzim için farklı derişimde başladı, en az etkilenen pürivat kinaz, en çok etkilenenler ise gliserol-3-fosfat dehidrogenaz, gliseraldehit-3-fosfat dehidrogenaz, fosfogliko kinaz ve alkol dehidrogenaz (ileri tepki) oldu. Sıcaklığın enzim aktivitesi üzerine etkisi 10-30 °C arası sıcaklıkta beş derece artırım ile test edildi. Enzimlerin aktivasyon enerjileri Arrhenius denklemi kullanılarak hesaplandı. Yukarı glikoliz ve gliserol dallanmasının (gliserol-3-fosfat dehidrogenaz) aktivasyon enerjilerinin alt taraftakiler ve etil alkol ayırımındakinden (alkol dehidrogenaz) daha yüksek olduğu görüldü.

Bu *in vitro* alıřmalardan elde edilen sonular matematiksel baėıntılar halinde modele yerleřtirildi. Bu Őekilde elde edilen model ıktıları, eřitli sıcaklık ve etil alkol deriřimlerinde gerekleřtirilen fermantasyonlar ile karřılařtırıldı. Model alkol fermantasyonlarında genel olarak grlen, fermantasyonun etil alkol birikmesi ile baskılanmasını tahmin edebildi. Dřk sıcaklıklarda daha az gliserol verimi grlmesi de model tarafından tahmin edilebildi. Ancak; zellikle yksek bařlangı etil alkol deriřimlerinde ve dřk sıcaklıklarda model sonuları deneysel sonulara tam olarak uymadı. Bu durum modellemede dikkate alınmamıř olan, hcrelerin bu Őartlarda oluřan stres tepkilerine baėlanabilir.

Anahtar Kelimeler: Maya, *Saccharomyces cerevisiae*, Metabolizma, Kinetik Modelleme, Alkol Etkisi, Sıcaklık Etkisi

ACKNOWLEDGEMENTS

I would like to express my sincere gratitude to Prof. Dr. Haluk Hamamcı for undertaking the job of being my supervisor and providing me the opportunity of a Ph.D. study. I would like to thank to him for his guidance, advices and support throughout this research.

I am also thankful to examining committee members, Prof. Dr. Sezai Türkel and Prof. Dr. Pınar Çalık for evaluating my progress and their critics on the work done for this thesis.

I am indebted and gratefull to all my labmates (past and present), who has provided a good and inspiring atmosphere in the laboratory. I would like to thank deeply to my dear friends and colleagues; Ebru, Şeyda, Gül, Tamay, Eda, Gökçen, Aysu, Ayşem, Beray, Peruze... My special thanks are devoted to Ali Oğuz for his invaluable help in the experiments and critics, for his moral support, patience and encouragement during my whole study.

The last but never the least I want to send all my love to my family and wish to thank them for their support throughout all these years.

TABLE OF CONTENTS

ABSTRACT	IV
ÖZ	VI
ACKNOWLEDGEMENTS	VIII
TABLE OF CONTENTS	IX
LIST OF TABLES	XII
LIST OF FIGURES.....	XIII
LIST OF ABBREVIATIONS	XV
CHAPTERS	
1. INTRODUCTION.....	1
1.1. The Yeast.....	1
1.2. Glycolysis and its regulation	3
1.3. Hexose transport.....	8
1.4. Branches from Glycolysis	9
1.4.1. Ethanol branch.....	9
1.4.2. Glycerol Branch.....	10
1.4.3. Storage Carbohydrates in Yeast	12
1.5. Ethanol and Temperature: Two Major Environmental Factors.....	13
1.5.1. Effect of Ethanol.....	13
1.5.2. Effect of Temperature.....	16
1.6. Modeling the Metabolism	17
1.6.1. Kinetic Models	18
1.6.2. Modeling the Glycolytic Pathway	22
1.7. Aim of the Study	24
2. MATERIALS AND METHODS	25
2.1. Chemicals	25
2.2. Organism	25

2.3. Culture and Growth Conditions	25
2.4. Analytical methods.....	26
2.5. Extraction of proteins	27
2.6. Enzyme Assays.....	28
2.6.1. Hexokinase assay.....	29
2.6.2. Phosphoglucose isomerase assay.....	29
2.6.3. Phosphofructokinase assay	29
2.6.4. Aldolase assay	30
2.6.5. Glyceraldehyde-3-phosphate dehydrogenase assay	30
2.6.6. Phosphoglycerate kinase assay.....	31
2.6.7. Phosphoglycerate mutase assay.....	31
2.6.8. Enolase assay.....	31
2.6.9. Pyruvate kinase assay	32
2.6.10. Triosephosphate dehydrogenase assay	32
2.6.11. Glycerol-3-phosphate dehydrogenase assay.....	32
2.6.12. Alcohol dehydrogenase assay.....	33
2.6.13. Pyruvate decarboxylase assay	33
3. RESULTS AND DISCUSSION	35
3.1. History of the model.....	35
3.1.1. Changes made from the original Teusink model.....	44
3.2. Ethanol Effect.....	49
3.2.1. Effect of Ethanol on Activities of Enzymes	51
3.2.2. Effect of Ethanol on Fermentation Kinetics.....	58
3.2.3. Model Studies Incorporating the Effect of Ethanol.....	61
3.3. Temperature effect	72
3.3.1. Effect of Temperature on Activities of Enzymes	72
3.3.2. Effect of Temperature on Fermentation Kinetics.....	80
3.3.3. Model Studies Incorporating the Effect of Temperature.....	83
4. CONCLUSIONS.....	85
REFERENCES.....	88
APPENDICES	
A. GROWTH CURVE OF YEAST	99

B. RATE EQUATIONS USED IN THE MODEL	100
C. STRUCTURE OF THE PROGRAM	106
D. MATLAB PROGRAM USED FOR THE MODEL	108
E. SAMPLES FOR FITS FOR THE EFFECT OF ETHANOL ON ACTIVITIES OF ENZYMES	123
CURRICULUM VITAE	125

LIST OF TABLES

TABLES

Table 1.1 Brief History of Yeast.....	2
Table 3.1 Comparison of steady state concentrations measured in the study of Teusink <i>et al.</i> (2000) with the ones obtained by our program and JWS Online	43
Table 3.2 Comparison of fluxes obtained by our program and JWS Online	44
Table 3.3 Values of parameters fitted for effect of ethanol on enzyme activities..	63
Table 3.4 Specific activities (v_{\max}) determined in <i>in vitro</i> assays and used in the model.....	64
Table A.1 Values of kinetic parameters used in the model.....	104
Table A.2 Values of parameters of phosphofructokinase kinetics.....	105

LIST OF FIGURES

FIGURES

Figure 1.1 Scheme of glycolysis	5
Figure 1.2 Scheme showing metabolite X being produced or consumed by various reactions	19
Figure 3.1 Scheme of reactions used in the Teusink <i>et al.</i> (2000) model	36
Figure 3.2 Equilibrium block between DHAP and GAP for TPI reaction.....	37
Figure 3.3 Concentration profile of Glc_in and bisphosphoglycerate (BPG) with different initial concentrations	41
Figure 3.4 Concentration profile of pyruvate (PYR) with different initial concentrations.....	42
Figure 3.5 Glycerol branch	46
Figure 3.6 Specific activity of ADH (ethanol as substrate) at varying concentrations of NAD ⁺	52
Figure 3.7 Inhibition patterns of enzymes with ethanol.....	56
Figure 3.8 Effect of initial extracellular ethanol concentration on glucose consumption and ethanol and glycerol productions.....	59
Figure 3.9 Inhibition of glucose consumption and, ethanol and glycerol production rates by ethanol.	61
Figure 3.10 <i>In silico</i> concentration profiles of extracellular glucose, ethanol and glycerol obtained with no initial ethanol and with 15% initial ethanol: inhibition effect of ethanol included just for hexose transport step and inhibition effect of ethanol included for all steps	67
Figure 3.11 <i>In silico</i> concentration profiles of extracellular glucose, ethanol and glycerol obtained: without ethanol inhibition effect, with inhibition effect of ethanol just on hexose transport step, and on all steps.....	68

Figure 3.12 Comparison of experimental glycerol production with simulations obtained by inclusion of glycerol transport step	71
Figure 3.13 Left column: Change of specific activities of enzymes with temperature (10-15-20-25-30-35°C); Right column: Arrhenius plots of corresponding enzymes	78
Figure 3.14 Activation energies of enzymes of glycolysis and its branches to glycerol and ethanol	79
Figure 3.15 Effect of culture temperature on glucose consumption and ethanol and glycerol productions.....	81
Figure 3.16 Effect of cultivation temperature on glucose consumption and, ethanol and glycerol production rates	82
Figure 3.17 Effect of cultivation temperature on ethanol and glycerol yields on glucose.....	82
Figure A.1 Growth curve of brewer's yeast in YPD medium.....	99
Figure A.2 Fits for the effect of ethanol on activity of hexokinase and of triosephosphate isomerase.....	123
Figure A.3 Fit for the effect of ethanol on activity of phosphoglycerate kinase and of glycerol-3-phosphate dehydrogenase.....	124

LIST OF ABBREVIATIONS

ACE	Acetaldehyde
ADH	Alcohol dehydrogenase
ADP	Adenosine diphosphate
AK	Adenylate kinase
ALD	Aldolase
AMP	Adenosine monophosphate
ATP	Adenosine triphosphate
BPG	1,3-bisphosphoglycerate
DHAP	Dihydroxyacetone phosphate
DTE	1, 4-dithioerythritol
E_a	Activation energy
EDTA	Ethylenediaminetetraacetic acid
ENO	Enolase
ETOH	Ethanol
F16bP	Fructose-1,6-bisphosphate
F26bP	Fructose-2,6-bisphosphate
F6P	Fructose-6-phosphate
G2P	2-phosphoglycerate
G3P	3-phosphoglycerate
G6P	Glucose-6-phosphate
G6PDH	Glucose-6-phosphate dehydrogenase
GAP	Glyceraldehyde-3-phosphate
GAPDH	Glyceraldehyde-3-phosphate dehydrogenase
Glc	Glucose
GLYC	Glycerol
Glyc3P	Glycerol-3-phosphate

GLYCPASE	Glycerol-3-phosphatase
GLYCPDH	Glycerol-3-phosphate dehydrogenase
HXK	Hexokinase
HXT	Hexose transport
K_{eq}	Equilibrium constant
K_m	Affinity constant
LDH	Lactate dehydrogenase
NAD^+	β -Nicotinamide adenine dinucleotide
NADH	β -Nicotinamide adenine dinucleotide, reduced
$NADP^+$	β -Nicotinamide adenine dinucleotide phosphate
NADPH	β -Nicotinamide adenine dinucleotide phosphate, reduced
ODE	Ordinary Differential Equation
PDC	Pyruvate decarboxylase
PEP	Phosphoenolpyruvate
PFK	Phosphofructokinase
PGI	Phosphoglucose isomerase
PGK	Phosphoglycerate kinase
PGM	Phosphoglycerate mutase
PMSF	Phenylmethanesulphonyl fluoride
PYK	Pyruvate kinase
PYR	Pyruvate
R	Universal gas constant
T	Temperature
TPI	Triosephosphate isomerase
TPP	Thiamine pyrophosphate
TRIO-P	Triose-phosphate
v_{max}	Maximum velocity

CHAPTER 1

INTRODUCTION

1.1. The Yeast

Yeasts can be considered man's oldest industrial microorganism. It's likely that man used yeast before the development of a written language. Hieroglyphics suggest that ancient Egyptians were using yeast and the process of fermentation to produce alcoholic beverages and to leaven bread over 5,000 years ago. *Saccharomyces cerevisiae* is undoubtedly the most important yeast species. In various forms, it may function as the wine yeast, brewer's yeast, distiller's yeast, or baker's yeast. Laboratory strains are extensively used in industry and in fundamental studies of biochemistry, genetics and molecular biology. It is one of the favoured model organisms for biological research, and is the first eukaryote whose genome is entirely sequenced. A brief history of yeast and research on it is listed in Table 1.1.

The yeasts are unicellular fungi and most of them are classified within the Ascomycetes. Yeast cells are usually spherical, oval, or cylindrical, and cell division generally takes place by budding. They are much larger than bacterial cells, and can be distinguished from bacteria by their size and by the obvious presence of internal cell structures (Madigan *et al.*, 1997).

Table 1.1 Brief History of Yeast (<http://biochemie.web.med.uni-muenchen.de/feldmann/>)

Chronology	Milestones
6000-2000 BC	Brewing (Sumeria, Babylonia)
1680	Yeast seen under the microscope (van Leewenhoek)
1835	Alcoholic fermentation associated with yeast
1839	Sugar as a food source for yeast growth
1857	Fermentation correlated with metabolism (Pasteur)
1877	Term enzyme (meaning “in yeast”) introduced
1880	Single yeast cell and pure yeast strains for brewing
1883	Alcohol and CO ₂ by cell free extracts
1915	Production of glycerol
1920	Yeast physiology reviewed
1949	First genetic map (Lindgren); mating type system
1930-1960	Yeasts’ taxonomy by Kluyver
1966	First tRNA structures from yeast
1978	First transformation of yeast (Hinnen, Hicks and Fink)
1990-1994	First commercial pharmaceutical products from recombinant yeast (Hepatitis B vaccine)
1990-1996	Completion of yeast genome project

According to the review of Hansen and Kielland-Brandt (Hansen and Kielland-Brandt, 1997) most lager brewing yeasts used today are probably related to the strain pure cultured and used by Emil Christian Hansen at the Carlsberg Laboratory, Denmark in late 18th century, which was later named *Saccharomyces carlsbergensis*. Ale yeast displays a wider range of genome structure. *Saccharomyces* brewing yeasts including *S. carlsbergensis* were included in *S. cerevisiae* and later is recognized as part of the *S. pastorianus* group, whereas ale yeasts form a diverse group rather close related to laboratory strains of *S. cerevisiae*.

Starting for the first half of the 20th century, yeast has regarded as a model organism especially for eukaryotic organisms, since yeast is unicellular and easy to cultivate and amenable to genetic manipulations, unlike other eukaryotes, such as plants and mammals. After its entire genome was sequenced, it is undoubtedly an excellent experimental system for molecular biology. The wealth of sequence information obtained in the yeast genome project is extremely useful as a reference against which sequences of human, animal or plant genes, and those of a multitude of unicellular organisms now under study may be compared.

Recent ideas of commercial utilization of yeast are supported by the several additional advantages of yeast (Kovar and Meyer, 2005). Ability of yeast to grow fast enables cultivation of yeast to high cell densities in non-expensive mineral media and large scale production and downstream are feasible. Unlike *Escherichia coli* for example, yeasts do not cause endotoxic reaction and food yeasts are highly acceptable for the production of pharmaceuticals. Yeast usually expresses heterologous genes using a natively strong and tightly regulated promoter and can secrete large amounts of proteins into the culture broth.

1.2. Glycolysis and its regulation

The glycolytic pathway is the most common pathway in the living organisms. It is found in microorganisms, animals and plants alike and is central to the energy metabolism independent of the fact that the organism's activity may be aerobic or anaerobic. The activity of this pathway is very important in industrial biotechnology in that the rate of the production of the primary compounds like citric acid, lactic acid and ethanol are dependent on it.

The dictionaries define glycolysis as the catabolism of carbohydrates like glucose or glycogen, by enzymes, with the release of energy and the production of lactic and pyruvic acids. A more scientific but still brief description states: Glycolysis is the initial pathway in the catabolism of carbohydrates, by which a molecule of

glucose is broken down to two molecules of pyruvate, with a net production of ATP molecules and the reduction of two NAD^+ molecules to NADH. Under aerobic conditions, these NADH molecules are reoxidized by the electron transport chain; under anaerobic conditions a different electron acceptor is used (Mathews *et al.*, 1999) The breakdown of storage polysaccharides and the metabolism of oligosaccharides yield glucose, related hexose sugars, and sugar phosphates, all of which find their way into the glycolytic pathway.

The 10 reactions between glucose and pyruvate can be considered in two distinct phases; the first five reactions make up an energy investment phase, in which sugar is metabolically activated by phosphorylation at the expense of ATP conversion to ADP, and the six carbon substrate is broken into 2 three-carbon sugar phosphates (Figure 1.1). The five reactions making up the second group are the energy generation phase. In this phase, two moles of triose-phosphates generated by cleavage of fructose-1,6-bisphosphate are converted into energy rich compounds (first 1,3-bisphosphoglycerate and then phosphoenolpyruvate), each of which transfers its high energy phosphate to ADP and thus forming ATP- the process is called substrate level phosphorylation. Thus, the net yield, per mole of glucose metabolized, is 2 moles of ATP and two moles of pyruvate.

During the glycolysis reducing equivalents are generated as well, in the form of NADH. NADH that is generated has to be reoxidized to NAD^+ and this is done by transferring the electrons to an electron acceptor so that the steady state and constant supply of NAD^+ is maintained. This receptor could be nitrate or sulfate ions in some microorganisms and some other organisms reduce organic substances. Lactic acid bacteria reduce pyruvate to lactate via the enzyme lactate dehydrogenase. Another important fermentation involves the cleavage of pyruvate into CO_2 and acetaldehyde. The latter is reduced to ethanol by alcohol dehydrogenase. As carried out by yeasts, this fermentation generates the alcohol in alcoholic beverages and CO_2 produced by pyruvate decarboxylation causes bread to rise while the ethanol produced evaporates during baking.

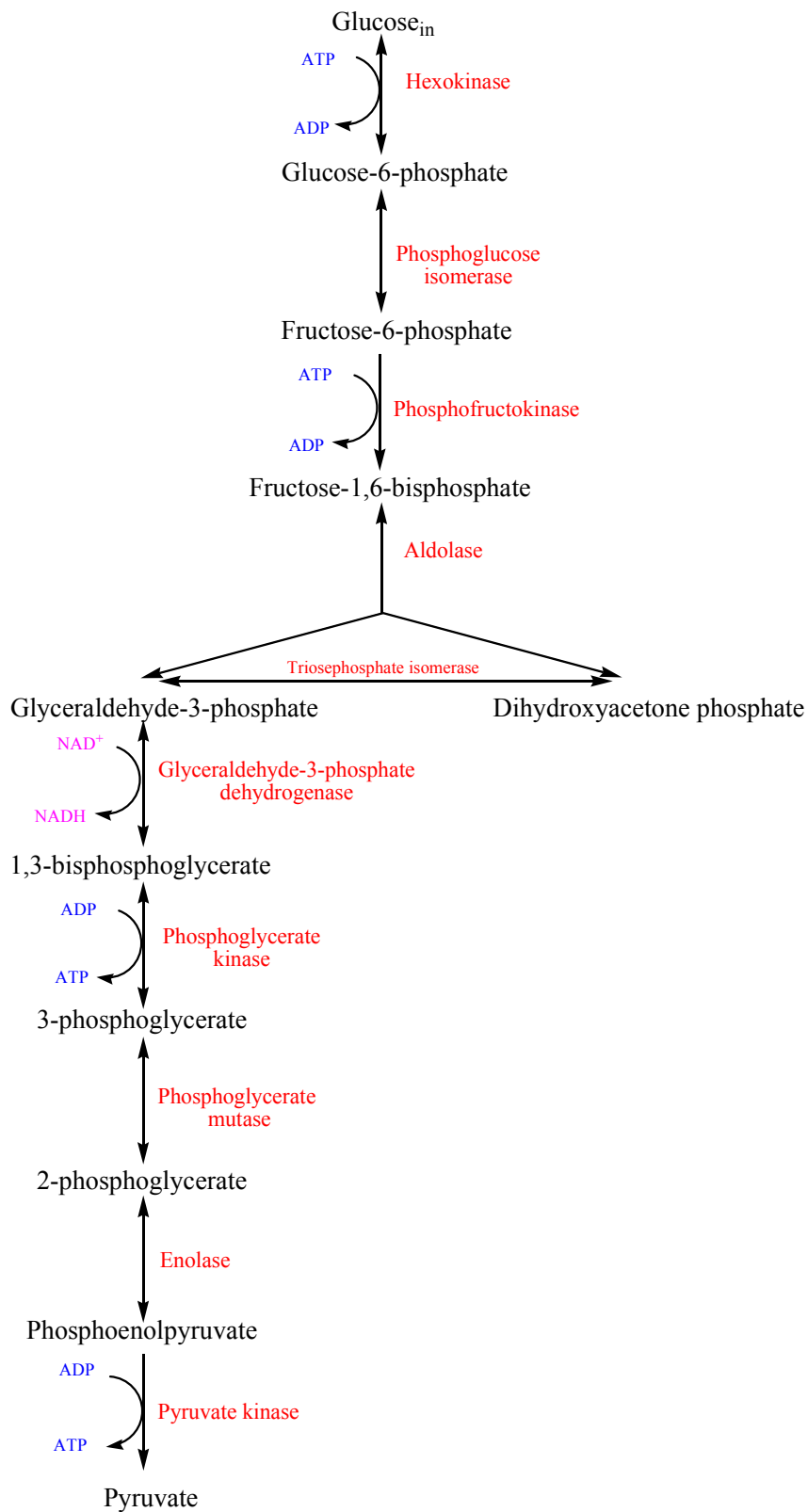


Figure 1.1 Scheme of glycolysis

Lying in the centre of metabolic pathways and being common in almost all organisms, glycolysis is probably the most intensively studied pathway. Yeast glycolysis and sugar metabolism in general, therefore, has been the focus of many researches. Regulation of the sugar metabolism draws attention since many industrial applications rely on the economical utilization of the substrates. Pasteur effect and the Crabtree effect, were two important issues concerning the sugar utilization in yeasts. Pasteur effect is defined by suppression of alcoholic fermentation in the presence of O₂. It occurs in yeasts that do not exhibit Crabtree effect. In *S. cerevisiae* this can be seen only in slowly growing cells, in which glycolytic flux is low. Crabtree effect, which was firstly defined in tumor cells (Crabtree, 1929), is the occurrence of aerobic alcoholic fermentation at high growth rates (Dedeken, 1966). If glucose concentration exceeds a certain value alcoholic fermentation sets even if O₂ is sufficient. This phenomenon is a very important in biomass directed applications such as baker's yeast and single cell production. When ethanol production occurs, the biomass yield on glucose decreases due to carbon flow through ethanol producing pathway. In aerobic batch cultures respirofermentative growth is observed, which is characterized by fast growth but low biomass yield. Full respiratory growth can be achieved in chemostat at low dilution rates and fed-batch cultures, in which sugar is added slowly. The specific glucose uptake rate increases with the specific growth rate up to a point, after which respirofermentative metabolism initiated. Below that critical specific growth rate *S. cerevisiae* produces biomass and CO₂ with a yield on glucose of 0.55 and 0.45 g g⁻¹, respectively. At high glucose uptake rates carbon flow through biomass is lower, around 0.12 g g⁻¹, and rest of the glucose is diverted to ethanol, CO₂ and other products. Under anaerobic conditions; *S. cerevisiae* can grow as long as ergosterol and unsaturated fatty acids are supplied. Energy is generated from glycolysis and ethanol is produced in relation to growth. Biomass yield is around 0.1 g g glucose⁻¹.

Flux through glycolysis determine the economy of the processes like fuel alcohol production and it should be adjusted in biomass directed applications control of the pathway has been an important question. Flux through a pathway is controlled

mainly by the amount of enzymes and by allosteric effectors. The key control points in the glycolytic pathway were suggested to be the sugar uptake, and the irreversible steps: hexokinase, phosphofructokinase and pyruvate kinase. Being far from equilibrium, these reactions have high potential to be the controlling steps. However overexpression studies generally did not lead a substantial increase in glycolytic flux. Phosphofructokinase overexpression did not enhance the glycolytic flux substantially in *S. cerevisiae* (Davies and Brindle, 1992). Similarly, overexpression of phosphofructokinase and pyruvate kinase did not increase citric acid production in *Aspergillus niger* (Ruijter *et al.*, 1997). Authors observed decreased fructose-2, 6-bisphosphate levels, which could decrease the specific activity of phosphofructokinase. With a more systematic approach, Schaaff *et al.* overexpressed each glycolytic enzyme of *S. cerevisiae* including the “key enzymes” and also pairs of them but, did not observed an increase in ethanol production rates (Schaaff *et al.*, 1989). This questioned the hypothesis that suggested a single flux-controlling enzyme. The control may be shared among more than one or all of the glycolytic enzymes. Smits *et al.* (2000) overexpressed simultaneously the seven enzymes of the lower part of glycolysis in; glyceraldehyde-3-phosphate dehydrogenase, phosphoglycerate mutase, phosphoglycerate kinase, enolase, pyruvate kinase, pyruvate decarboxylase and alcohol dehydrogenase. The recombinant strain exhibited higher enzyme level than the host strain. Upon a glucose pulse to aerobic glucose-limited continuous culture, specific CO₂ production rate was increased in the host and the recombinant strain. The increase was higher in the recombinant strain, which showed an increased fermentative capacity. However, the ethanol yield was the same in both strains. One should note that the overexpression of one enzyme may effect expression of other enzymes via the metabolite levels or via protein burden.

Glucose transport is the other candidate for being the controlling step of glycolysis. Otterstedt *et al.* (2004) could alter the mode of metabolism of *S. cerevisiae* by changing this step. They generated a strain in which glucose uptake was dependent on a chimeric hexose transporter mediating a reduced sugar uptake.

This strain respired glucose even at high glucose levels, i.e., it did not exhibit Crabtree effect.

1.3. Hexose transport

Although it is not included in the glycolysis reaction scheme, transport of glucose across the plasma membrane into the cell is the first step of glucose metabolism. *Saccharomyces cerevisiae* can deal with extremely broad ranges of glucose concentrations and the glucose can be metabolized effectively at concentrations higher than 1.5 M down to micro molar concentrations. This implies the presence of a complex and highly regulated glucose uptake system (Buziol *et al.*, 2002).

Monosaccharide transport in *S. cerevisiae* is a facilitated diffusion process as in many other mammalian cells. This is in contrast to many other lower eukaryotes and plant cells (and also prokaryotes) where hexose transport occurs frequently by proton symport mechanism (Ciriacy and Reifenberger, 1997).

S. cerevisiae has 20 genes that encode proteins similar to glucose transporters (HXT1 to HXT17, GAL2, SNF3, and RGT2). In these SNF3 and RGT2 encode proteins that function not as transporters but as sensors of extracellular glucose that generate an intracellular signal for glucose induced transcription of the HXT genes. Glucose ensures its own efficient metabolism by serving as an environmental stimulus that regulates the quantity, types, and activity of glucose transporters, both at transcriptional and post transcriptional levels (Özcan and Johnston, 1999).

All hexose transporters, except HXT12 - from a pseudogene- have been demonstrated to be able to transport hexoses. The most important hexose transporters under physiological conditions seem to be HXT1-4 and HXT6-7 (Maier *et al.*, 2002). D-glucose, D-fructose, D-mannose has been recognized as the natural substrates for the hexose transporter system, while transport of D-galactose

requires a separate transporter, which is synthesized upon induction by galactose (Ciriacy and Reifengerger, 1997).

S. cerevisiae cells express only the glucose transporters appropriate for the amount of extracellular glucose available. This is due to the combined action of different regulatory mechanism, including transcriptional regulation of various HXT genes in response to extracellular glucose and to inactivation of Hxt proteins under certain conditions. Also, modulation of the affinity of certain glucose transporters for glucose interaction between different transporters may contribute to the ability of yeast cells to adapt to different extracellular glucose concentrations (Özcan and Johnston, 1999).

Glucose transport in yeast exhibits dual kinetics, with a high-affinity (low K_m , 1 to 2 mM) and a low –affinity system (high K_m , 15 to 100 mM). High and low affinity glucose represents the sum of several transporters rather than being the result of individual transporters (Özcan and Johnston, 1999).

1.4. Branches from Glycolysis

1.4.1. Ethanol branch

Cytosolic pyruvate can be decarboxylated to acetaldehyde by pyruvate decarboxylase, which in turn is reduced to ethanol by the action of alcohol dehydrogenase.

In aerobic sugar limited cultures of *S. cerevisiae*, PDC activity increases above the critical dilution rate (growth rate) at which alcoholic fermentation is initiated (Postma *et al.*, 1989). For the production of beverages with reduced amount of alcohol, it might be of interest to reduce the activity of PDC. However, when three *pdc* genes (*pdc 1*, *pdc5* and *pdc6*) of *S. cerevisiae* that encode active PDC were knocked-out, the organism could not grow on glucose as the sole carbon source

unless small amounts of ethanol or acetate were added to the medium (Flikweert *et al.*, 1999). It was concluded that PDC was indispensable for growth of *S. cerevisiae*, providing the cytosolic acetyl-CoA to be used in lipid synthesis.

Alcohol dehydrogenase (ADH) reduces acetaldehyde, which is produced from pyruvate by the action of pyruvate decarboxylase, to ethanol by oxidizing NADH. *S. cerevisiae* contains five ADH forms. ADH I is cytosolic and constitutive. It is the major enzyme in fermentative growth, reducing acetaldehyde to ethanol. ADH II is also cytosolic but absent from glucose-grown cells and ADH III is mitochondrial (Ciriacy, 1997). ADH IV is a formaldehyde dehydrogenase and has no effect on ethanol production (Drewke *et al.*, 1990). The function of ADH V is currently unknown (Smith *et al.*, 2004). More recently, ADH VI and VII were shown to exist in yeast (reviewed in (de Smidt *et al.*, 2008)).

Under anaerobic conditions or under glucose excess, *S. cerevisiae* converts most of the substrate to ethanol. Thus, the biomass yield is lower than obtained in aerobic glucose limited culture. The anaerobic conversion of glucose to ethanol is a redox neutral process. The NAD^+ consumed in the reaction catalyzed by glyceraldehyde-3-phosphate in glycolysis is regenerated when ethanol is produced. However, when intermediates of glycolysis are withdrawn for synthesis of cellular materials, more NAD^+ is consumed, thus a surplus of NADH occurs. This will eventually stop the metabolism unless another sink for regeneration of NAD^+ works. This sink is glycerol branch.

1.4.2. Glycerol Branch

Glycerol is one of the earliest chemicals which was bulk produced by fermentation. Nowadays, it is produced mainly as a by product of fat, oil, biofuel and biodiesel industries but there is still an interest in its metabolism because of several factors, positive or negative. On the positive side fermentative production is green chemistry, and also it is a very important and a desired metabolite in wine

making. On the other hand its production is not wanted when ethanol, as a chemical, is being produced. In either case the interest in its metabolism is not merely academic and has also industrial justification.

Glycerol production is known to serve at least two important functions in yeast: (a) as a sink for the excess NADH which is produced by anabolic reactions during anaerobic conditions, and (b) as an osmolyte balancing a high external osmotic pressure during e.g. salt stress. The strategy behind most of the applied methods for enhancing the production of glycerol is in a sense “indirect”, since it aims at creating conditions during which the NADH generation in metabolism is maximized (this can be achieved, for example, by addition of steering chemicals like sulfite). The consequent carbon flux redistribution is caused by the necessity for NAD⁺ regeneration, giving increased glycerol production. A second strategy relies on direct interference with the carbon flux, for example by blocking the isomerization reaction between DHAP and GAP or by inhibiting the later part of glycolysis. In this case, the redox balance will be distorted causing a redistribution of fermentation products in order to meet the need for generation of NADH. The latter strategy can be accomplished for example by overexpression of enzymes in the glycerol pathway, such as glycerol-3-phosphate dehydrogenase and/or down regulation of enzymes in the later part of glycolysis, such as alcohol dehydrogenase. In this case, the increased glycerol formation results in a need for increased NADH production, which has to be met by an increased production of oxidized compounds, e.g. carboxylic acids (Taherzadeh *et al.*, 2002).

Glycerol is formed in two steps: first, the formation of glycerol-3-phosphate (Glyc3P) from DHAP by the action of the glycerol-3-phosphate dehydrogenase (GLYCPDH), and second, subsequent formation of glycerol by the action of glycerol-3-phosphatase (GLYCPASE). There are two isogenic genes for GLYCPDH, GPD1 and GPD2. Expression of GPD1 increases under osmotic stress conditions, while that of GPD2 is subject to redox control and stimulated under anoxic conditions (Ansell *et al.*, 1997; Michnick *et al.*, 1997).

1.4.3. Storage Carbohydrates in Yeast

Trehalose and glycogen have been considered as the storage or reserve carbohydrates in yeast. Glycogen is a glucose polymer made up of linear chains of twelve to eighteen glucose residues linked by $\alpha(1\rightarrow4)$ glycosidic bonds and branched by the formation of $\alpha(1\rightarrow6)$ linkages. Trehalose is a disaccharide formed by two glucose moieties linked by an $\alpha(1\rightarrow1)$ linkage, thus forming a non-reducing end. Glycogen accumulates in the cell while nutrients are still abundant such as, during the growth of yeast while glucose remains in the medium, and it is mobilized during the stationary phase of growth when yeast cells are deprived of nutrients. Trehalose, on the other hand, is barely detectable during exponential growth in glucose and accumulates during the transition from exponential to stationary phase and reaches its maximum during the stationary phase (François *et al.*, 1997). Both carbohydrates are synthesized from glucose-6-phosphate, a glycolytic intermediate, and UDP-glucose.

Trehalose has been concerned in stress response, particularly the response to hyperosmolarity, heat shock and oxidative stress. A high content of trehalose protects cells from autolysis and increases leavening capacity in dough (François and Parrou, 2001). Trehalose synthesis also among the responses to near-freezing and cold shock temperatures in yeast (Al-Fageeh and Smales, 2006). Yeast cells grown under increased osmolarity showed more ethanol tolerance than controls (Sharma, 1997). The role of trehalose in stress resistance is described by its ability to protect membranes from desiccation and to exclude water from the protein surface thereby, protect proteins from denaturation in hydrated cells (François and Parrou, 2001).

Disruption of the *TPS1* gene, which encodes trehalose-6-phosphate synthase, the first enzyme of the trehalose synthesis pathway, prevented *S. cerevisiae* growing on glucose (Thevelein and Hohmann, 1995). This mutant accumulated hexose phosphates; on the other hand ATP and inorganic phosphate are consumed rapidly. This shows that the hexokinase step is too fast for the rest of the metabolism to

cope with in *tps1* mutant (Teusink *et al.*, 1998). The product TPS1, trehalose-6-phosphate, was shown to inhibit hexokinase II *in vitro* (Blazquez *et al.*, 1993). These findings demonstrate the role of trehalose-6-phosphate regulating the glycolysis by restricting the influx of glucose into glycolysis.

1.5. Ethanol and Temperature: Two Major Environmental Factors

1.5.1. Effect of Ethanol

Like pH and temperature accumulation of alcohol in organisms' natural habitat or in fermentation medium represents an environmental stress. In microbial alcohol production, for example, fermentation may terminate pre-maturely due to accumulation of ethanol. While ethanol is seen as a desirable by-product of the fermentation process, its accumulation during fermentation can result in a significant chemical stress on the physiological status of the yeast cell. Ethanol, as a chemical stress agent, inhibits cell growth and viability, and causes changes in metabolic pathways, increases in fermentation times, changes in yeast cell wall and membrane structure and function, and modifications in gene expression (Lentini *et al.*, 2003). Need to supplement fossil fuels with alternative fuels increased the attention to ethanol based products. High levels of ethanol are needed to be reached at the end of fermentation in order to decrease production costs. Therefore, mechanism of ethanol toxicity should be revealed for more effective industrial exploitation of microorganisms including *Saccharomyces spp.*

Saccharomyces species are most probably the most alcohol resistant eukaryotic organisms. They are able to grow up to concentrations of 8-12% (v/v), to survive exposure to concentrations of up to 15% (v/v), and to ferment glucose to produce ethanol up to concentrations of around 12% (v/v) for normal fermentations and up to 20% (v/v) during sake fermentations (reviewed in (Ingram and Buttke, 1984)). It was traditionally believed that maximum amount of ethanol that could be produced by specific strain depends on the relative abilities of those strains to

tolerate ethanol. In this respect, ethanol tolerances was in the order of sake yeast>wine yeast>distillers' yeast>brewers' yeast. However, after the energy crises, much interest has arisen on the physiological and genetic nature of the ethanol tolerance. It was then showed that ethanol tolerance of *Saccharomyces* yeast is not simply due to an intrinsic ability of these yeasts to tolerate differing levels of ethanol. Indeed, the maximum level of ethanol that a given strain of yeast can produce is dramatically influenced by wort nutritional conditions (especially with regards to unsaturated lipids and assimilable nitrogen), environmental parameters employed (especially temperature), and whether the carbohydrate substrate is added sequentially (as in the sake industry) or is all present at the time of inoculation (as in brewing, distilling, and enology) (Casey and Ingledew, 1986). Jones (1989) states that high alcohol tolerant strains do not necessarily give high ethanol yields from sugars nor ferment rapidly.

There is no widely accepted definition of ethanol toxicity. Inhibition and cessation of growth, decrease in fermentative ability, viability loss, and maximum level of produced ethanol are generally used to quantify the ethanol toxicity. The mechanism of ethanol inhibition effect has been attempted to relate with the ethanol inhibition of growth and fermentation rates, of glycolytic enzymes, of membrane potential, ethanol induced lipolysis of phospholipids, and reduction in water activity.

Ethanol inhibits fermentation and growth on glucose of *Saccharomyces cerevisiae*. Ethanol affects the maximum specific rates of fermentation and growth but not its affinity for glucose, that is, it inhibits the growth and fermentation non-competitively (Leao and van Uden, 1982; Luong, 1985). There are many studies concentrated on establishing mathematical correlation between growth and fermentation rates in the absence and presence of ethanol (linear, exponential, hyperbolic, or more complex relations have been derived depending mostly on the strain, nutritional composition, and cultural and growth conditions), with a final goal of describing the kinetic behavior of alcoholic fermentation (Luong, 1985; Casey and Ingledew, 1986; Marin, 1999; Medawar *et al.*, 2003; Ricci *et al.*, 2004).

Inhibition of growth with ethanol was usually worked with added ethanol. However, it was reported that produced ethanol is much more toxic than added ethanol (Nagodawithana and Steinkraus, 1976; Casey and Ingledew, 1986). It was first thought that this difference is caused by the accumulation of produced ethanol inside the cell (Nagodawithana and Steinkraus, 1976). This possibility was ruled out by later works with more accurate analysis results which have shown that ethanol does not accumulate within the cell (Guijarro and Lagunas, 1984; Dombek and Ingram, 1986; Dasari *et al.*, 1990). One possible explanation for different patterns of toxicity with added ethanol is osmotic effect due to high substrate concentrations usually encountered in ethanolic fermentations. For rapid fermentations, in which sharp decrease in viability is observed with rapid ethanol formation, it was showed that the difference was not due to intracellular ethanol accumulation or to differences in glucose concentration between cultures, rather, it was partly due to inability of cells to adapt quickly enough to sudden increase in ethanol concentration and was partly due to increased demand for magnesium at higher ethanol concentrations (Dombek and Ingram, 1986; Dasari *et al.*, 1990; Walker and Maynard, 1997; Birch and Walker, 2000). Inhibition retarding effect of magnesium was also shown by other authors (Dombek and Ingram, 1986; Walker and Maynard, 1997; Birch and Walker, 2000).

Plasma membrane is the site where nutrient uptake from the medium and excretion of by-products of metabolism in to the environment takes place. The primary target site for the effect of ethanol is believed to be the membrane, affecting the transport rates of nutrients. Inhibitory effect of ethanol and other alkanols on glucose transport had been studied by Leao and van Uden (1982). Their work with D-xylose (an unmetabolized monosaccharide by *S. cerevisiae*) showed that affinity of transport system of *S. cerevisiae* for the glucose was not affected by the alkanols tested (ethanol, isopropanol, propanol, and butanol), rather the effect was exclusively on the v_{max} , effect being exponential. They also relate the degree of inhibition with the lipid-buffer partition coefficients of alkanols, the higher the lipid-buffer partition coefficient the higher the inhibition caused by the same amount. Similar results were obtained for the rate of glucose utilization (Gray and

Sova, 1956). Studies for the uptake of amino acids (Leao and van Uden, 1984), maltose (Loureirodias and Peinado, 1982) and ammonium (Leao and van Uden, 1983) have also showed similar results, non-competitive inhibition with alkanols, effect being exponential.

The enzymes of the glycolytic pathway are one of the likely targets for product inhibition of ethanol. There are not many studies about the effect of ethanol on the activities of glycolytic enzymes. Nagodawithana *et al.* (Nagodawithana *et al.*, 1977) investigated the effect of ethanol on HXK, PFK, ALD, and GLYCPDH of *Saccharomyces uvarum*, formerly *S. carlsbergensis*. Hexokinase and GLYCPDH were inhibited noncompetitively by ethanol and PFK and ALD were not inhibited within the concentration range tested. There was just one study in which all glycolytic enzymes of bakers' yeast were examined in terms of ethanol inhibition (Millar *et al.*, 1982). The latter study investigated the effect of ethanol both in terms of denaturation and on activities of purified enzymes. It was suggested in both studies that inhibitions of glycolytic enzymes with ethanol may play a role in the slowing down of the glycolytic rate.

1.5.2. Effect of Temperature

Changes in environmental conditions are the most common stresses that organisms face. Organisms encounter large temperature changes in environment during seasonal and diurnal temperature cycling. Temperature is also an important factor in industrial exploitation of microorganisms. For example, beer and wine productions by *Saccharomyces* species are commonly at 10-20 °C, while industrial alcohol production by this yeast is carried out at higher temperatures.

Adaptation of organisms to high or sub-optimal temperatures was mostly studied through heat or cold shock experiments. The response of both prokaryotes and eukaryotes to heat shock includes the induction or up-regulation of heat shock proteins. Similarly, cells respond to cold stress by overexpression of a group of

proteins, called cold shock proteins. Responses of yeast to cold (10-18 °C) are quite different than to near freezing conditions (below 10 °C). This correlates with the ability of yeast to grow at 10-18 °C but growth stops below 10 °C (Al-Fageeh and Smales, 2006). Cold induced changes include membrane lipid composition and fluidity, transport functions, translational efficiency, protein folding and nucleic acid structure (Tai *et al.*, 2007).

Temperature has two major effects on enzymes. Below certain point, increase in temperature increases the catalytic rate, whereas above that point thermal denaturation occurs. Reactant molecules get more kinetic energy as temperature increases, so that more collisions occur. Temperature dependence of enzyme catalyzed reactions is defined by Arrhenius equation:

$$k_{cat} = A \cdot e^{\left(\frac{-E_a}{R \cdot T}\right)} \quad (1.1)$$

where, E_a is the activation energy, A is the Arrhenius constant, and R is the universal gas constant. According to this equation, increase in temperature or decrease in activation energy results in increase in activity. However, Arrhenius equation does not take into account the temperature dependent effect of allosteric effectors nor temperature dependent degradation. Besides, amount and capacity of the enzymes may be different at different temperatures through regulation of transcription, mRNA degradation, protein synthesis and degradation and post translational modification (Tai *et al.*, 2007; Postmus *et al.*, 2008).

1.6. Modeling the Metabolism

Mathematical modeling is a very powerful tool in physics, chemistry, and engineering for interpretation and prediction of natural phenomena and experimental results (Gombert and Nielsen, 2000). Mathematical models of metabolism have a special interest within biotechnology since products of

metabolism find many applications in real life. Microorganisms are used either as a cell factory, or their products of metabolism like organic acids, alcohol, pharmaceuticals, even flavour compounds find great deal of application areas.

Metabolic models are tools that can be used to address many different questions. The aim of modeling could be structural understanding, exploratory simulation, interpretation and evaluation of measured data, analysis of a system, prediction and design, or optimization (Wiechert, 2002). Metabolic models are used to improve our understanding of metabolic regulation by quantifying essential parts or aspects of the metabolic system.

Gombert and Nielsen (2000) grouped mathematical models of metabolism on the basis of their structure: stoichiometric models, which are based on the time invariant characteristics of metabolic networks, and kinetic models, which are based on stoichiometry and enzyme and microbial kinetics. Stoichiometric models do not require kinetic parameters and information about kinetic mechanism of each enzyme, so it can be applied to complete metabolic network. Metabolic flux analysis (MFA) is used for the calculation of intracellular reaction rates at steady state or pseudo-steady state by solving the mass balance based mathematical models (Çalık and Özdamar, 2002). Beside calculating the “carbon flow” MFA can be used to calculate non-measured extracellular fluxes, to calculate maximum theoretical yields, to identify the existence of different pathways, to examine the influence of alternative pathways on the distribution of fluxes, and to identify possible rigid branch points in a pathway (Nissen *et al.*, 1997).

1.6.1. Kinetic Models

A metabolic system consists of a network of coupled enzymic reactions and membrane associated transport steps. Such networks can be schematically represented by sequence of reactions in which each reaction can be characterized by its participating enzyme, metabolites, cofactors, effectors, and reaction

stoichiometry. These reactions and transport steps connects metabolite pools through which pools affect each other by mass action.

When the kinetics of cellular processes are known in detail, it is possible to describe the dynamics of these processes by combining kinetics with the known stoichiometry of the pathway. The aim in using detailed kinetic models using ordinary differential equations (ODEs) is to get a quantitative understanding of the functioning of the living cell. In this approach, characterization of individual components, enzymes, and their interactions are needed. The ultimate and very ambitious goal of kinetic models is to build a computer replica of a living cell (Snoep and Westerhoff, 2004). In constructing these kinds of models of pathway of known structure, the kinetics of individual enzymes needed to be measured and/or necessary data should be subtracted from literature. Effects of co-factors, pH, ions, and temperature and so on are used to parameterize the model, beside the kinetic data (Giersch, 2000).

For a metabolite X, rate of change of its concentration is equal to the sum of rates of reactions producing X (X is the product) minus the sum of the reactions that consumes it (X is the substrate) (Figure 1.2, equation 1.2).

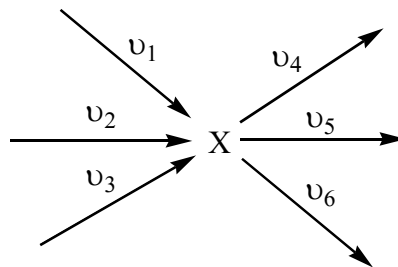


Figure 1.2 Scheme showing metabolite X being produced or consumed by various reactions

$$\frac{d[X]}{dt} = (\nu_1 + \nu_2 + \nu_3) - (\nu_4 + \nu_5 + \nu_6) \quad (1.2)$$

Therefore, rate of change of the concentration of X depends on the relative magnitudes of the reactions that produces or consumes it. In this example, stoichiometry of X is equal to one. This always may not be the case; metabolites as reactants (or products) may not have a stoichiometric coefficient equal to unity, in which case one should consider these differing stoichiometries. In a system of reactions which contains n step with m metabolites, X_i being any metabolite and ν_j being the rate of any reaction or transport step, the stoichiometric coefficient c_{ij} describes the stoichiometry by which X_i participates in reaction step j. In this case, equation 1.3 holds;

$$\frac{d[X_i]}{dt} = c_{i1} \cdot \nu_1 + c_{i2} \cdot \nu_2 + c_{i3} \cdot \nu_3 + \dots + c_{in} \cdot \nu_n \quad (1.3)$$

This equation can be re-written in short as;

$$\frac{d[X_i]}{dt} = \sum_{j=1}^n c_{ij} \cdot \nu_j \quad (1.4)$$

In order to describe the dynamic behaviour of a metabolic system, such an equation (equation 1.4) is written for each participating metabolite. For a metabolic network, set of ODEs can be solved by the use of aggregated rate equations such as Michaelis-Menten, Hill or Monod-Wyman-Changeux type, kinetic parameters of which (ν_{max} , K_m , K_i , K_{eq} etc.) are determined experimentally for each enzyme. Any constraint on concentrations of a group of metabolites

described by a conservation relation can be used in solving such networks of reactions.

Kinetic expressions are the results of many decades of work by many laboratories yet they still have a lot of shortcomings: they are determined *in vitro* so one can never be sure of the similar conditions *in vivo*. The conditions *in vivo* may be considerably different from the ones *in vitro*, and many scientists still doubt that modeling living organism behavior, even partially, is possible by mathematical expressions obtained from *in vitro* assays. Regulation of the activity of enzymes by metabolites produced elsewhere in the cell metabolism may be overlooked. Kinetic data obtained under different conditions cannot be combined. Enzymes that are present in a classically defined compartment may be sub-compartmented due to binding of membranes, to the cytoskeleton or other enzymes. In addition, the concentration of enzymes in the cell is much higher than in the usual test tube experiment (Teusink *et al.*, 2000). Such factors combined could be important arguments against modeling activities.

Having put this word of caution, it can now be started to present the benefits of stoichiometric and kinetic modeling of the metabolism. The primary benefit that one can expect from modeling something is to understand it. How can one manage and understand hundreds of biochemical processes simultaneously? After ages of qualitative or quasi-quantitative modeling, a mathematical biochemistry approach is coming within reach. The biochemical processes are described by the appropriate differential or algebraic equations, the parameter values are taken from experimental studies, and are integrated numerically (Jonker *et al.*, 2002). Thus, the individual kinetic expressions with the powerful language of mathematics convey the information in such a condensed manner which would otherwise require pages of essays to explain. The second benefit would be to be able to predict the behaviour of the metabolism so that the fermentation conditions and enzyme levels can be adjusted so that the specific aims will be achieved.

Describing and predicting the dynamic changes occurring within the cell and its environment, it is necessary to model the reaction rates using kinetic expressions. However, it is almost impossible to include all individual reactions due to the complexity of biological systems. Therefore, in dynamic models, only most important reactions or pathways of interest are modeled by the help of kinetic expressions (Lei and Jorgensen, 2001). When constructing a mathematical model of metabolism: first thing to do is to define all reactions, specifying the kinetics of each reaction and setting up the mass balances for each metabolite contained in the network as described above. There are different approaches developed to simplify and solve such systems (Visser *et al.*, 2000; Hynne *et al.*, 2001; Lei and Jorgensen, 2001; Dano *et al.*, 2006).

1.6.2. Modeling the Glycolytic Pathway

The glycolytic pathway is one the most common pathways of the living world. Mathematical modeling of this very important pathway has been attempted in the past and the efforts are being increased by every passing year and increasing biochemical knowledge. Even though it is not possible to truly model and predict such a complex system, modeling helps us to express the accumulated knowledge in a condensed manner, to study and learn the system better.

Among the kinetic models totally based on or including glycolysis, there are few of worth to mention. The first one is the work done by Rizzi *et al.* (1997); in which they attempted the modeling of metabolic dynamics of *S. cerevisiae*. Their model was based on rate equations for the individual reactions and aimed to predict changes in the levels of intra- and extracellular metabolites after a glucose pulse, which means their analysis was focused on a time scale of seconds. The model structure and experimental observations were related to the aerobic growth of the yeast. The model was based on material balance equations of the key metabolites in the extracellular environment, the cytoplasm and the mitochondria, and includes mechanistically based, experimentally matched rate equations for the individual

enzymes. They used MFA to calculate discharge fluxes from glycolysis and TCA. Maximal rates were calculated by using rate equations and measured intracellular concentrations.

Second work belongs to Westerhoff group (Teusink *et al.*, 2000). They came up with a model most of whose kinetic data was taken on the same system at the same time, this model is unique in that sense. Their model included hexose transport, all glycolytic enzymes from glucose to ethanol, and branches to the glycerol, glycogen, trehalose, and succinate for fermenting non-growing yeast cell. Model made use of the kinetic equations for each glycolytic enzyme and set of ODEs describing the time dependence of metabolite concentrations. System was solved with the values of constants obtained in that study with few literature and adjusted values.

In their study Hynne *et al.* (2001) presented a method to fit a model of biochemical pathway to experimentally determined metabolite (substrate) concentrations and dynamical properties at a stationary state. Kinetic parameters were calculated from substrate concentrations and metabolic fluxes determined experimentally by simple algebra without integration of kinetic equations. They applied this approach to glycolysis including branches to glycerol and ethanol and glycolytic oscillations.

The most recent work has been carried out by Bosch *et al.* (2007). They investigated the role of internal sugar signalling mechanism by measuring the intracellular levels of upper glycolytic metabolites and adenine nucleotides in HXT1, HXT7 and TM6* mutant strains with progressively reduced uptake capacities as compared to wild type, and found out that the reduction in sugar consumption caused an accumulation of hexose phosphates upstream of PFK and reduction of F16bP levels. With the help of their mathematical model, they suggested that these effects may be explained by the changes in the kinetics of PFK and PGI, and by modified sensitivities of PDH and/or TCA cycle enzymes towards NAD^+ and NADH.

1.7. Aim of the Study

The simulations of alcoholic fermentation using the detailed kinetic models were either not attempted or were not satisfactory in predicting the fermentation. In this work it was attempted to simulate alcoholic fermentations by a model based on a previous study, which used kinetics of enzymes to model the glycolysis of *Saccharomyces cerevisiae* focusing on the intracellular concentrations of intermediary metabolites (Teusink *et al.*, 2000). The first aim was to collect kinetic data from literature to construct a model describing the glycolysis in yeast and its branches using MATLAB as the programming language. In an effort to describe the alcoholic fermentation, the effects of two main environmental factors, ethanol concentration and temperature, were investigated and incorporated into the model.

To construct a model, the kinetic parameters measured in that study was used along with some data generated in this study and some literature data. Mainly, it was tried to incorporate the effect of accumulating ethanol on the kinetics of the enzymes of the pathway into the model. In this work, the effect of increasing ethanol concentration and temperature on the enzymes of the glycolytic pathway was tried to be determined experimentally and then it was tried to incorporate this into the detailed kinetic model and test it for the simulation of the ethanolic fermentation.

CHAPTER 2

MATERIALS AND METHODS

2.1. Chemicals

The chemicals used in all experiments were all of analytical grade and commercially available from Sigma, Aldrich, Merck, and Fluka. Coupling enzymes used in enzyme assays were either Sigma or Fluka.

2.2. Organism

Commercial yeast strain *Saccharomyces* strain (brewers' yeast) used in the study was obtained from Efes Brewery.

2.3. Culture and Growth Conditions

Brewers' yeast was maintained on YPD agar plates (yeast extract 1%, peptone 2%, glucose 2%, and 1.5% agar (w/v)) at 4°C. For long term storage, they were stored in 20% (v/v) glycerol stock at -80 °C.

Yeast was pregrown in 20 ml YPD medium in 100 ml cotton plugged Erlenmeyer flask. Preculture was inoculated from the glycerol stock and incubated at 30°C and 200 rpm for about 12 h, at which time absorbance at 600nm was around 1.0. This was used to inoculate the main culture, composed of yeast extract (1%), peptone

(2%), and glucose (5%). Twenty ml of preculture was added to 180 ml main culture medium in 500 ml Erlenmeyer flask and incubated at 30°C and 140 rpm. Cells were harvested after 15-16 h, when OD₆₀₀ reached around 9.0 (see Appendix A for the growth curve). Absorbances were followed by Shimadzu UV 1202 (Japan) spectrophotometer. These cells were used for enzyme assays.

Effects of ethanol and temperature on glucose consumption and ethanol and glycerol production were investigated in short term under non-growing conditions. Four temperatures (10, 15, 20, 30 °C) and three ethanol concentrations (5, 10, 15 %) were investigated. Cells grown in YPD (glucose 5%) medium until OD₆₀₀ of 9.0 were collected by centrifugation (Sorvall RC5C, Thermo, USA) at 5000 g for 5 min at 4 °C. They were washed twice by 50 mM potassium phosphate buffer at pH 6.5 and resuspended in 200 mM phosphate buffer (pH 6.5). Dry cell weight of this suspension was determined by microwave drying and same buffer was added to adjust the cell concentration to 22 mg dry weight ml⁻¹. Glucose solution (10% w/v), concentrated ethanol, and 25 ml screw capped bottles containing 12.75 ml of cell suspension were placed in an incubator or in a water bath at desired temperature and left 45-60 min. for temperature equilibration before the experiment commenced. Appropriate amounts of ethanol and water and 5 ml of glucose solution were added to previous yeast suspension to a total volume of 25 ml, so that concentrations of the buffer, glucose and cells were 100 mM, 2%, and 11 mg dry cell weight ml⁻¹, respectively. Bottles were incubated without shaking for 70 min and 300 µl samples were taken at every seven minutes. Before taking the samples bottles were shaken by inverting. Samples were put into Eppendorf tubes on ice and centrifuged immediately at 12500 g for 1 min at 4 °C. Supernatants were kept at -20 °C until HPLC analyses.

2.4. Analytical methods

Glucose, glycerol and ethanol concentrations were determined by HPLC using an organic acid analysis column (Phenomenex, Torrance, CA, USA), and a

differential refractometer (Schambeck RI2000, Germany). The detector cell was kept at 35 °C. The column was kept at 60 °C and was eluted with 5 mM H₂SO₄ at a flow rate of 0.6 ml min⁻¹. Glucose, lactate and ethanol standard solutions of known concentrations were used for calibration. Signal from the detector was processed by CCDS data acquisition software (Dizge Analitik, Turkey).

Dry cell weight was measured by filtering cells on cellulose-acetate filters (0.45 mm pore size) and drying the filters in microwave oven for 15 min. Filters were cooled for 20 min. in desiccator before weighing. Filters were pre-weighed after drying for 10 min. in the microwave.

2.5. Extraction of proteins

Yeast cells at OD₆₀₀ of 9.0 were collected by centrifugation at 5000xg for 5 min. (Sorvall RC5C, Thermo, USA). Cells were washed twice with 20 mM potassium phosphate buffer (pH 7.0) and suspended in the same buffer at a volume (ml) equal to the wet weight (mg) of cells. Suspension was pipetted slowly into liquid nitrogen. The droplets formed at the pipette tip were frozen immediately as they dropped in the liquid nitrogen. Droplets were kept at -80 °C until further use.

Frozen cells were brought to powder form by Mikro-D95 dismembrator (Sartorius, Germany). For the extraction of proteins, biomass droplets and steel balls were put in PTFE container, which were pre-cooled in liquid nitrogen. This container was shaken for 60 seconds at 2000 rpm. This procedure crushed the biomass drops to a powder form, which was then suspended in cold extraction buffer (as specified in enzyme assay procedures). Cell debris was removed by centrifugation at 12500xg for 30 min at 4 °C (Hettich Micro 200R, Germany). Supernatant (crude extract) was used for enzyme assays, protein concentration of extracts were determined by Lowry method (Lowry *et al.*, 1951) modified by Hartree (1972) with bovine serum albumin as the standard.

2.6. Enzyme Assays

Almost all enzyme activities were measured by monitoring the oxidation of NADH at 340 nm in spectrophotometer (Shimadzu UV-1202, Japan) except hexokinase, phosphoglucose isomerase, and alcohol dehydrogenase (reverse direction-ethanol as the substrate) which were measured by monitoring the reduction of NADP⁺, NADP⁺, and NAD⁺, respectively.

For all enzymes, one unit of enzyme activity was defined as the μ mole substrate converted per min. Protein extracts were diluted with extraction buffer when necessary. All assays were performed with at least two concentrations of cell extract. Activities obtained by these experiments differed by less than 10%. Extinction coefficient of NADH was taken as 6.22 mM⁻¹ cm⁻¹. Assays were done in 1.4 ml special glass cells (Hellma, Germany) having a light path of 1 cm and assay volume was 1 ml for all assays except PFK assay which was 1.2 ml. Activities were calculated by following formula:

$$Activity = \frac{Slope(\Delta A / \text{min})}{\varepsilon(6.22)} \cdot \frac{Assay_volume}{Crude_volume} \cdot Dil.factor \quad (2.1)$$

Activities were reported as specific activities, which were defined as the unit of enzyme per mg of protein in the crude extract. Crude extracts generally contained 0.8-2 mg protein ml⁻¹. Extraction buffer, assay buffer, and reagents contained in the assay are given under assay headings below. When the amount of coupling enzyme was increased in studying the effect of ethanol on activities of enzymes, it is indicated in parenthesis.

For the study of the effect of ethanol on activities of enzymes, all assays were measured at 30 °C. Temperature effect on activities of enzymes was tested at 10-15-20-25-30-35 °C.

All reagents and coupling enzymes were prepared with ultrapure water (resistance = 18.2 M Ω ·cm).

2.6.1. Hexokinase assay

Extraction buffer: 20 mM potassium phosphate buffer (pH 7.0) containing 1 mM PMSF.

Assay buffer: 50 mM PIPES buffer (pH 7.0) containing 100 mM KCl and 5 mM MgSO₄

Reagents: 0.2 mM NADP⁺, 5 mM ATP, 2.8 U/ml G6PDH, and 10 mM glucose as substrate.

2.6.2. Phosphoglucose isomerase assay

Phosphoglucose isomerase activity was measured in the reverse direction.

Extraction buffer: 20 mM potassium phosphate buffer (pH 7.0) containing 1 mM PMSF.

Assay buffer: 50 mM PIPES buffer (pH 7.0) containing 100 mM KCl and 5 mM MgSO₄

Reagents: 0.2 mM NADP⁺, 2.8 U/ml G6PDH, and 2 mM F6P as substrate.

2.6.3. Phosphofructokinase assay

Extraction buffer: 50 mM potassium phosphate buffer (pH 7.0) containing 2 mM MgCl₂, 1 mM DTE, and 1 mM PMSF.

Assay buffer: 70 mM PIPES buffer (pH 7.0) containing 5 mM MgCl₂

Reagents: 0.15 mM NADH, 1 mM ATP, 1 mM ADP, 0.1 mM F26bP, 1.5 U/ml ALD, 67.5 U/ml TPI, 2.5 U/ml GLYCPDH, and 5 mM F6P as substrate.

2.6.4. Aldolase assay

Extraction buffer: 20 mM potassium phosphate buffer (pH 7.0) containing 1 mM PMSF.

Assay buffer: 50 mM PIPES buffer (pH 7.0) containing 100 mM KCl and 5 mM MgSO₄

Reagents: 0.15 mM NADH, 50 U/ml TPI, 4.3 U/ml GLYCPDH, and 2 mM F16bP as substrate.

2.6.5. Glyceraldehyde-3-phosphate dehydrogenase assay

For the forward direction:

Extraction buffer: 20 mM potassium phosphate buffer (pH 7.0) containing 2 mM MgCl₂ and 1 mM PMSF.

Assay buffer: 50 mM PIPES buffer (pH 7.0) containing 100 mM KCl and 5 mM MgSO₄

Reagents: 2 mM NAD⁺, 5 mM cysteine-HCl, 10 mM arsenate, 0.5 mM glyceraldehyde-3-phosphate as substrate.

For the reverse direction:

Extraction buffer: 20 mM potassium phosphate buffer (pH 7.0) containing 1 mM PMSF.

Assay buffer: 50 mM PIPES buffer (pH 7.0) containing 100 mM KCl and 5 mM MgSO₄

Reagents: 0.15 mM NADH, 1 mM ATP, 0.9 mM EDTA, 0.2 mM DTE, 5 U/ml PGK (10 U/ml for ethanol effect), and 2 mM 3-PG as substrate.

2.6.6. Phosphoglycerate kinase assay

Extraction buffer: 20 mM potassium phosphate buffer (pH 7.0) containing 1 mM PMSF.

Assay buffer: 50 mM PIPES buffer (pH 7.0) containing 100 mM KCl and 5 mM MgSO₄

Reagents: 0.15 mM NADH, 1 mM ATP, 0.9 mM EDTA, 8 U/ml GAPDH, and 5 mM 3-PG as substrate.

2.6.7. Phosphoglycerate mutase assay

Extraction buffer: 20 mM potassium phosphate buffer (pH 7.0) containing 1 mM PMSF.

Assay buffer: 50 mM PIPES buffer (pH 7.0) containing 100 mM KCl and 5 mM MgSO₄

Reagents: 0.15 mM NADH, 1 mM ADP, 0.5 mM glycerate-2,3- bisphosphate, 0.9 mM EDTA, 14 U/ml LDH, 7 U/ml PYK, 0.95 U/ml ENO, and 2 mM 3-PG as substrate.

2.6.8. Enolase assay

Extraction buffer: 20 mM potassium phosphate buffer (pH 7.0) containing 1 mM PMSF.

Assay buffer: 50 mM PIPES buffer (pH 7.0) containing 100 mM KCl and 5 mM MgSO₄

Reagents: 0.15 mM NADH, 1 mM ADP, 0.9 mM EDTA, 14 U/ml LDH, 7 U/ml PYK, and 0.2 mM 2-PG as substrate.

2.6.9. Pyruvate kinase assay

Extraction buffer: 100 mM PIPES buffer (pH 7.0) containing 10 mM KCl and 1 mM PMSF.

Assay buffer: 70 mM PIPES buffer (pH 7.0) containing 100 mM KCl and 2 mM MgCl₂

Reagents: 0.2 mM NADH, 2 mM ADP, 1 mM F16bP, 10 U/ml LDH, and 2 mM PEP as substrate.

2.6.10. Triosephosphate dehydrogenase assay

Extraction buffer: 100 mM potassium phosphate buffer (pH 7.0) containing 1 mM DTE, 2 mM MgCl₂, and 1 mM PMSF.

Assay buffer: 50 mM PIPES buffer (pH 7.0) containing 10 mM MgCl₂

Reagents: 0.15 mM NADH, 2.5 U/ml GLYCPDH (5 U/ml for ethanol effect), and 0.8 mM DL-glyceraldehyde-3-phosphate (diluted with 10 mM K-PO₄ buffer at pH 7.0) as substrate.

2.6.11. Glycerol-3-phosphate dehydrogenase assay

Extraction buffer: 10 mM triethanolamine (TEA) buffer (pH 7.5) containing 1 mM DTE, 1 mM EDTA, and 1 mM PMSF.

Assay buffer: 20 mM imidazole-HCl buffer (pH 7.0) containing 1 mM MgCl₂

Reagents: 0.1 mM NADH, 1 mM DTE, and 1.34 mM DHAP as substrate.

Since TEA buffer interfered with Lowry method in protein determination, standard curve was prepared by inclusion of same amount of TEA that would come from crude. Therefore, specific activity of GLYCPDH was calculated by protein amount calculated from this standard curve.

2.6.12. Alcohol dehydrogenase assay

Extraction buffer: 100 mM potassium phosphate buffer (pH 7.0) containing 1 mM EDTA, 1 mM DTE, and 1 mM PMSF.

Assay buffer: 50 mM PIPES buffer (pH 7.0) containing 100 mM KCl and 5 mM MgSO₄

Reagents:

- Reverse direction: 2 mM NAD⁺ and 100 mM ethanol as substrate.
- Forward direction: 0.15 mM NADH, and 5 mM acetaldehyde as substrate

2.6.13. Pyruvate decarboxylase assay

The effect of temperature on pyruvate decarboxylase (PDC) was investigated using a NADH linked assay like the other enzymes. For this assay extraction and assay buffers and reagents were as follows:

Extraction buffer: 20 mM potassium phosphate buffer (pH 7.0) containing 1 mM EDTA, 1 mM DTE, and 1 mM PMSF.

Assay buffer: 50 mM PIPES buffer (pH 7.0) containing 100 mM KCl and 5 mM MgCl₂

Reagents: 0.15 mM NADH, 0.2 mM TPP, 110 U/ml ADH, and 50 mM PYR as substrate.

The effect of ethanol concentration on PDC could not be investigated by NADH linked continuous assay since the most reasonable coupling enzyme for the assay, alcohol dehydrogenase was inhibited extremely by its product, ethanol. Therefore, a stop assay was developed, in which crude extract was incubated with the pyruvate and TPP, and ethanol, without the coupling enzyme alcohol dehydrogenase. Remaining pyruvate was measured enzymatically as described below.

The extraction and assay buffer used were the same as above. Pyruvate concentration was decreased to 10 mM in order to be measured accurately. Otherwise the percentage of the remaining pyruvate would be too high that sensitivity of the pyruvate assay would not be sufficient to detect the difference. With this concentration of pyruvate, activity was 30% lower than that of 50 mM. Similarly, relatively higher amount of crude extract (20-40 % of the assay volume) was used in the enzyme assay and incubation time was also longer (15 minutes). TPP concentration was also five times that of used in continuous assay. Assays were conducted in Eppendorf tubes containing 1 ml assay mixture in water bath at 30 °C. One hundred and fifty milliliter samples were taken from the assay at 5, 10 and 15 min. and mixed with the same volume of 500 mM EDTA to stop the enzymatic activity.

Remaining pyruvate was determined enzymatically by measuring the oxidation of NADH while pyruvate is reduced to lactate by lactate dehydrogenase. Assay was conducted in 50 mM phosphate buffer (pH 7.0) containing 0.2 mM NADH. After the sample was added absorbance at 340 nm was recorded and LDH (10 U ml⁻¹) was added to start the reaction. After the decrease in absorbance stopped the absorbance was recorded and subtracted from the initial absorbance. The difference was used to calculate the amount of pyruvate present initially, since the NADH and pyruvate were utilized stoichiometrically in equal amounts. Decrease in the pyruvate concentration was linear in the course of the assay (15 minutes), suggesting that enzyme was stable during the assay.

CHAPTER 3

RESULTS AND DISCUSSION

3.1. History of the model

The modelling of the pathways using the kinetic expressions of the comprising enzymes is advancing. The glycolytic pathway, being one of the most important pathways and also one of the better known pathways, has been of interest of such models. Among these models, the Teusink's publication (Teusink *et al.*, 2000) was remarkable in the sense that very few adjusted parameters were used for the simulation. In their study, they measured almost all kinetic constants contained in kinetic equations of each glycolytic enzyme of bakers' yeast. Their model included hexose transport, all glycolytic enzymes from glucose to ethanol and, for the branched model, branches to the glycerol, glycogen, trehalose, and succinate for fermenting non-growing yeast cell (Figure 3.1). Model makes use of the kinetic equations for each glycolytic enzyme (see Appendix B for details) and set of ordinary differential equations (ODEs) describing the time dependence of metabolite concentrations. This model, while as admitted by the authors, did not very well describe the system and required several adjustments to "catch up" *in vivo* measured fluxes, but shed light on what was there to improve upon. In support of this approach, I based my work on their branched model, and looked for points that could be incorporated into it or to be changed that would lead to better simulation of the yeast fermentations, with a final goal of better understand the metabolism and its regulation.

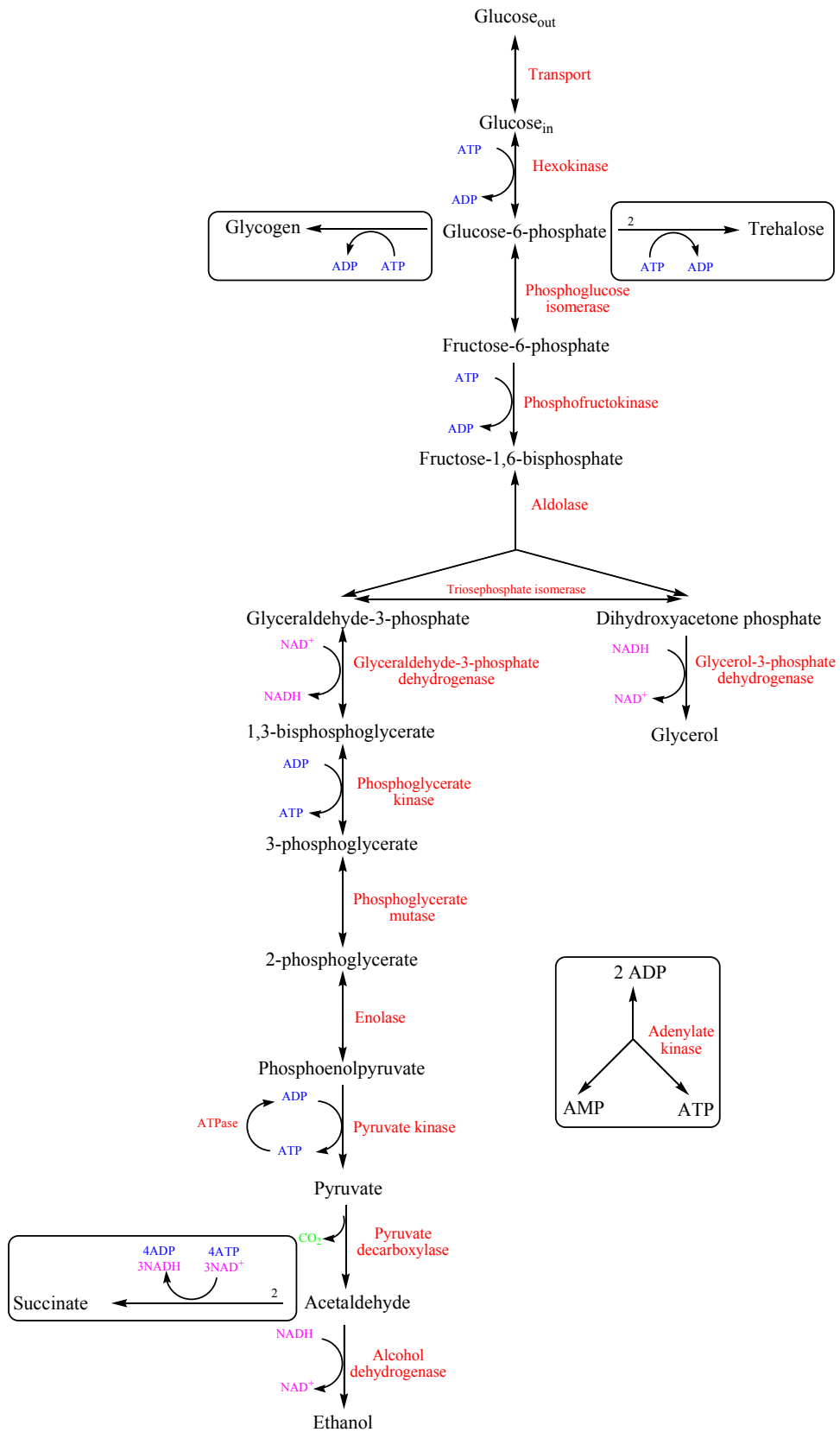


Figure 3.1 Scheme of reactions used in the Teusink *et al.* (2000) model

Before going into details of the program written to solve the set of ODEs to have time profile of metabolite concentrations and rates of reactions, there are few things to mention about the variables of the previous work;

In the model, triosephosphate isomerase (TPI) reaction was modelled as an equilibrium block between dihydroxyacetonephosphate (DHAP) and glyceraldehyde-3-phosphate (GAP) (Figure 3.2). TRIO represented the free variable, calculated as the sum of these two concentrations. So, concentration relations for DHAP and GAP (eqn. 3.3&3.4) obtained by solving equations (3.1) and (3.2) were used in the kinetic equations where appropriate.

$$\left. \begin{aligned}
 [TRIO - P] &= [DHAP] + [GAP] & (3.1) \\
 K_{eq,TPI} &= \frac{[GAP]}{[DHAP]} & (3.2)
 \end{aligned} \right\} \begin{aligned}
 [DHAP] &= \frac{[TRIO - P]}{1 + K_{eq,TPI}} & (3.3) \\
 [GAP] &= \frac{[TRIO - P] \cdot K_{eq,TPI}}{1 + K_{eq,TPI}} & (3.4)
 \end{aligned}$$

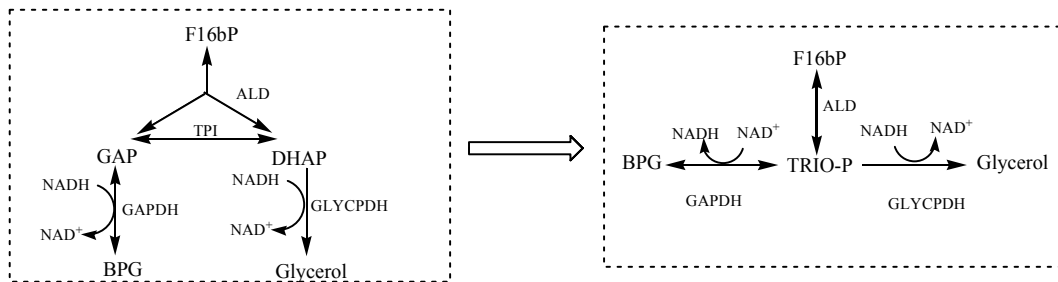


Figure 3.2 Equilibrium block between DHAP and GAP for TPI reaction

In addition to this, adenylate kinase reaction was also modelled as an equilibrium block between ATP, ADP, and AMP. P, sum of high-energy phosphates in adenine

nucleotides, was used as the free variable for the equilibrium block. Solving moiety conservation relation for adenine nucleotides (eqn. 3.5) (Hofmeyr *et al.*, 1986; Teusink *et al.*, 2000), metabolic pool defined for P (eqn. 3.6), and equilibrium equation (eqn. 3.7) for adenylate kinase (AK) reaction gives solution for the concentrations of ATP, ADP, and AMP. So, these relations (eqns 3.7&3.8) for adenine nucleotides were used in the kinetic equations of enzymes where appropriate.

$$[ATP] + [ADP] + [AMP] = sumAXP \quad (3.5)$$

$$P = 2 \cdot [ATP] + [ADP] \quad (3.6)$$

$$K_{eq,AK} = \frac{[AMP] \cdot [ATP]}{[ADP]^2} \quad (3.7)$$

$$ATP = \frac{4 \cdot K_{eq,AK} \cdot P + sumAXP - P + (8 \cdot K_{eq,AK} \cdot P \cdot sumAXP - 4 \cdot K_{eq,AK} \cdot P^2 + sumAXP^2 - 2 \cdot sumAXP \cdot P + P^2)^{\frac{1}{2}}}{2(-1 + 4 \cdot K_{eq,AK})} \quad (3.8)$$

$$ADP = \frac{-4 \cdot K_{eq,AK} \cdot P - sumAXP + P + (8 \cdot K_{eq,AK} \cdot P \cdot sumAXP - 4 \cdot K_{eq,AK} \cdot P^2 + sumAXP^2 - 2 \cdot sumAXP \cdot P + P^2)^{\frac{1}{2}}}{(-1 + 4 \cdot K_{eq,AK})} \quad (3.9)$$

Online version of this model, which is also present in the model database of JWS Online Cellular Systems Modelling (Olivier and Snoep, 2004) and can be run, was used to check the program outputs built in this study. There are some software packages for metabolic modelling like biochemical kinetic simulator GEPASI (Mendes, 1993), metabolic simulator SCAMP (Sauro, 1993), some other programs written in SBML. However, in order to have more flexibility and have more power on model and its variables a program that simulates the model was written in

MATLAB 6.5. It solves the set of ODEs, given in equations 3.10 through 3.23, describing the time dependence of concentrations of metabolites of glycolysis and its branches.

$$\frac{d[Glc_{in}]}{dt} = v_{HXT} - v_{HXK} \quad (3.10)$$

$$\frac{d[G6P]}{dt} = v_{HXK} - v_{PGI} - v_{glycogen} - 2 \cdot v_{trehalose} \quad (3.11)$$

$$\frac{d[F6P]}{dt} = v_{PGI} - v_{PFK} \quad (3.12)$$

$$\frac{d[F16bP]}{dt} = v_{PFK} - v_{ALD} \quad (3.13)$$

$$\frac{d[TRIO-P]}{dt} = 2 \cdot v_{ALD} - v_{GAPDH} - v_{GLYCPDH} \quad (3.14)$$

$$\frac{d[BPG]}{dt} = v_{GAPDH} - v_{PGK} \quad (3.15)$$

$$\frac{d[G3P]}{dt} = v_{PGK} - v_{PGM} \quad (3.16)$$

$$\frac{d[G2P]}{dt} = v_{PGM} - v_{ENO} \quad (3.17)$$

$$\frac{d[PEP]}{dt} = v_{ENO} - v_{PYK} \quad (3.18)$$

$$\frac{d[PYR]}{dt} = v_{PYK} - v_{PDC} \quad (3.19)$$

$$\frac{d[ACE]}{dt} = v_{PDC} - v_{ADH} - 2 \cdot v_{SUCC} \quad (3.20)$$

$$\frac{d[P]}{dt} = -v_{HXK} - v_{PFK} + v_{PGK} + v_{PYK} - v_{ATPase} - v_{glycogen} - v_{trehalose} - 4 \cdot v_{SUCC} \quad (3.21)$$

$$\frac{d[NAD^+]}{dt} = v_{GLYCPDH} - v_{GAPDH} + v_{ADH} - 3 \cdot v_{SUCC} \quad (3.22)$$

$$\frac{d[NADH]}{dt} = v_{GAPDH} - v_{GLYCPDH} - v_{ADH} + 3 \cdot v_{SUCC} \quad (3.23)$$

The program was composed of two parts: one main program containing all necessary information needed to solve the ODEs (i.e. values of all kinetic constants for each enzyme, type of ODEsolver, which is an embedded program in MATLAB to solve ODEs, commands to write the calculated concentrations of metabolites and values of rates to an excel file, relations for the calculation of maximum velocities at different temperatures (see section 3.3.3), etc.) and one sub-program containing ODEs, subfunctions for kinetic equations of enzymes and for equations for the effect of ethanol on activities of enzymes as will be explained in section 3.2. When the main program is executed, ODEsolver calls the sub-program and integrates the differential equations by using kinetic expressions and the constants, interval of integration (time span), initial conditions and the options specified. By solving the ODEs, metabolite concentrations were calculated for every increment and, at intervals specified by the user, the concentrations were written in an excel file automatically. In order to write the values of rates in the excel file, rates are calculated again in the main program using the concentrations calculated by the ODEsolver. See Appendix C for the structure of the program, and see Appendix D for the final version of the program.

The program was executed many times to correct the syntax and logical errors. The errors were recognized by observing abnormal concentration and rate values. Although all errors were corrected, program still output some unexpected results. This problem was overcome by changing the ODEsolver from ODE45 which uses an explicit Runge-Kutta formula, the Dormand-Prince pair, to ODE23s. Solver ODE23s is used for the stiff problems and based on a modified Rosenbrock formula of order 2. In order to test the program, extreme initial concentration values were input to the program. Even when an extreme value for one of the initial conditions for intracellular metabolites was input into the model, steady

state values converged to the same value (Figure 3.3, 3.4). These verified the validity of the program.

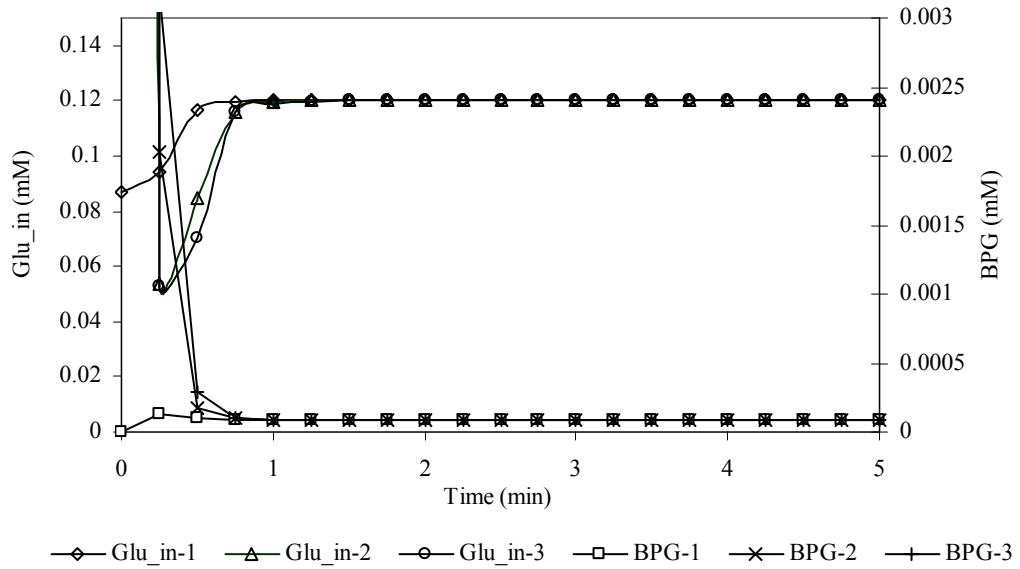


Figure 3.3 Concentration profile of Glc_in and bisphosphoglycerate (BPG) with different initial concentrations $Glc_0=5$ mM (0.087-0, 5-10, 10-10 for Glu_in-BPG pair for 1-2-3 respectively)

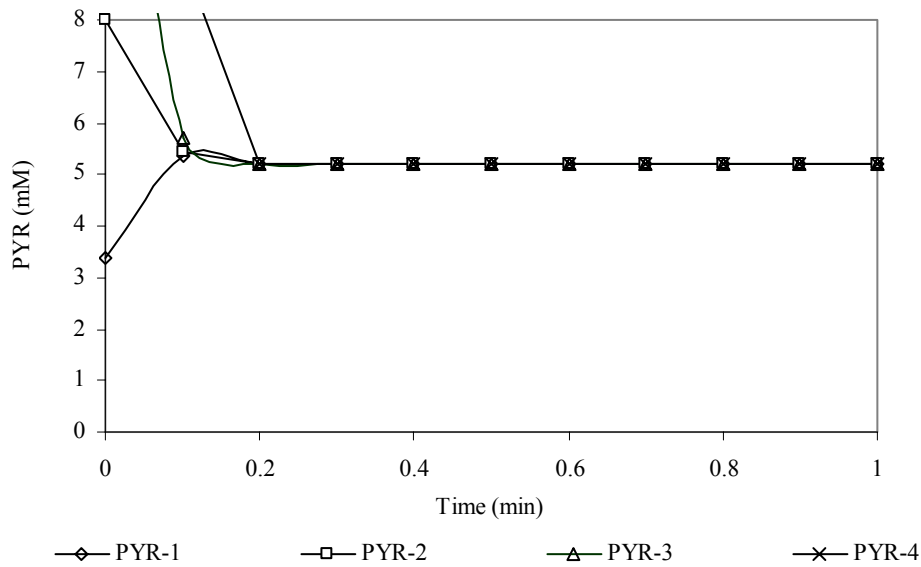


Figure 3.4 Concentration profile of pyruvate (PYR) with different initial concentrations when Glco=5 mM (3.36, 8.0, 15 and 30 mM for PYR-1, 2, 3, 4 respectively)

In this first version of the program concentrations of trehalose, glycogen, succinate, glycerol-3-phosphate, and extracellular glucose and ethanol were kept constant as in the previous work and the program output almost the same steady state values obtained at JWS Online (Table 3.1 and 3.2). Percent differences for fluxes were varied between 1.3 and 1.8%, with the exception of ATPase reaction in which the difference was 16.7%. Higher differences were obtained in intracellular metabolite concentrations, up to 30%. Utilisation of four ATP in the succinate branch was not included in JWSonline version of the model although it was included in the original paper (Teusink *et al.*, 2000). This was the main reason for the differences observed between the results obtained by the program in this study and the ones obtained in JWSonline. In addition to that, different calculation methods used by the programs in solving ODEs could have resulted in such discrepancy.

Table 3.1 Comparison of steady state concentrations measured in the study of Teusink *et al.* (2000) with the ones obtained by the program and JWS Online (extracellular glucose, ethanol, and glycerol concentrations were constant at 50, 50, and 0.15 mM respectively)

Intracellular Metabolite	Concentration (mM)			% Difference
	Experimental^a	from JWS online	from MATLAB version of the model	
Glu_in		0.099	0.12	21.2
Glu-6P	2.45	1.033	0.84	-18.7
F6P	0.62	0.11	0.08	-27.3
F16P	5.51	0.6	0.55	-8.3
TRIO-P		0.796	0.74	-7.0
DHAP	0.81		0.71 ^b	
GAP			0.032 ^b	
BPG		0.00033	0.00023	-30.3
G3P	0.9	0.372	0.32	-14.0
G2P	0.12	0.045	0.04	-11.1
PEP	0.07	0.074	0.059	-20.3
PYR	1.85	8.52	8.11	-4.8
ACE	0.17	0.17	0.17	0
EtOH			50	
GLY3P	0.15		0.15	
Glycerol				
NAD	1.2	1.55	1.55	0
NADH	0.39	0.045	0.045	0
P		6.31	5.7	-9.7

^a data taken from Teusink *et al.*(2000); ^b Calculated from TRIO-P

Table 3.2 Comparison of fluxes obtained by our program and JWS Online (extracellular glucose, ethanol, and glycerol concentrations were constant at 50, 50, and 0.15 mM respectively)

Rates	Flux ($\text{mmol}\cdot\text{L}_{\text{cytosol}}^{-1}\cdot\text{min}^{-1}$)		
	from JWS online	MATLAB version of JWS online model	% Difference
v_{HXT}	88.15	86.81	1.5
v_{HXK}	88.15	86.81	1.5
v_{PGI}	77.35	76.01	1.7
v_{PFK}	77.35	76.01	1.7
v_{ALD}	77.35	76.01	1.7
v_{GAPDH}	136.5	134.07	1.8
v_{PGK}	136.5	134.07	1.8
v_{PGM}	136.5	134.07	1.8
v_{ENO}	136.5	134.07	1.8
v_{PYK}	136.5	134.07	1.8
v_{PDC}	136.5	134.07	1.8
v_{ADH}	129.22	126.89	1.8
v_{GLYCPDH}	18.2	17.95	1.3
v_{glyco}	6	6	0
v_{trehal}	2.4	2.4	0
v_{SUCC}	3.64	3.59	1.3
v_{ATPase}	99.1	82.55	16.7

3.1.1. Changes made from the original Teusink model

Firstly, isomerisation reaction between dihydroxyacetonephosphate (DHAP) and glyceraldehyde-3-phosphate (GAP) catalyzed by triosephosphate isomerase (TPI) was included as reversible Michaelis-Menten in the model (Rizzi *et al.*, 1997;

Hynne *et al.*, 2001), so that DHAP and GAP were both present explicitly. Constants for kinetic equation (equation 3.24) were taken from Rizzi *et al.* (1997).

$$v_{tpi} = \frac{v_{m_{tpi}} \cdot \left(DHAP - \frac{GAP}{K_{eq,tpi}} \right)}{K_{DHAP} \cdot \left(1 + \frac{GAP}{K_{GAP}} \right) + DHAP} \quad (3.24)$$

Secondly, we concentrated on the glycerol branch. Glycerol is formed in two steps: first, the formation of glycerol-3-phosphate (Glyc3P) from DHAP by the action of the glycerol-3-phosphate dehydrogenase (GLYCPDH), and second, subsequent formation of glycerol by the action of glycerol-3-phosphatase (GLYCPASE). In the branched version of the previous model, lumped glycerol branch was included and reversible Michaelis-Menten kinetics was used to describe the branch. Cronwright *et al.* (2002) were modelled the glycerol formation as a two step process: In their study, GLYCPDH activity was simulated by using a reversible two-substrate, two-product rate equation with noncompetitive inhibition (equation 3.25; Figure3.5). Since at physiological concentrations, ATP, ADP, NAD⁺, and F16bP inhibits GLYCPDH activity (Nader *et al.*, 1979; Albertyn *et al.*, 1992; Cronwright *et al.*, 2002), these have been included as modifiers in the equation. Exclusion of these terms decreased the value of the control coefficient from 0.85 (Cronwright *et al.*, 2002) to 0.69 for this enzyme of glycerol branch.

$$v_{glycpdh} = \frac{v_{m_{glycpdh}} \cdot \left(NADH \cdot DHAP - \frac{NAD \cdot Gly3P}{K_{eq,glycpdh}} \right)}{\left(1 + \frac{F16bP}{K_{F16bP}} + \frac{ATP}{K_{ATP}} + \frac{ADP}{K_{ADP}} \right) \cdot \left(1 + \frac{NADH}{K_{NADH}} + \frac{NAD}{K_{NAD}} \right) \cdot \left(1 + \frac{DHAP}{K_{DHAP}} + \frac{Gly3P}{K_{Gly3P}} \right)} \quad (3.25)$$

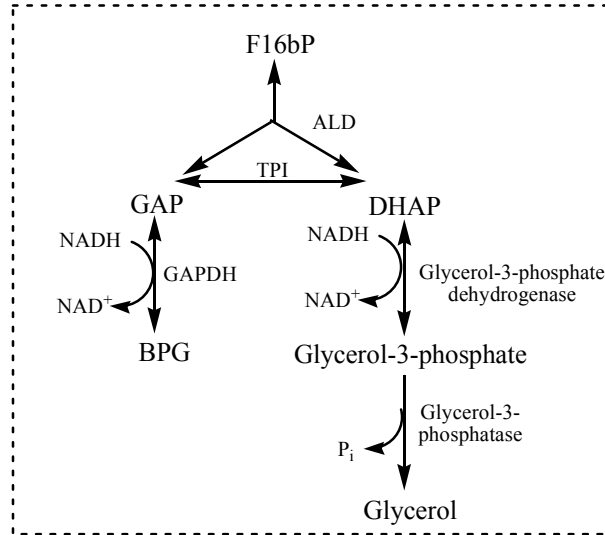


Figure 3.5 Glycerol branch

GLYCPASE activity was simulated by using irreversible noncompetitive inhibition kinetics. The reaction has one substrate and two products, one of which is a modifier (inhibitor). The inhibitor is noncompetitive with the substrate (equation 3.26).

$$v_{glycpase} = \frac{v_{m_{glycpase}} \cdot \left(\frac{Gly3P}{K_{Gly3P}} \right)}{\left(1 + \frac{Gly3P}{K_{Gly3P}} \right) \cdot \left(1 + \frac{P_i}{K_{P_i}} \right)} \quad (3.26)$$

It is known that rate determining step in glycerol branch is the reaction catalyzed by GLYCPDH (Remize *et al.*, 2001; Cronwright *et al.*, 2002). However, since this two step scheme reflects the actual case, and we want to examine each step in detail we also included GLYCPASE reaction beside GLYCPDH in the model.

As a result of changes above, separate ODEs for time dependence relations for Gly3P and for DHAP and GAP instead of TRIO-P (equation 3.14) were included in the set of ODEs (eqns 3.27-3.29).

$$\frac{d[DHAP]}{dt} = v_{ALD} - v_{TPI} - v_{GLYCPDH} \quad (3.27)$$

$$\frac{d[GAP]}{dt} = v_{ALD} - v_{TPI} - v_{GAPDH} \quad (3.28)$$

$$\frac{d[Glyc3P]}{dt} = v_{GLYCPDH} - v_{GLYCPASE} \quad (3.29)$$

As noted before, in the previous work (Teusink *et al.*, 2000) extracellular concentrations of glucose, ethanol, and glycerol were kept constant which condition is only possible in chemostat cultivations. Actually beer, wine and industrial alcohol productions are batch processes; so that alcohol and glycerol concentrations increase while sugar concentration decreases over time. One of the aims of our work is to describe the production rates of ethanol and glycerol and the consumption of extracellular glucose. Therefore, at this point, three more ODEs describing the time dependencies of these metabolites were included (equations 3.30-3.32). One should note that the system for the reactions (glycolysis and its branches) is the biotic phase (cell volume). Thus, the metabolites that are secreted to the liquid medium are diluted by a factor equal to the ratio of the volume of the reactor and total cytosolic cell volume. Similarly, rate of glucose consumption in the reaction volume is slower by this factor than consumption in cell volume. In order to take this into account, the kinetic equations of the reactions for glucose consumption, and glycerol and ethanol production were divided by this factor, the “volume effect” factor. So that extracellular concentrations of these metabolites could be calculated in the actual time scale. The total cell volume was taken as constant that is, the increase in the total cell volume due to growth was not taken into account, since the model describes non-growing conditions. The cell cytosolic

volume was assumed to be 1.67 μl per mg dry yeast weight (about 3.75 μl cytosol per mg protein) (Teusink *et al.*, 2000; Cronwright *et al.*, 2002). Total cell volume thus can be calculated by knowing or assuming the total cell dry weight in the reactor.

$$\frac{d[\text{Glc}_o]}{dt} = -\nu_{HXT} \quad (3.30)$$

$$\frac{d[\text{Glyc}]}{dt} = \nu_{GLYCPASE} \quad (3.31)$$

$$\frac{d[\text{EtOH}]}{dt} = \nu_{ADH} \quad (3.32)$$

In contrary to earlier works (Nagodawithana and Steinkraus, 1976), more recent studies with more accurate analysis results have shown that ethanol does not accumulate within the cell (Guijarro and Lagunas, 1984; Dombek and Ingram, 1986; Dasari *et al.*, 1990). Therefore, intra- and extracellular concentrations of ethanol was assumed to be the same. Similarly, other extracellular metabolite glycerol was also assumed to be equal inside and outside the cell. Most of the *in silico* trials were performed in this way. However, afterwards, transport step for glycerol diffusion was also included in the model as will be explained and discussed later.

At this point, separate ODEs for ATP, ADP, and AMP (equations, 3.33, 3.34, and 3.35 respectively) were added instead of free variable P (equation 3.21). AMP was kept constant, i.e. time dependence is equal to zero, since there were no reaction neither consuming nor producing this metabolite in the model.

$$\frac{d[ATP]}{dt} = -v_{HXX} - v_{glycogen} - v_{trehalose} - v_{PFK} - v_{ATPase} - 4 \cdot v_{SUCC} + v_{PGK} + v_{PYK} \quad (3.33)$$

$$\frac{d[ADP]}{dt} = v_{HXX} + v_{glycogen} + v_{trehalose} + v_{PFK} + v_{ATPase} + 4 \cdot v_{SUCC} - v_{PGK} - v_{PYK} \quad (3.34)$$

$$\frac{d[AMP]}{dt} = 0 \quad (3.35)$$

3.2. Ethanol Effect

While ethanol is seen as a desirable product of the fermentation process, its accumulation during fermentation can result in a significant chemical stress on the physiological status of the yeast cell. Ethanol as a chemical stressor inhibits cell growth and viability, and causes changes in metabolic pathways, increases in fermentation times, changes in yeast cell wall and membrane structure and function, and modifications in gene expression (Lentini *et al.*, 2003).

In the simulations starting with high glucose concentrations, we noticed that ethanol production rate as well as glucose consumption rate did not change throughout unlike the real cases. For example, in wine fermentations, where sugar concentrations are above 20% (w/v), ethanol production decreases gradually especially towards the end of the fermentation.

At the beginning, we theoretically included a “made up” inhibition term to kinetic equations of enzymes (including hexose transport) and noticed that decrease in production/consumption rates became more realistic (see Figure 3.11 for the difference in the patterns of simulations). Therefore, it was decided to work on inhibition effect of ethanol on individual enzymes.

It is a well known fact that ethanol exerts product inhibition; however there is no consensus on the point that this effect is exerted in the yeast cell. The enzymes of

the glycolytic pathway are likely targets however there are counter arguments. The yeast cell ceases to grow long before the glycolytic pathway stops to function; so there must be other point of effect even if glycolytic enzymes are affected by the increasing ethanol concentration. In this work, it was tried to determine experimentally the effect of increasing ethanol concentration on the enzymes of the glycolytic pathway and it was also tried to incorporate this into the kinetic model and tested it for the simulation of the ethanolic fermentation.

There were not many studies about the effect of ethanol on the activities of glycolytic enzymes. Nagodawithana *et al.* (1977) investigated the effect of ethanol on HXK, PFK, ALD, and GLYCPDH of *Saccharomyces uvarum*, formerly *S. carlsbergensis*. There was just one study in which all glycolytic enzymes of bakers' yeast were examined in terms of ethanol inhibition (Millar *et al.*, 1982).

Since, ethanol tolerances of different strains differ, and since there are some discrepancies between the studies mentioned above we decided to examine the effect of ethanol on activities of enzymes of glycolysis and its branches to glycerol and ethanol.

Another point for possible ethanol inhibition is the sugar transport step. Inhibitory effect of ethanol on sugar transporters had been studied by a few authors. In their work with D-xylose (a monosaccharide unmetabolizable by *S. cerevisiae*), Leao and van Uden (1982) showed that affinity of transport system of *S. cerevisiae* for the sugar was not affected by ethanol but the effect appeared to be exclusively on the v_{\max} . They expressed the alkanol effect on glucose transport system as in equation 3.36 where v_{\max}^o is the maximum uptake rate without alkanol, x is the alkanol concentration, and k is the inhibition constant characteristics for the alkanol and 0.616 L mol^{-1} in the case of ethanol.

$$v = v_{\max}^o \cdot e^{-kx} \cdot \frac{S}{K_m + S} \quad (3.36)$$

In their study Pascual *et al.* (1988) found out that glucose transport rate is also inhibited by ethanol in noncompetitive manner. In their paper they did not give the value of inhibition constant, so it was calculated by drawing Lineweaver-Burk plots of their data and found it to be 3.4 M (data not shown). They were reported that up to 2 M (92 g L⁻¹) ethanol, glucose uptake velocity did not change although Leao and van Uden (1982) observed a change even at 40 g L⁻¹ of ethanol.

3.2.1. Effect of Ethanol on Activities of Enzymes

In studying the effect of ethanol on activities of glycolytic enzymes, enzyme assays were carried out by including ethanol at varying concentrations in final assay volume, and rates (or specific activities) were compared with the rates in the absence of ethanol, except ADH assay using ethanol as substrate (see Appendix A for growth curve; see assay details in Chapter 2). In order to avoid any possible activity loss due to excessive incubation of crude extract with ethanol, all reactions were started with the addition of properly diluted crude extracted immediately after the addition of ethanol. When coupling enzyme(s) used in the assay, coupling(s) were increased at the highest ethanol concentration tested and compared with the results obtained with original amounts used. In most of the assays, increasing the amounts of coupling enzymes did not yield in activity increase. Therefore, coupling amounts was not increased for any of the assays except PGK in GAPDH assay and GLYCPDH in TPI assay. Latter two enzymes were doubled to be in the safe side. Pyruvate decarboxylase activity could not be measured by the regular coupled assay (coupling with ADH) since ADH is product inhibited, so stop assay was used instead. For the assay of GAPDH in forward direction, NAD⁺ reduction is followed. Since ethanol and NAD⁺ are substrates for ADH, a background activity was seen in the assay. A specific ADH inhibitor, pyrazole, was incorporated into the assay but the problem could not be solved completely (data not shown). Therefore effect of ethanol on forward activity of GAPDH was not included in the model and effect on reverse activity was used as a whole instead.

For the enzyme assays utilizing NADH, there was a possibility that the ADH in crude extract; might reduce NAD^+ formed, back to NADH during the course of reaction, since ethanol is also its substrate. In that case, observed activity would be lower than the actual value. In order to rule out this possibility, ADH activity was measured with varying concentrations of NAD^+ (Figure 3.6). In all assays, crude extract concentration was adjusted to ensure that NADH oxidation was below 0.016 mM (0.1 absorbance change at 340nm) per minute. Since this amount of NAD^+ was not sufficient for ADH to show profound activity said affect was not likely to occur.

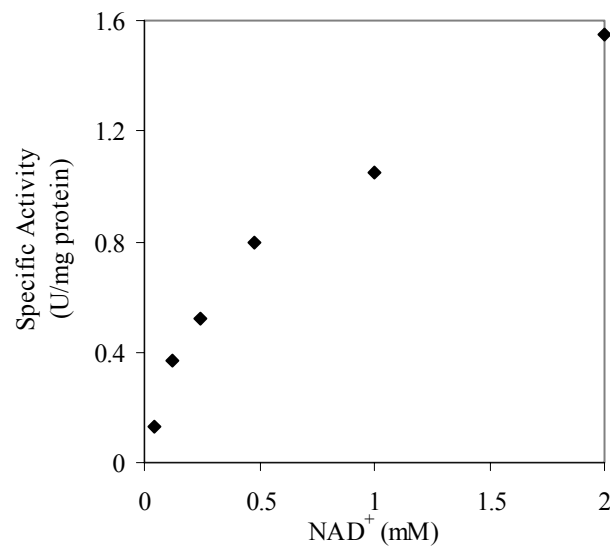
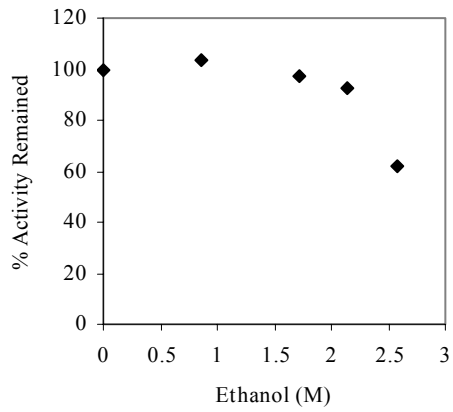
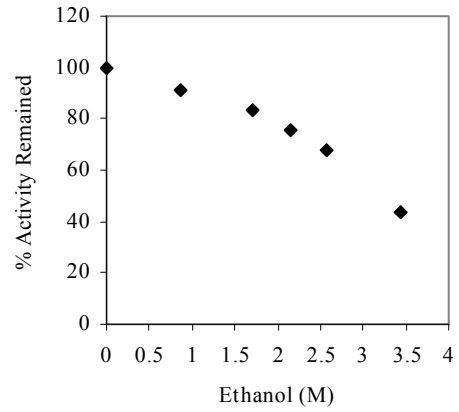
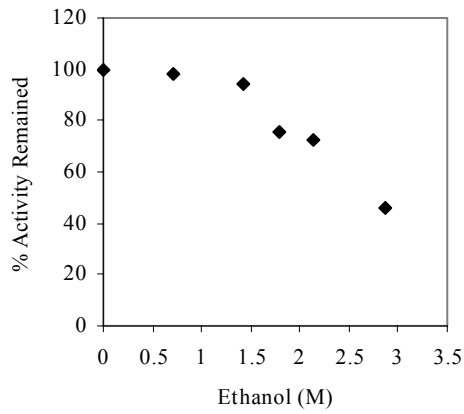
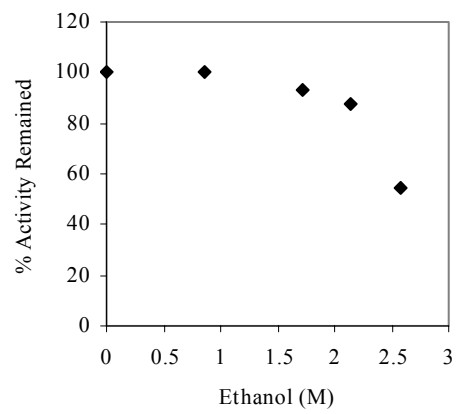
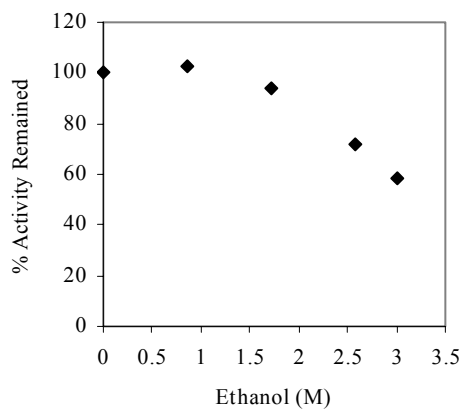
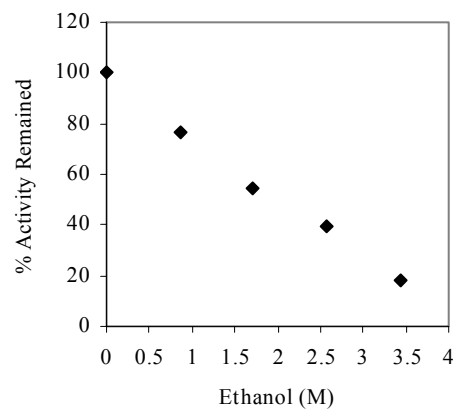


Figure 3.6 Specific activity of ADH (ethanol as substrate) at varying concentrations of NAD^+

Yeasts encounter varying degrees of ethanol during fermentations; among the processes, it encounters relatively higher ethanol concentrations in wine, sake, and industrial ethanol productions. Therefore, the concentration range tested in *in vitro* studies was selected by considering this fact and the assumption that the intra- and

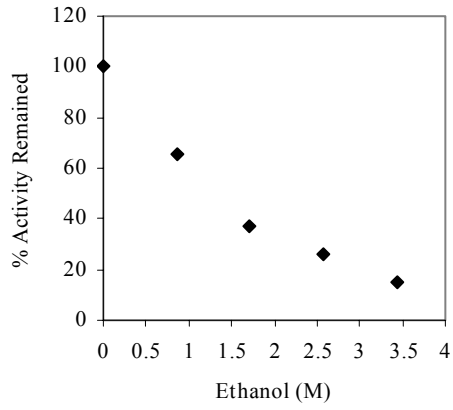
extracellular ethanol concentrations are the same (Guijarro and Lagunas, 1984; Dombek and Ingram, 1986; Dasari *et al.*, 1990). Effect of ethanol was tested in the range of 0 to 20% (v/v) (0 to 158 g/L). All enzymes were inhibited by ethanol to some degree and these inhibitions started at different ethanol concentrations (Figure 3.7). Two different trends could be generalized. HXK, PFK, ALD, TPI, PYK, and ADH (reverse) falls within the first group, in which little effect was observed at relatively low ethanol concentrations, i.e. up to 10% (v/v) ethanol, and effect was more profound at higher ethanol concentrations with varying degrees for each enzyme. The so called “key” glycolytic enzymes, HXK, PFK, and PYK, fall within this group. The second group, in which gradual decrease in activity was observed with increasing concentrations of ethanol, includes PGI, GLYCPDH, GAPDH, PGK, PGM, ENO, PDC, and ADH (forward). Among the enzymes of the second group, PGI, PGM, ENO, and PDC were less sensitive than others. Within all enzymes studied, the least affected enzyme by increasing ethanol concentration (within the range tested) was PYK. The most significant inhibitions were of GLYCPDH, GAPDH, PGK, and as expected ADH (forward).

One of the possible mechanisms for the inhibition enzyme activities with ethanol is the reduction of water activity (Hallsworth, 1998). Proteins are susceptible to hydrogen bond disruption due to the bound water. Protein conformation changes as a result of displacement of this water. Fifteen percent of ethanol (v/v) reduces water activity to about 0.94 and 20% (v/v) to about 0.92 (Hallsworth, 1998). Therefore, it is possible that the activities of enzymes may have been influenced due to this effect on conformation.

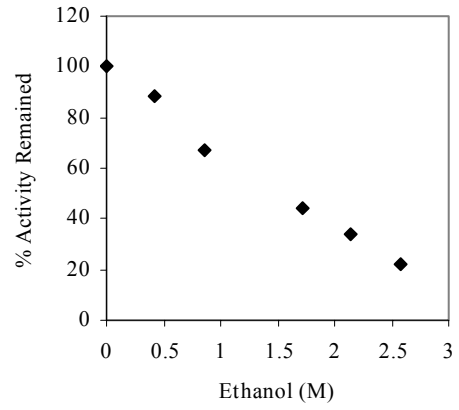
H XK**P GI****P FK****A LD****T PI****G LYCPDH**

Continued on next page

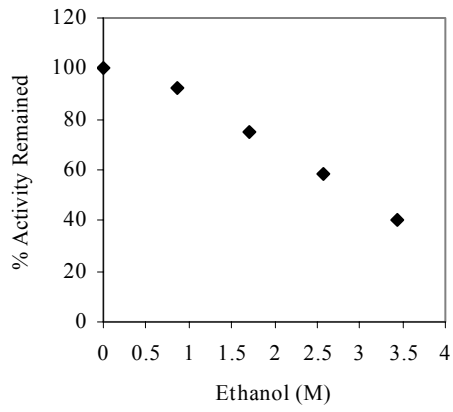
GAPDH



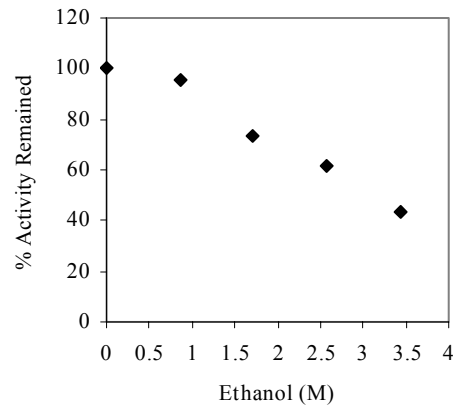
PGK



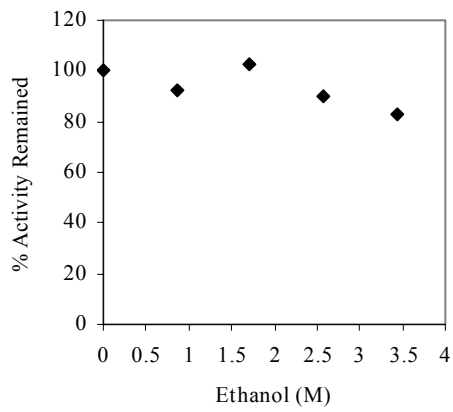
PGM



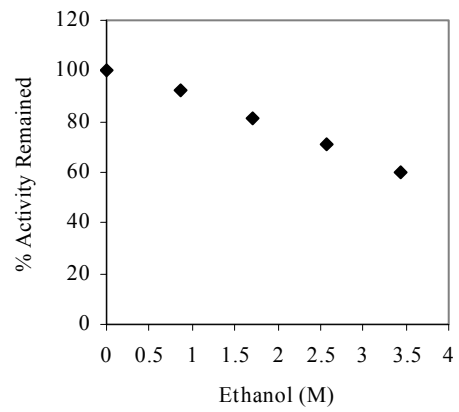
ENO



PYK



PDC



Continued on next page

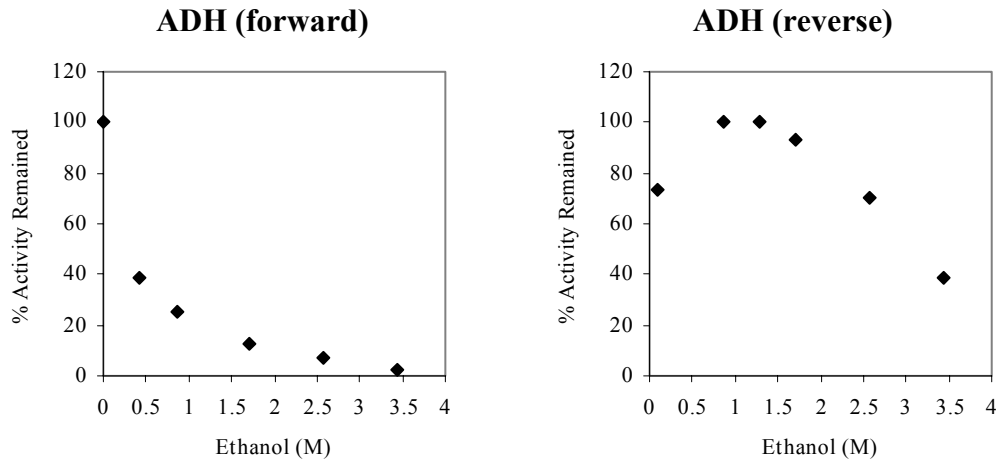


Figure 3.7 Inhibition patterns of enzymes with ethanol

Another possible effect would be the ethanol acting as “inhibitor molecule” in classical sense, that is, ethanol acting as competitive or non-competitive inhibitor. Millar *et al.* (1982) suggested two sorts of inhibition: one is competitive type in which ethanol binds to active site and inhibits substrate binding, and the second non-competitive type in which ethanol binds to another site on an enzyme surface other than the active site. They expected the competitive effects to be gradual and express themselves in a hyperbolic decay, and little effect observed at low ethanol concentrations for non-competitive type. In this sense, GLYCPDH, GAPDH, PGK, PDC, and ADH (reverse) would fall within former group and HXK, PGI, PFK, ALD, TPI, PGM, ENO, PYK, and ADH (reverse) within the latter one. For example, more detailed analysis of inhibition of HXK by ethanol revealed that it is inhibited noncompetitively (Nagodawithana *et al.*, 1977; Millar *et al.*, 1982). Similarly for the GLYCPDH, non-competitive type inhibition was observed which was tested only with one inhibitor concentration (15% (v/v) ethanol) (Nagodawithana *et al.*, 1977). However, for other enzymes, further analysis is needed to be sure whether the inhibition is of the type competitive or non-competitive.

There were two contradictory reports on the effect of ethanol on HXK. In the first one, HXK was inhibited even at 5% (v/v) ethanol, although slightly, and even higher inhibition was observed at 10% (v/v), activity decreased almost to 75% (Nagodawithana *et al.*, 1977). Activity was not affected up to 15% (v/v) ethanol in the second report (Millar *et al.*, 1982). In spite of the different inhibition patterns in these two studies, they both found inhibition of non-competitive type as noted above. Although trend observed in our study was almost the same with the second report i.e. almost no inhibition was detected up to 12.5% (v/v) ethanol, activity was decreased to about 60% at 15% (v/v) of ethanol.

Aldolase activity decreased sharply to 55% of its original activity at 15% (v/v) of ethanol unlike the studies mentioned above (Nagodawithana *et al.*, 1977; Millar *et al.*, 1982), in which activity was not affected at all till the point of rapid denaturation (concentration was not reported) (Millar *et al.*, 1982). Although Nagodawithana *et al.* (1977) reported that PFK activity was not inhibited by 15% ethanol, Millar *et al.* (1982) observed a reduction in activity at this concentration, as in our case. Trend and values obtained in our study was almost the same with the one obtained in latter work. GLYCPDH was significantly inhibited even at 5% (v/v) ethanol. The only article reporting the inhibition of GLYCPDH (Nagodawithana *et al.*, 1977) did not contain practical numerical value to compare.

The most profound difference between this work and the work of Millar *et al.* (1982) was on the GAPDH activity. Considerable decline in activity was practiced in this study even at 5% (v/v) ethanol, while moderate decrease was seen even at 10% ethanol in the previous report.

For the other enzymes, similar trends were obtained with previous work (Millar *et al.*, 1982). However, inhibitions were started with lower concentrations of ethanol for PGI, TPI, PGK, and PYK and lesser inhibition was observed with ENO and PDC.

The previous work (Millar *et al.*, 1982) investigated the effect of ethanol on purified enzymes of bakers' yeast at 20°C either in conditions which give optimum activity, or at pH 6.5. However, in this study, all enzyme assays were performed at 30°C and pH 7.0 and conditions were not adjusted to favor optimum conditions, instead same conditions were used for all enzymes. Therefore, these and the different yeast strain (brewers' yeast) used in this study could account for the above differences observed with the previous study.

3.2.2. Effect of Ethanol on Fermentation Kinetics

It has been known that ethanol accumulation through the fermentation causes premature inhibition of fermentation (Ingram and Buttke, 1984; Casey and Ingledew, 1986). This effect on brewers' yeast was tested in the presence of different amounts of initial ethanol. Cells were pre-grown in YPD containing 5% (w/v) glucose and harvested in exponential phase. Glucose concentration in the medium was 1.5-2% at the time of harvest. These cells were suspended in 100 mM phosphate buffer at pH 6.5, containing 20 g glucose L⁻¹, at a final concentration of 11 g dry weight L⁻¹ in screw capped bottle. After equilibrating the temperature to 30 °C, fermentation was started by the addition of ethanol and glucose in static incubator. This experimental design ensured observing the effect in short time (70 min) under non-growing conditions for the yeast. Performing the experiments in this way reduced the complexity of the system so that yeast possibly depended mainly on glycolysis and its branches to ethanol, glycerol, and reserve carbohydrates. Initial ethanol concentration was either 0, 5, 10, or 15% (v/v). Comparison of glucose consumption and glycerol and ethanol production are shown in Figure 3.8.

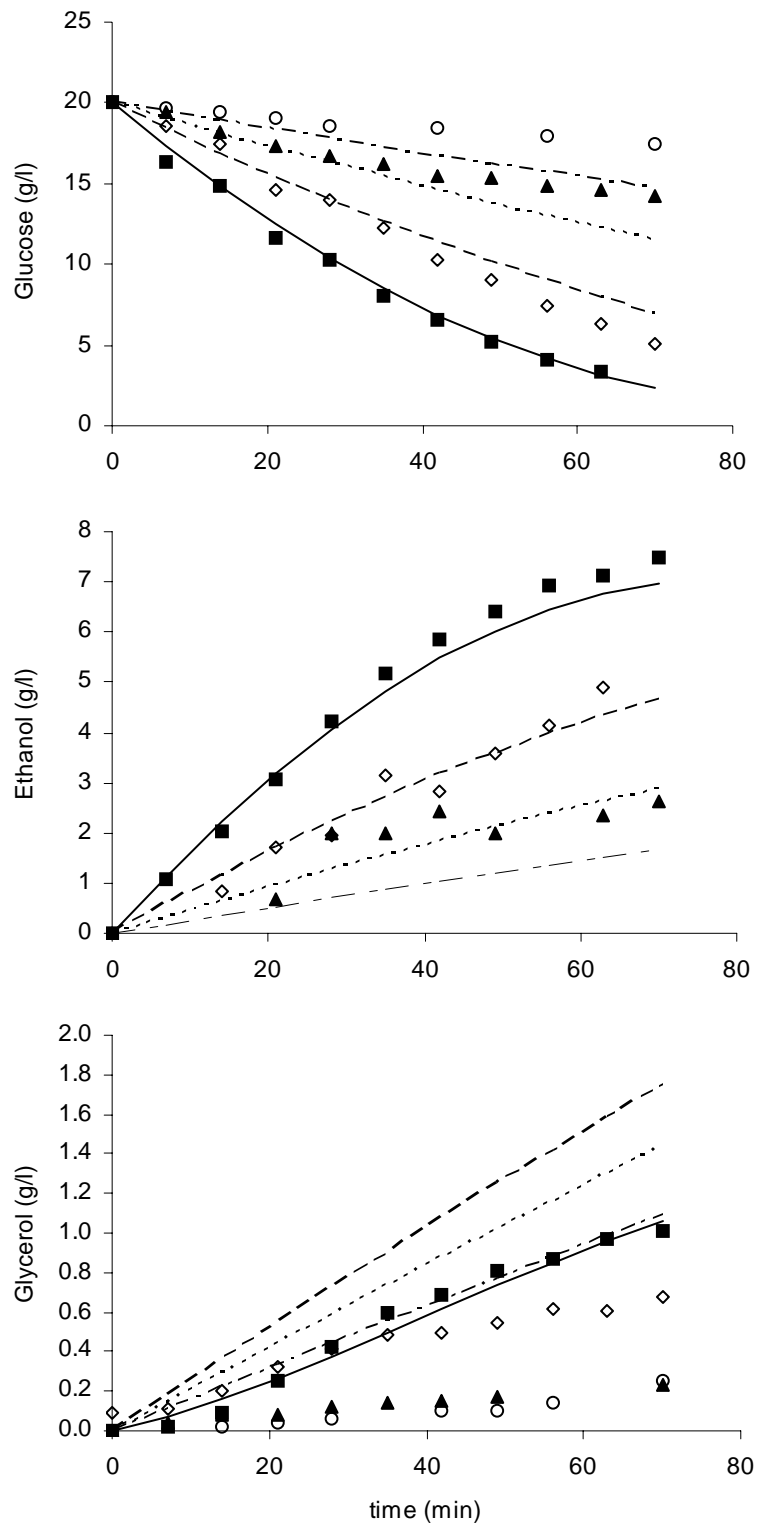


Figure 3.8 Effect of initial extracellular ethanol concentration on glucose consumption (top) and ethanol (middle) and glycerol (bottom) productions Lines represent the model simulation. no ethanol: ■, — ; 5% ethanol: ◇, --- ; 10% ethanol: ▲, -.-.-; 15% ethanol: ○, -.-.- (v/v).

In all cases, glucose consumption and ethanol production started as soon as glucose was added to the cell suspension, that is, no lag was observed. The time elapsed since the cells were harvested from YPD medium, including the centrifugation and washing steps and temperature equilibration, did not result in an activity loss of the cells. Without initial ethanol, about 17 g L⁻¹ glucose was consumed with concomitant production of 7.5 g L⁻¹ ethanol and about 1 g L⁻¹ glycerol within 70 min. Through the end of fermentation, small decline in consumption and production rates were observed. With the increasing initial concentrations of ethanol, consumption and production rates were decreased. At higher starting ethanol concentrations (10 and 15 %), since the produced ethanol was quite smaller than the initial amount HPLC analysis were not very reliable. High fluctuations were observed in the ethanol data; data for 15% starting ethanol was not even included in the figure. Incorporation of 5% ethanol to the fermentation medium resulted in a relatively smaller decrease in rates as compared to 10 and 15%. The effect was drastic at higher concentrations. Less than 6 and 3 g L⁻¹ of glucose were consumed in 10 and 15%, respectively. Rates were influenced by the initial ethanol concentrations almost linearly (Figure 3.9). Linear relation was shown between the fermentative ability and the concentration of ethanol in yeast by several authors (as reviewed in (Casey and Ingledew, 1986)). Inhibition of fermentative ability can be attributed to inhibition of the enzymes and the transport of sugars, besides other factors like the inhibition of growth, which is not considered in the scope of this study (See Section 1.5.1).

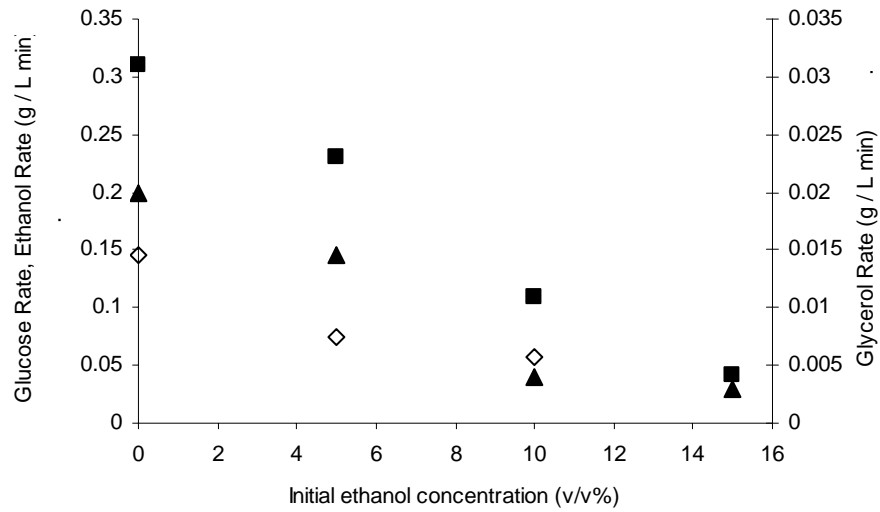


Figure 3.9 Inhibition of glucose consumption (■) and, ethanol (◇) and glycerol (▲) production rates by ethanol

3.2.3. Model Studies Incorporating the Effect of Ethanol

Using the data obtained for the changes in the *in vitro* activities of enzymes with increasing ethanol concentrations, equation for each enzyme was fitted by the non-linear least squares method by using curve fitting tool of MATLAB. Equations were in the form of equation 3.37 (Table 3.3; see Appendix E for samples of fits) where *residual_activity* was defined as the relative activity compared to the activity observed without ethanol.

$$residual_activity = a - b \cdot e^{c \cdot [EtOH]} \quad (3.37)$$

Kinetic equation for each respective enzyme is multiplied by this factor, which is calculated for the ethanol concentration in the cell volume at every time points. Ethanol inhibition of transporters was included either as an exponential term as

explained before (Leao and van Uden, 1982) or as non-competitive inhibition term as in equation 3.38 where v_{\max}^{app} is the maximum uptake rate observed with ethanol and v_{\max}^o is that without ethanol, and $K_{i,EtOH}$ is the inhibition constant calculated from Pascual *et al.* (1987). Possible effect of ethanol on glycogen, trehalose, and succinate branches were assumed to be the same with the effect on HXT and that for the GLYCPASE with the effect on GLYCPDH. For in silico calculations of intra- and extracellular metabolites, ATP, ADP, and AMP concentrations were assumed to be constant at 2.52, 1.32, and 0.25 mM respectively as measured in Teusink *et al.* (2000).

$$v_{\max}^{app} = \frac{v_{\max}^o}{\left(1 + \frac{[EtOH]}{K_{i,EtOH}}\right)} \quad (3.38)$$

In order to compare the fermentations performed with different amounts of initial ethanol with computer simulations, program was executed with the v_{\max} values obtained in this study (Table 3.4). Specific activities of enzymes obtained at 30°C were assumed to be the maximum velocities of corresponding enzymes since the saturating conditions were used in the assays for most of the enzymes. For glucose uptake step, kinetics of low affinity system was used in simulations for our fermentation experiments, because 1.5-2% (w/v) glucose remained in the pre-growth medium at the time of harvest of cells, which were then resuspended in buffer containing 2% (w/v) glucose. There are two uptake systems expressed in *S. cerevisiae* : a constitutive low affinity system with high K_m values and a glucose repressed high affinity system (Walsh *et al.*, 1994; Teusink *et al.*, 1998; Özcan and Johnston, 1999). High glucose concentrations used in our systems should have repressed the high affinity system. While running the program, K_m of 55 mM for intra- and extracellular glucose and v_{\max} of 163.7 mmol $L_{\text{cyt}}^{-1} \text{min}^{-1}$ (Teusink *et al.*, 1998) was used.

Table 3.3 Values of parameters fitted for effect of ethanol on enzyme activities
(equation of the type $a - b \cdot e^{c[EtOH]}$)

Enzyme	a	b	c
HXK	1.0	33.29 x 10 ⁻⁶	36.29 x 10 ⁻⁴
PGI	1.16	15.97 x 10 ⁻²	43.65 x 10 ⁻⁵
PFK	1.06	57.63 x 10 ⁻³	82.93 x 10 ⁻⁵
ALD	1.0	32.03 x 10 ⁻⁵	28.19 x 10 ⁻⁴
TPI	1.01	10.78 x 10 ⁻³	12.33 x 10 ⁻⁴
GAPDH	0	-1.0	-53.65 x 10 ⁻⁵
PGK	0	-1.0	-48.57 x 10 ⁻⁵
PGM	1.33	33.23 x 10 ⁻²	30.25 x 10 ⁻⁵
ENO	1.3	30.1 x 10 ⁻²	31.21 x 10 ⁻⁵
PYK	1.02	19.27 x 10 ⁻³	66.64 x 10 ⁻⁵
PDC	1.997	1.0	99.2 x 10 ⁻⁶
ADH (forward)	0	-1.0	-14.29 x 10 ⁻⁴
ADH (reverse)	1.02	17.39 x 10 ⁻³	10.52 x 10 ⁻⁴
GLYCPDH	0	-1.0	-38.5 x 10 ⁻⁵

Table 3.4 Specific activities (v_{\max}) determined in *in vitro* assays and used in the model

ENZYMES	Specific Activity (U mgprotein⁻¹)	Specific Activity (mmol Lcyt⁻¹ min⁻¹)
HXK	1.7	452
PFK	0.69	184
ALD	1.26	334.7
TPI	25.87	6898.1
GAPDH (forward)	0.92	245.3
GAPDH (reverse)	6.3	1681.3
PGK	5.86	1561.3
PGM	9.99	2664
ENO	1.88	502.7
PYK	1.54	409.6
PDC	1.1	293.3
ADH (forward)	7.05	1880
ADH (reverse)	2.1	560
GLYCPDH	0.16	41.6

The v_{\max} values that we measured in *in vitro* enzyme assays were generally successful to simulate extracellular substrate and product concentrations while giving reasonable intracellular metabolite concentrations. The only modifications needed were for GAPDH and GLYCPDH steps. GAPDH capacity should be increased in order to avoid excessive accumulation of F16bP and DHAP. This may

be due to possible non-saturating condition used in terms of substrate GAP in assaying the forward reaction or loss of activity of this enzyme during the extraction of proteins from cells, i.e. extraction efficiency which is also important for all enzymes tested. Extend of modification depended on the modification made in GLYCPDH step. Initially model contained the kinetics adapted from Cronwright *et al.* (2002) for GLYCPDH since it takes all effectors of the enzyme (including F16bP, ATP, and ADP) into account. However, significantly lower glycerol production was obtained when this equation was used, due to the inhibitory effect of these metabolites on the enzyme. When this equation was used, GAPDH capacity should have been increased 3 times while that of GLYCPDH at least 1.6 times. Even with this amount of increase, model could not simulate the extracellular glycerol obtained in the fermentation. Further increase in capacity of GLYCPDH was needed to catch up with the level of glycerol produced. Afterwards, simulation trials were conducted with kinetic equation in which F16bP, ATP, and ADP were not effectors anymore. In that case, result for glycerol production was closer to real case (Figure 3.8) with 2 fold increase in GAPDH activity. . Need for such increases in activities of enzymes may be related with the extraction efficiency of enzymes and actual conditions in cytosol.

At first, the ethanol effect on enzymes determined in *in vitro* assays was applied to all steps of glycolysis and branches including the hexose transport step. When the noncompetitive effect type was applied on transporter (equation 3.38) with an inhibition constant calculated from the data of Pascual *et al.* (1987), the model was unable to simulate that much decrease in rates with increasing initial ethanol concentration obtained experimentally (data not shown). Therefore, it was decided to continue with exponential type inhibition effect (Leao and van Uden, 1982). *In silico* test results are given in Figure 3.8 as lines. Secondly, the effect was applied only to transport step regarding the discussions about the hexose transport step controlling the glycolytic flux (Teusink *et al.*, 1998; Diderich *et al.*, 1999; Reijenga *et al.*, 2001; Elbing *et al.*, 2004). There was no difference in extracellular metabolite concentrations without initial ethanol in these two sets of simulations, i.e. lines of concentrations coincided for two sets of simulations in Figure 3.10-A.

At higher initial ethanol concentrations, similarly, there was no difference between glucose profiles obtained *in silico* and slight difference between ethanol ones (Figure 3.10-B, at 15% ethanol difference between two sets of simulations were the highest (at most 14%)). Discrepancy in glycerol concentration was larger; about 30% when simulated with 15% initial ethanol, and 24% when simulated with 10% initial ethanol. Then, in order to examine same thing in fermentation with high glucose concentration, program was run for 1 M of glucose concentration for above mentioned two sets (Figure 3.11). In this case, there was also no difference between the simulations with inhibitory ethanol effect on all steps and with just on HXT, even between glycerol profiles. From these observations, it can be concluded that, ethanol inhibition of hexose transport was sufficient for the observed decrease in the glycolytic flux, which may in turn support the idea that the hexose transport step is the rate limiting step of glycolysis. Glucose transport has often been considered as an important step in determining the rate of glycolysis in yeast (Bisson *et al.*, 1993; Diderich *et al.*, 1999). *S. cerevisiae* mutant showing transport capacity of 9% of that of wild type did not produce ethanol in batch culture (Elbing *et al.*, 2004). Diderich *et al.* (1999) concluded that the high proportion of the control of the glycolytic flux resided in the glucose transport step in de-repressed *S. bayanus*. When intracellular glucose levels were negligible, transport step is not influenced by the rest of the metabolism thus may control flux completely. This may be the case for the low affinity transport where the intracellular concentration is lower than the affinity of the transporter (Teusink *et al.*, 1998). Intracellular glucose measured in repressed cells (i.e. low affinity transport) was lower than the low affinity K_m , thus should not inhibit the transport. Whereas, in de-repressed cells, intracellular levels were high enough (as high as K_m) to inhibit the transport rate by 50% so that they may not control the flux through glycolysis, in which case the high intracellular glucose levels should be the result of the metabolic signals arisen from other steps (Teusink *et al.*, 1998).

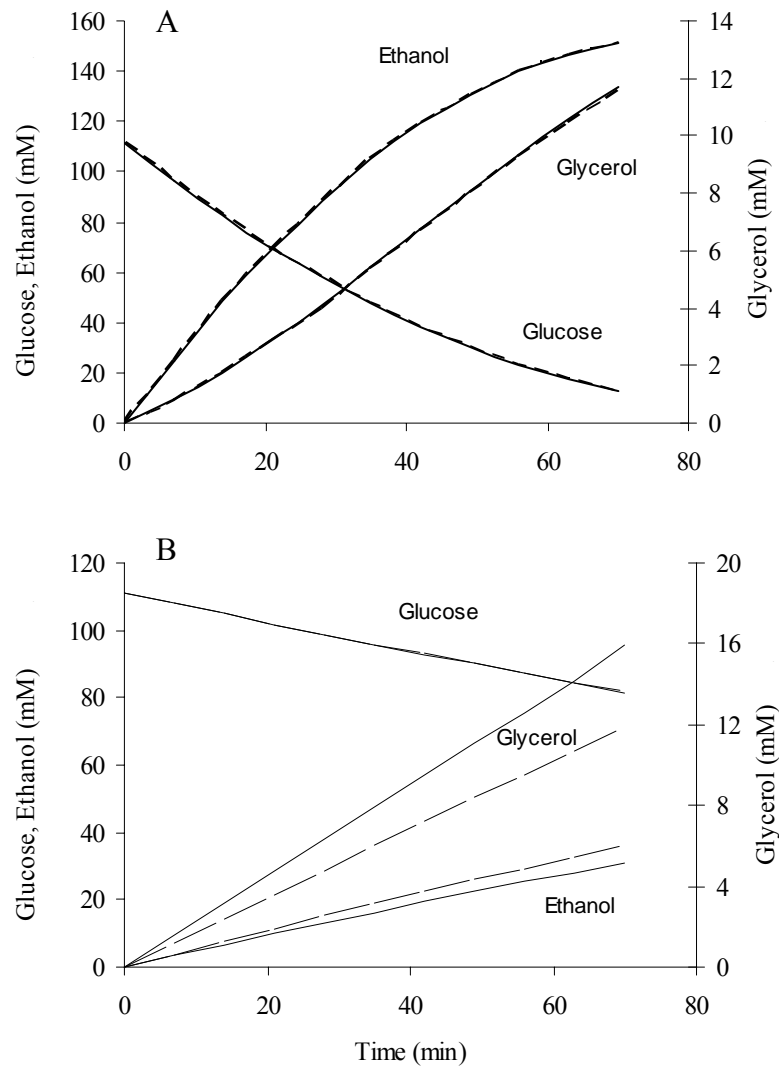


Figure 3.10 *In silico* concentration profiles of extracellular glucose, ethanol and glycerol obtained with no initial ethanol (A) and with 15% initial ethanol (B): inhibition effect of ethanol included just for hexose transport step, — ; inhibition effect of ethanol included for all steps, ---

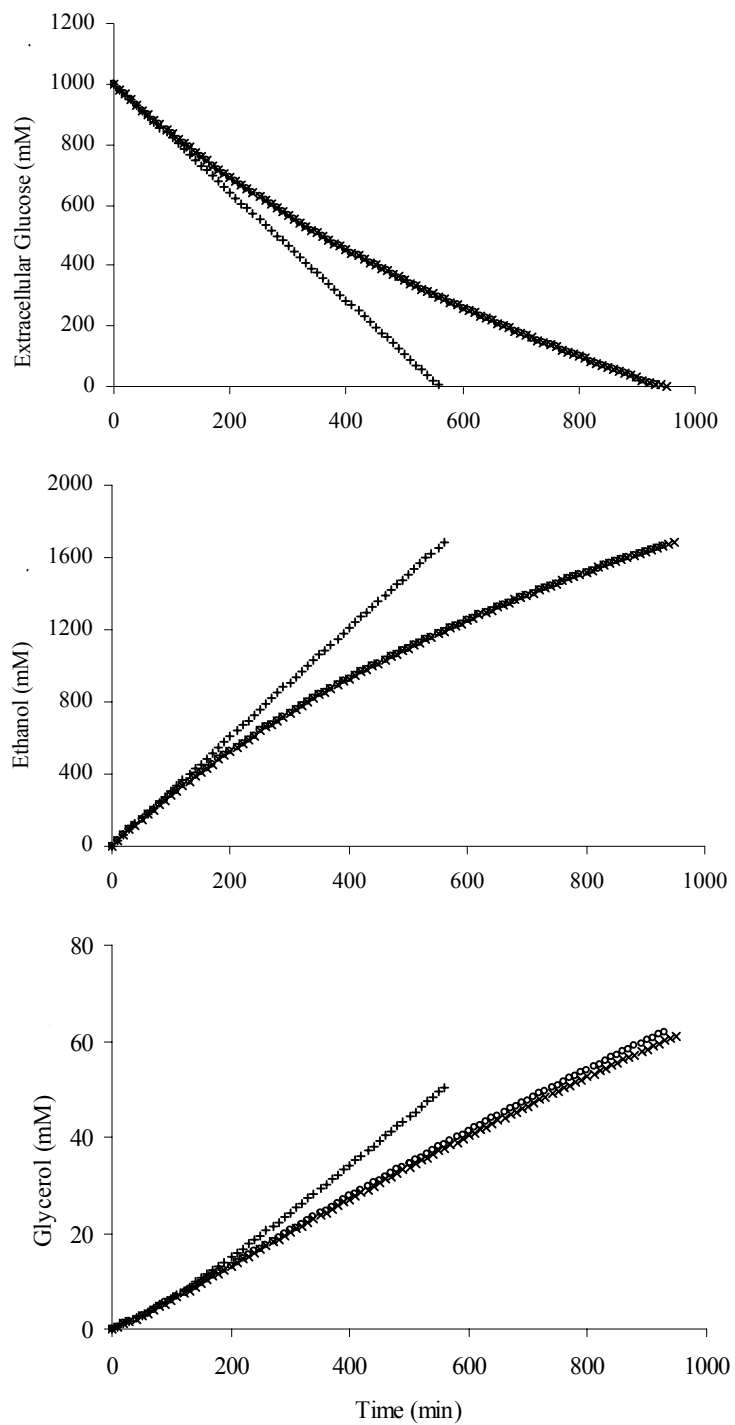


Figure 3.11 *In silico* concentration profiles of extracellular glucose, ethanol and glycerol obtained: without ethanol inhibition effect (+), with inhibition effect of ethanol just on hexose transport step (o), and on all steps (x).

There were two modeling works we met in the literature using inhibition effect of ethanol on transport step. The first one is a structured, nonsegregated model of *S. cerevisiae* (Steinmeyer and Shuler, 1989) and the second one modeled sugar uptake kinetics coupling with stoichiometric model (Pizarro *et al.*, 2007). However, they both adjusted the inhibition parameters for ethanol to fit the experimental fermentation data and do not concentrate on kinetics of individual enzymatic reactions occurring within the cell.

Our model failed to simulate the reduced glycerol production rate, observed with the addition of ethanol initially. In short term fermentative ability experiments, increasing the initial ethanol resulted in decreased amount of glycerol as it is obvious from the lower glucose consumption. However, in computer experiments with high initial concentrations of ethanol (5, 10, or 15%), considerably higher amount of glycerol production were estimated as compared to experimental observations (Figure 3.8). Amounts in these tests were even higher than the simulations without initial ethanol. *In silico*, lower yields of ethanol in high ethanol tests accompanied with higher glycerol yields, which makes sense stoichiometrically and in terms of redox balance. Because, lower ethanol production due to the inhibition of ADH by ethanol directed the flux through glycerol production, as long as the proportions of fluxes through other branches remained the same. Also, excess of NADH had to be reoxidized by another route, in this case by glycerol production, resulting in increased yield of glycerol. Physiologically cells may respond the ethanol stress through increased production of trehalose or glycerol accumulation, which were not considered in the model till this observation. These responses may have decreased the extracellular amount of glycerol as observed in fermentations in this study. Glycerol is exported out of the plasma membrane by passive diffusion or through the protein channel, Fps1p, by facilitated diffusion (Nevoigt and Stahl, 1997; Remize *et al.*, 2001). It has been known that the glycerol is accumulated inside the cell during osmotic stress (Blomberg and Adler, 1989; Andre *et al.*, 1991; Nevoigt and Stahl, 1997); very high intracellular glycerol concentrations were reported (Albertyn *et al.*, 1992; Wojda *et al.*, 2003; Ferreira *et al.*, 2005). Yeast cells accumulate glycerol, proline,

and trehalose under water stress to protect structure and function of hydrated cell component (Hallsworth, 1998). The osmoprotectants glycerol and erythritol protect against ethanol-induced water stress in *Aspergillus nidulans* (Hallsworth *et al.*, 2003). Alexandre *et al.* (2001) observed that the mRNA levels of genes involved in glycerol synthesis and catabolism increased upon addition of 7% ethanol to exponentially growing *S. cerevisiae* in 30 min. However, Kaino and Takagi (Kaino and Takagi, 2008) did not observe any intracellular glycerol accumulation in *S. cerevisiae* upon exposure to 9% of ethanol, whereas when yeast cells were exposed to 1 M sorbitol stress, the expression of GPD1 encoding glycerol-3-phosphate dehydrogenase was induced, leading to glycerol accumulation. In order to include such possibility of glycerol accumulation, glycerol transport step (equation 3.39) with concomitant re-design of related ODEs (equations 3.40-41) was inserted in to the model.

$$v_{glyc-trans} = k_{glyc-trans} \cdot (Glyc_{in} - Glyc_{ex}) \quad (3.39)$$

$$\frac{d[Glyc_{in}]}{dt} = v_{GLYPASE} - v_{glyc-trans} \quad (3.40)$$

$$\frac{d[Glyc_{ex}]}{dt} = v_{glyc-trans} \quad (3.41)$$

where $k_{glyc-trans}$ is the rate constant for glycerol transport and was taken as 1.9 min^{-1} for non-stressed conditions (Bosch *et al.*, 2008). In order to obtain the glycerol amount achieved at the end of 70 min of incubation, this constant should be reduced to 0.02 min^{-1} . When the program was run with this constant for 5-10-15% ethanol, less extracellular glycerol was calculated than no initial ethanol case. However, results were still far from simulating the experimental results for glycerol production with increasing ethanol concentration (Figure 3.12).

Another important protectant against water stress is the disaccharide trehalose. It was suggested by Sharma (Sharma, 1997) that the increased tolerance to ethanol stress of cells grown under hyper-saline conditions was because of the increased trehalose content of these cells. Also, Kaino and Takagi (Kaino and Takagi, 2008) observed almost ten fold increase in trehalose content within one hour when cells were exposed to 9% ethanol. Ethanol stress induced genes involved in both trehalose synthesis and degradation, which may allow the yeast to adjust trehalose content rapidly (Alexandre *et al.*, 2001). When the program was run with 10 times increased production rate of trehalose, although the amount of glycerol produced decreased, results were still far from simulating the experimental results with even worse simulation of ethanol production. Gradual increase in trehalose production and/or in intracellular glycerol accumulation could be one of the possible approaches to solve the problem.

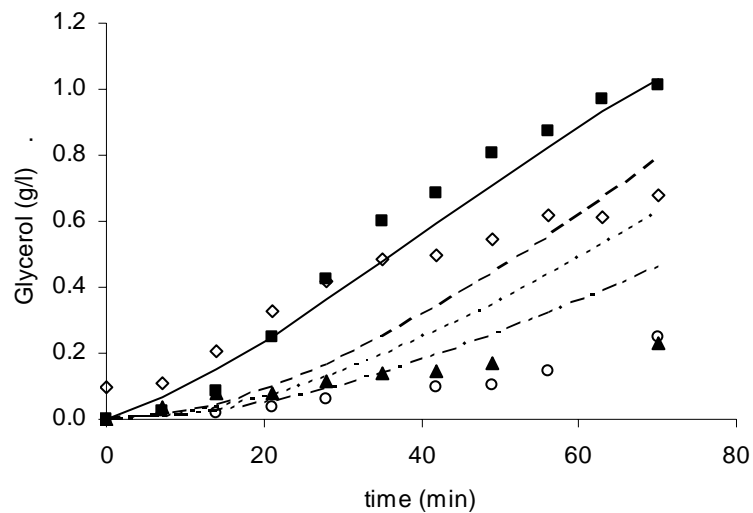


Figure 3.12 Comparison of experimental glycerol production with simulations obtained by inclusion of glycerol transport step as explained in the text. Lines represent the model simulation. no ethanol: ■, — ; 5% ethanol: ◇, - - - ; 10% ethanol: ▲, - ; 15% ethanol: ○, - (v/v)

3.3. Temperature effect

Temperature influences the structural and functional properties of cellular systems, both at physical and chemical level. Alterations occurred in kinetic properties of enzymes with the culture temperature is among the latter effect. Rates of enzyme reactions increases with increasing temperature up to a point where protein denaturation starts. This effect on the rates of reactions can partially be explained by Arrhenius relation for kinetic rate constant (equation 3.42).

$$k_{cat} = A \cdot e^{\left(\frac{-E_a}{R \cdot T}\right)} \quad (3.42)$$

where k_{cat} is the rate constant, A is the pre-exponential constant, also known as the frequency factor, T is the absolute temperature, E_a is the activation energy in J mol^{-1} , and R is the universal gas constant and is equal to $8.314 \text{ J K}^{-1} \text{ mol}^{-1}$.

3.3.1. Effect of Temperature on Activities of Enzymes

To incorporate relations for the change in reaction rates of enzymes included in the model with culture temperature, enzyme assays were conducted at different temperatures (10 to 35°C with 5°C increments). Crude extracts to be assayed were obtained from biomass collected from the culture carried out at 30°C. I focused on the direct effect of temperature on reaction rates and in the context of this study temperature induced effects at the level of transcription, protein turnover, and post-translational modifications during the course of fermentation was not taken into consideration. The effect of temperature on enzyme kinetics was assumed to be related with the overall capacity of an enzyme, that is, overall change in enzyme

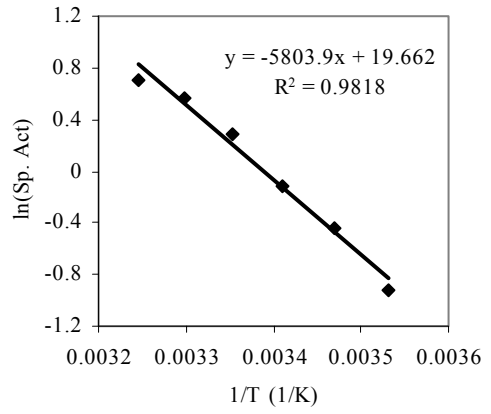
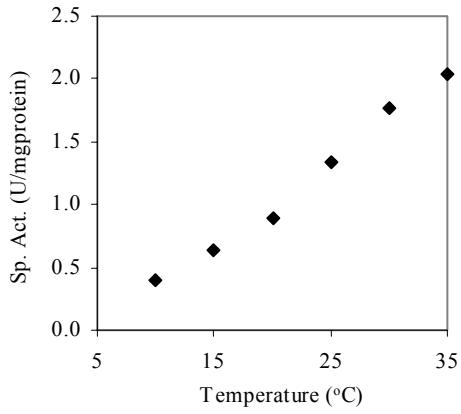
activity by a factor calculated by Arrhenius relation. Thus, rearranging equation 3.42 yields;

$$\ln sp.act. = \ln A - \frac{E_a}{R} \cdot \frac{1}{T} \quad (3.43)$$

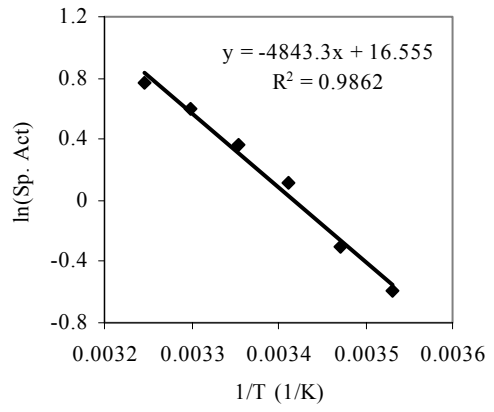
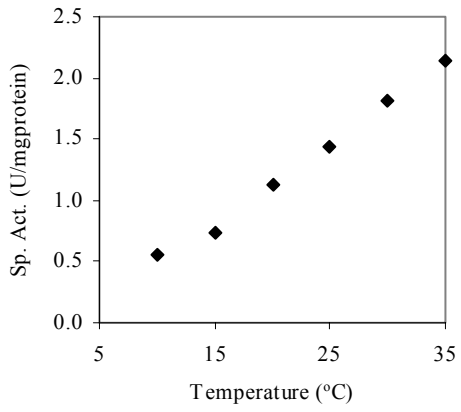
Then, the graph of $\ln (sp.act.)$ versus $(1/T)$ should be linear if a reaction follows Arrhenius relation, and the slope of the line is equal to $(-E_a/R)$ from which activation energy can be calculated. For all enzymes investigated, linear relation between the natural logarithm of specific activity and inverse of absolute temperature could be obtained (Figure 3.13) from which corresponding activation energies were calculated (Figure 3.14). When using the data, exclusion of data points obtained at 35°C resulted in a slight increase in activation energies but for most of the enzymes the difference was less than 10% except for ALD, GLYCPDH, ADH (forward), and ADH (reverse) for which difference was more than 10%. Therefore, these data was not omitted in all but those four enzymes since exclusion of these data resulted in better correlation coefficients for these enzymes.

One important observation for the enzymes tested (glycolysis and its branches to glycerol and ethanol, main products of fermentation in alcoholic beverages industry) was the relatively higher activation energies (so higher temperature dependencies) of higher part of the glycolysis and glycerol branch (GLYCPDH) than that of lower part enzymes as well as ethanol branch (ADH). This observation may account for the higher production (rates) of glycerol at higher temperatures than the lower temperatures. Brewing is performed at relatively lower temperatures (about 10°C for lager yeast) than wine fermentations especially the red wine (with a general fermentation temperature of 25-28 °C) in which the glycerol amount is higher than the white one (temperatures ranging between 10 to 20 °C).

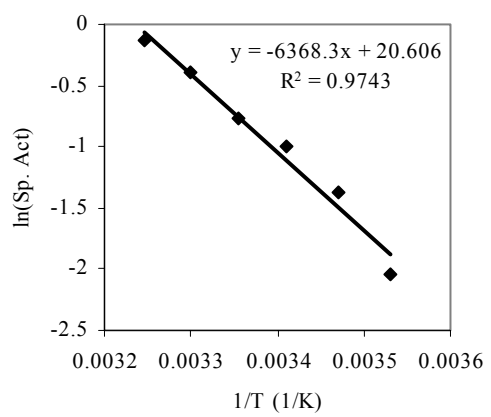
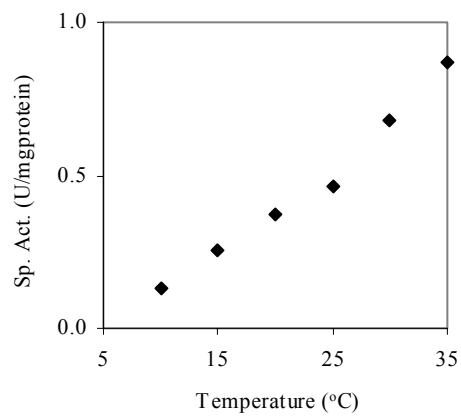
HXK



PGI

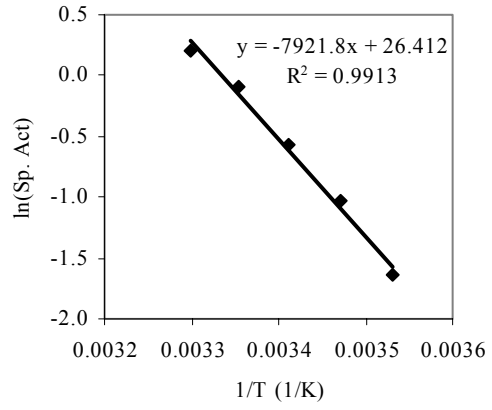
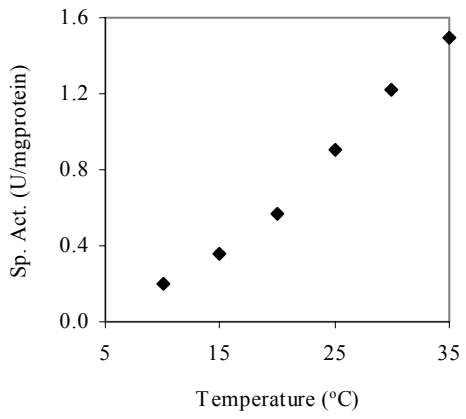


PFK

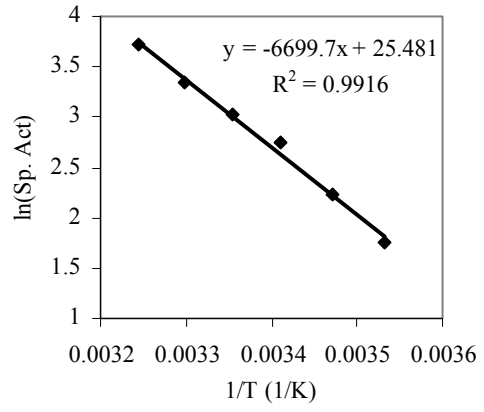
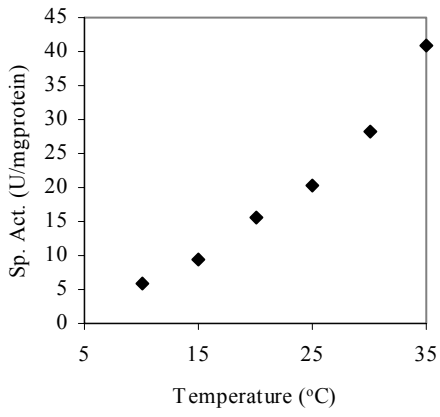


Continued on next page

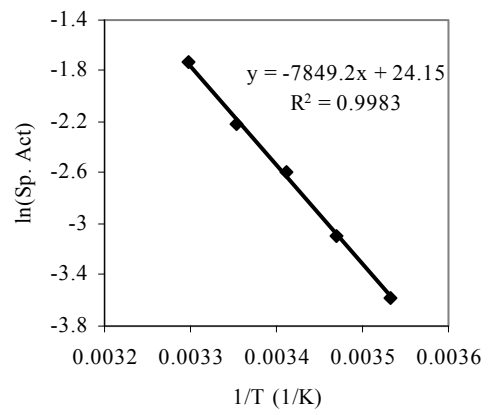
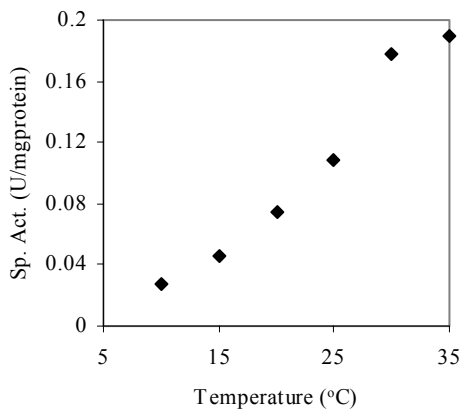
ALD



TPI

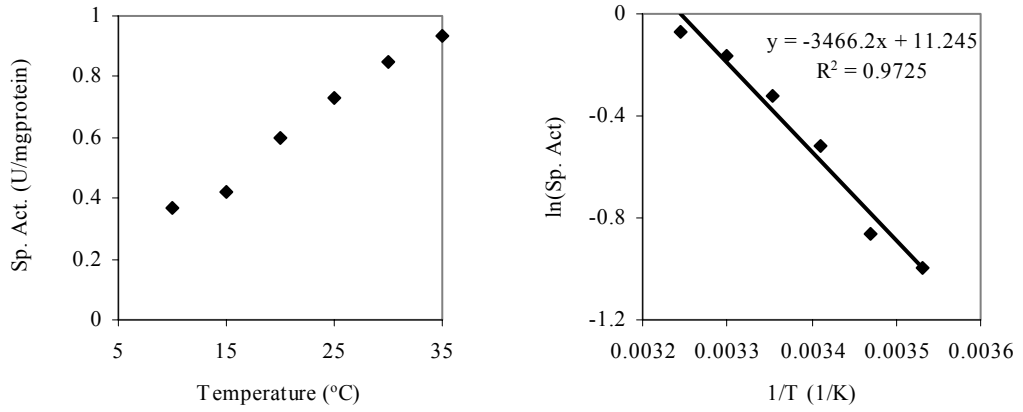


GLYCPDH

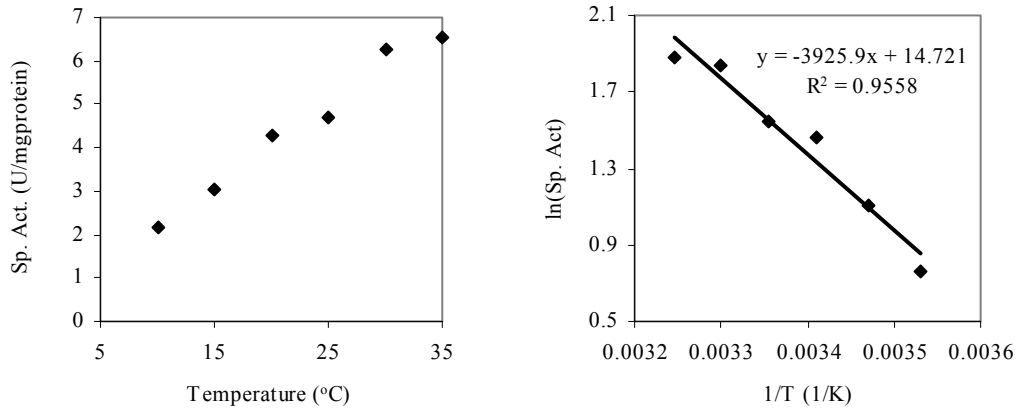


Continued on next page

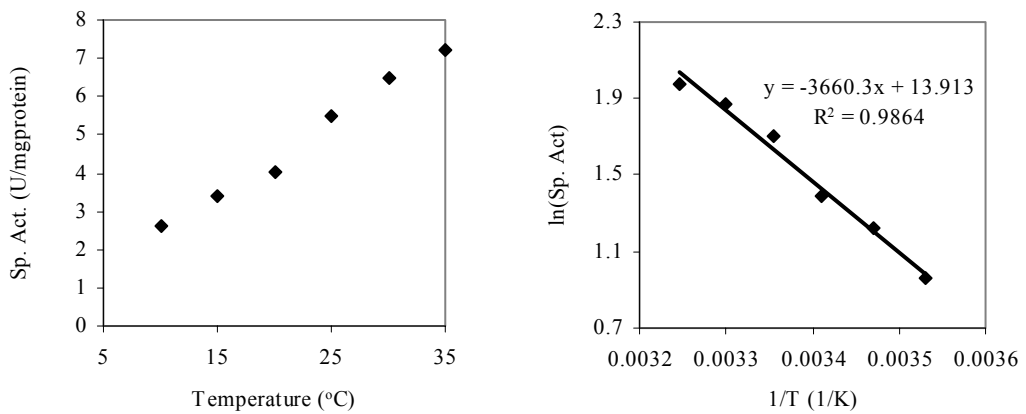
GAPDH (forward)



GAPDH (reverse)

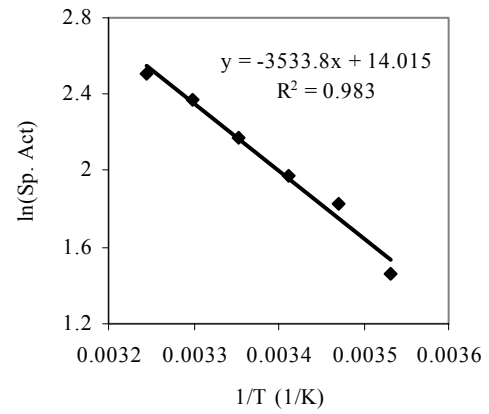
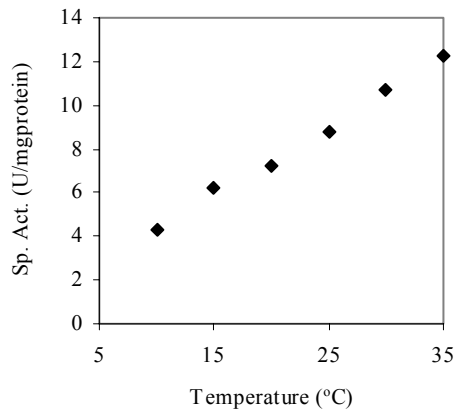


PGK

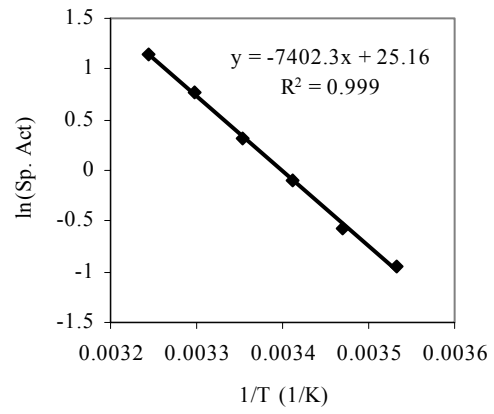
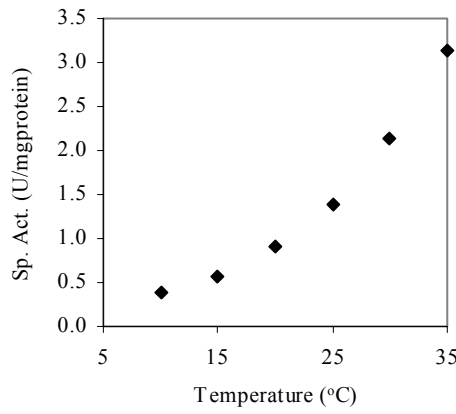


Continued on next page

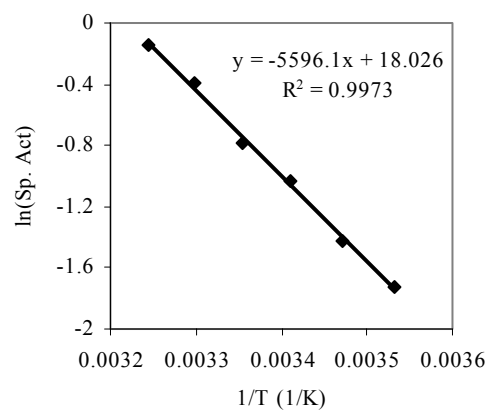
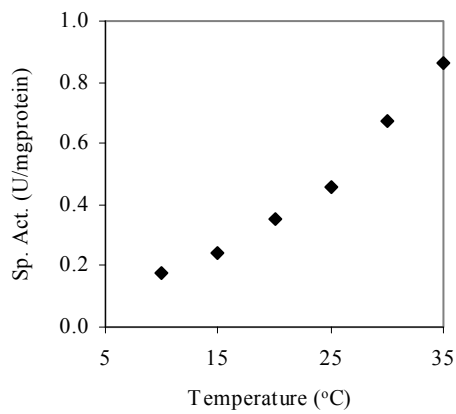
PGM



ENO

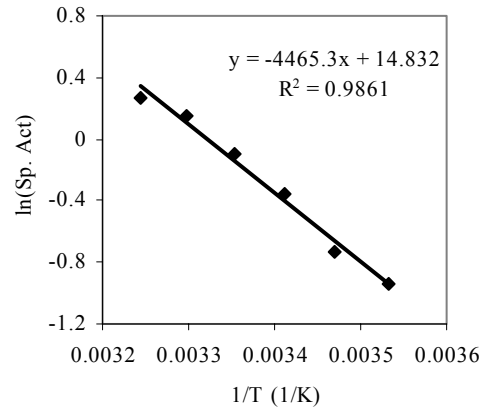
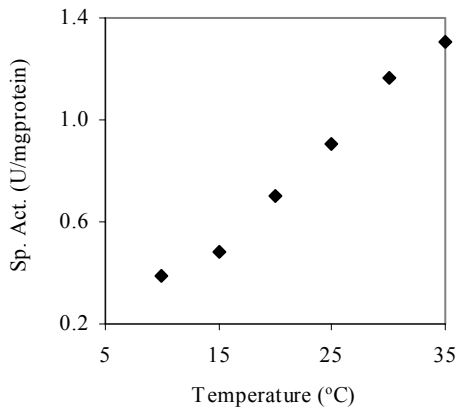


PYK

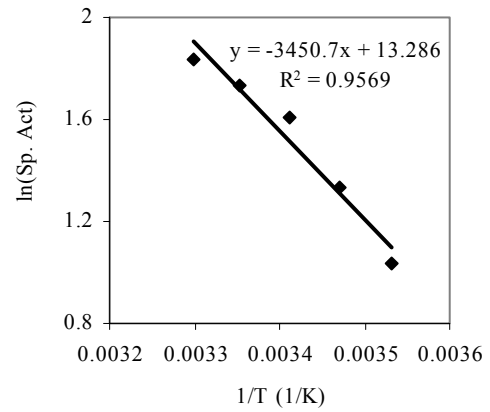
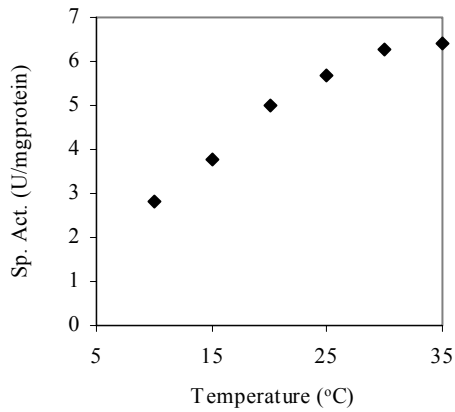


Continued on next page

PDC



ADH (forward)



ADH (reverse)

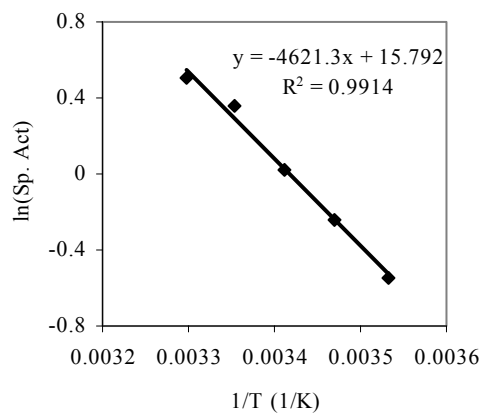
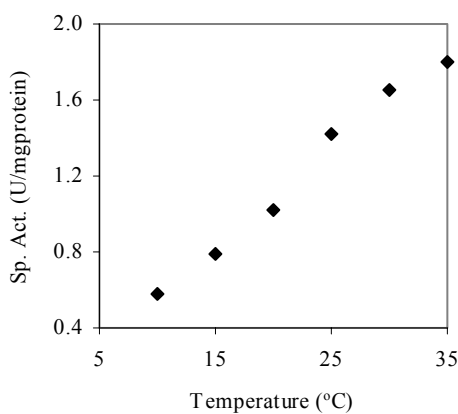


Figure 3.13 Left column: Change of specific activities of enzymes with temperature (10-15-20-25-30-35°C); Right column: Arrhenius plots of corresponding enzymes

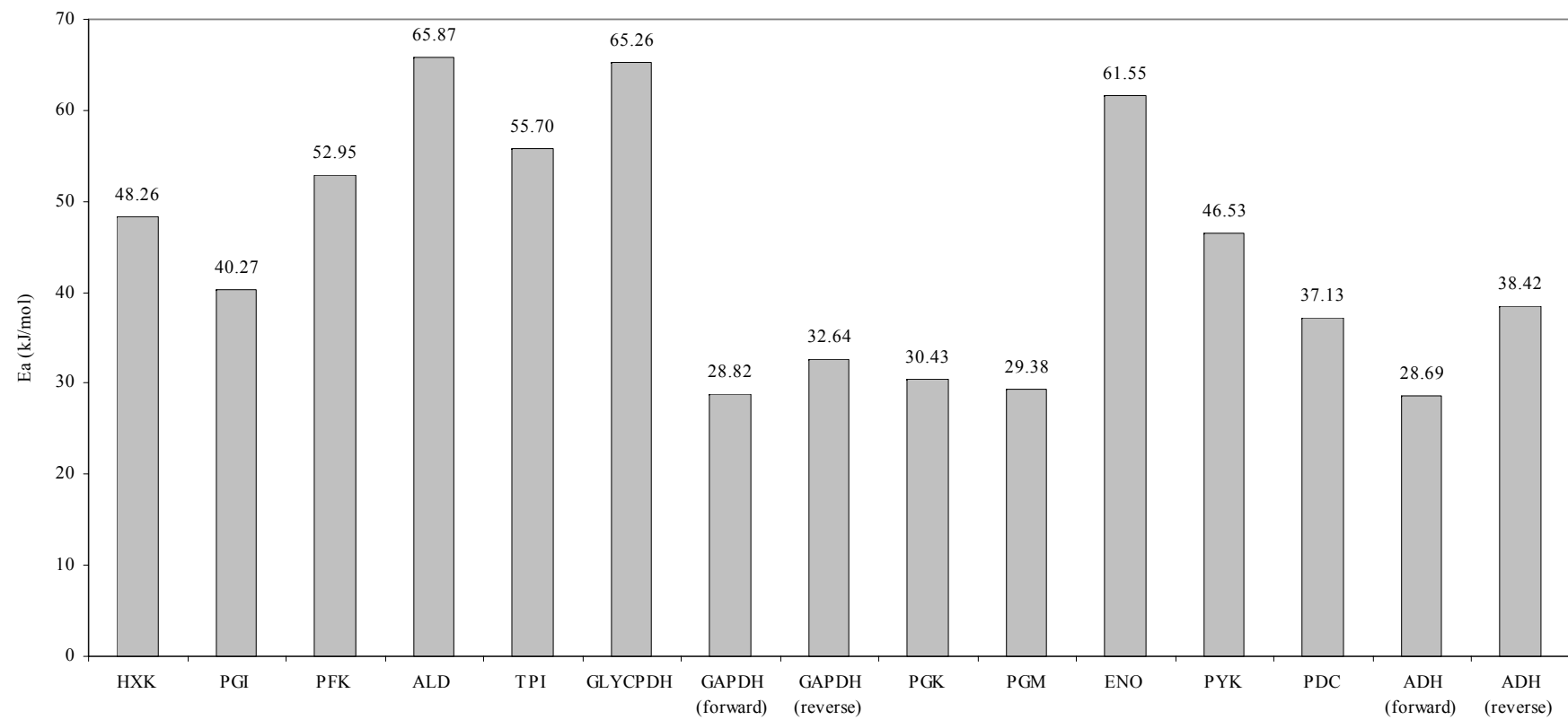


Figure 3.14 Activation energies of enzymes of glycolysis and its branches to glycerol and ethanol

The highest activation energy was of ALD. Enolase had exceptionally higher activation energy ($61.55 \text{ kJ mol}^{-1}$) as compared to the other enzymes of lower glycolysis. This value for ENO is in agreement with the values $53.3\text{-}63.3 \text{ kJ mol}^{-1}$ obtained in (Westhead and Malmstrom, 1957), which was calculated from the measurements under different assay conditions. The E_a of the first enzyme of glycerol branch GLYCPDH was almost two fold higher than the enzymes of ethanol branch, PDC and ADH. This is in accordance with the higher glycerol yield at higher temperatures.

3.3.2. Effect of Temperature on Fermentation Kinetics

The effect of temperature on fermentation kinetics was investigated under the same conditions that were used for ethanol effect studies. Temperatures ranged from 10 to 30°C, namely 10, 15, 20, and 30°C. Temperatures were selected considering the yeast based processes, such as brewing temperature is as low as 10 °C, while wine production is at higher temperatures (18-20 °C). Industrial ethanol production is carried out even at higher temperatures. Experiments were performed as described in section 3.2.2, except addition of ethanol. Cells were equilibrated to the desired temperature for about 30 min, before glucose was added to start the fermentation. Comparison of glucose consumption and glycerol and ethanol production are shown in Figure 3.15. Generally, rates did not change in 70 min except at 30°C rates decreased slightly through the end. Rates increased almost linearly with temperature above 15 °C while further decrease in temperature from 15 to 10 °C had a slight effect (Figure 3.16). As expected, as the culture temperature decreased, the amount of glucose consumed and ethanol and glycerol produced decreased. However, effects on consumption/production rates were not the same for all. Temperature had a drastic effect on glycerol yield on glucose (Figure 3.17). Glycerol yield was more than five fold higher at 30 °C than was at 10 °C, while ethanol yield was affected only to some extent. This observation also correlates with enhanced glycerol production at higher temperatures.

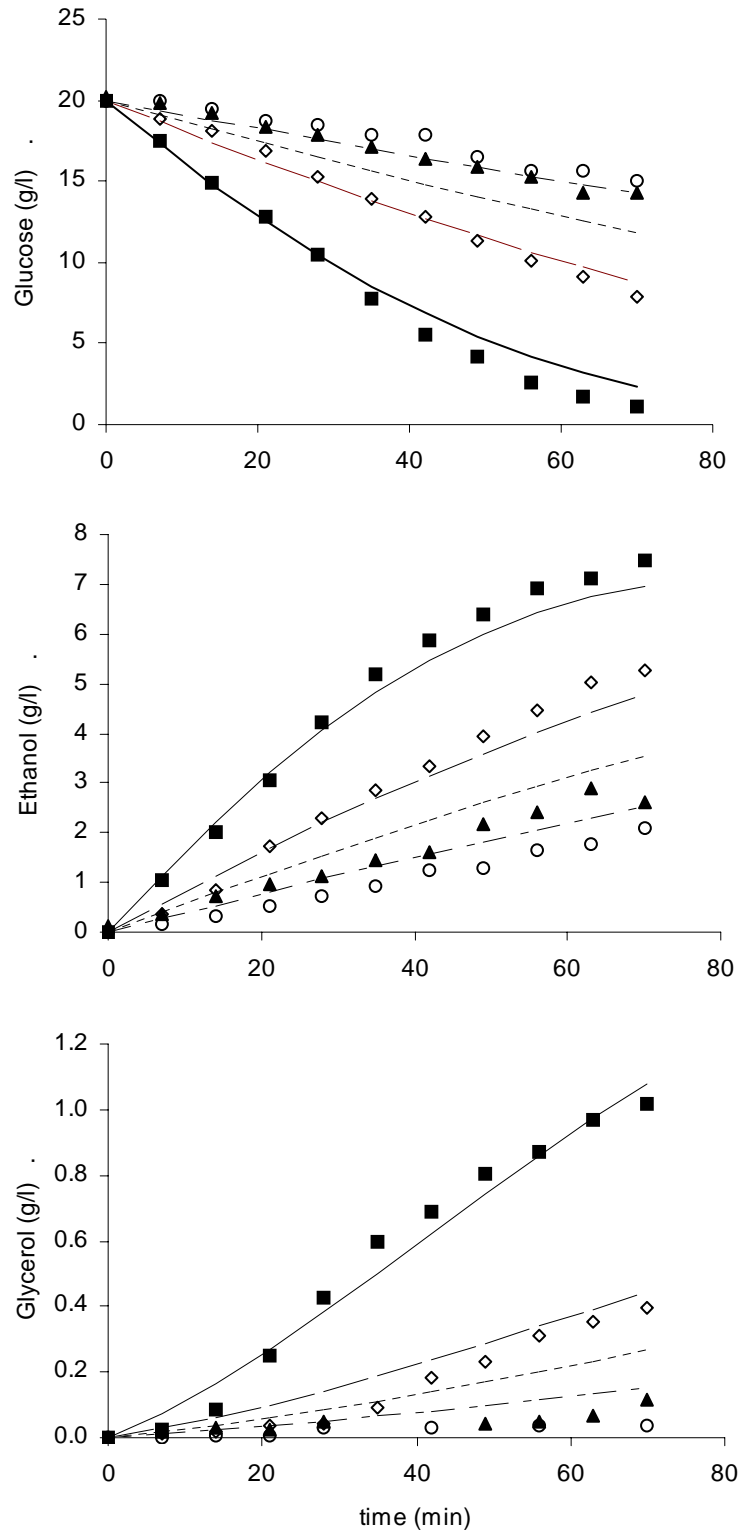


Figure 3.15 Effect of culture temperature on glucose consumption (top) and ethanol (middle) and glycerol (bottom) productions. Lines represent model simulation. 30°C: ■, —; 20°C: ◇, ---; 15°C: ▲, -.-.-; 10°C: ○, -.-.-.

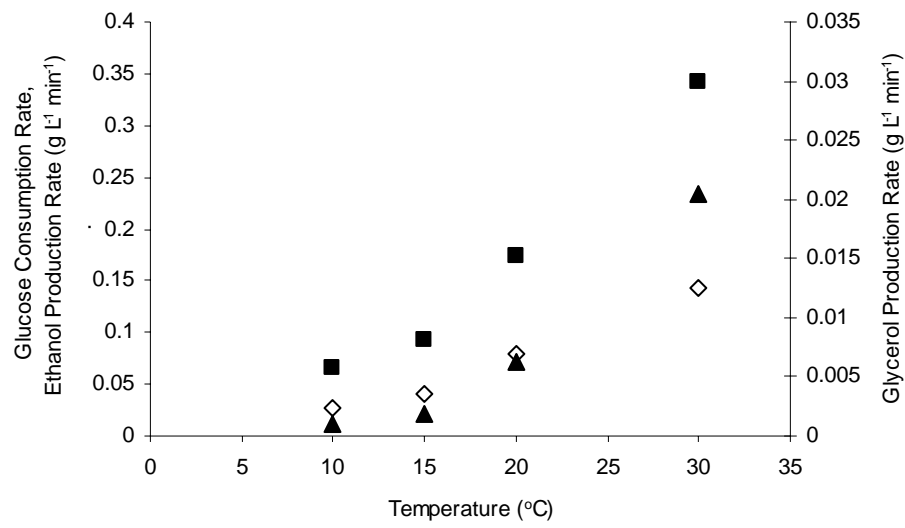


Figure 3.16 Effect of cultivation temperature on glucose consumption (■) and, ethanol (◇) and glycerol (▲) production rates

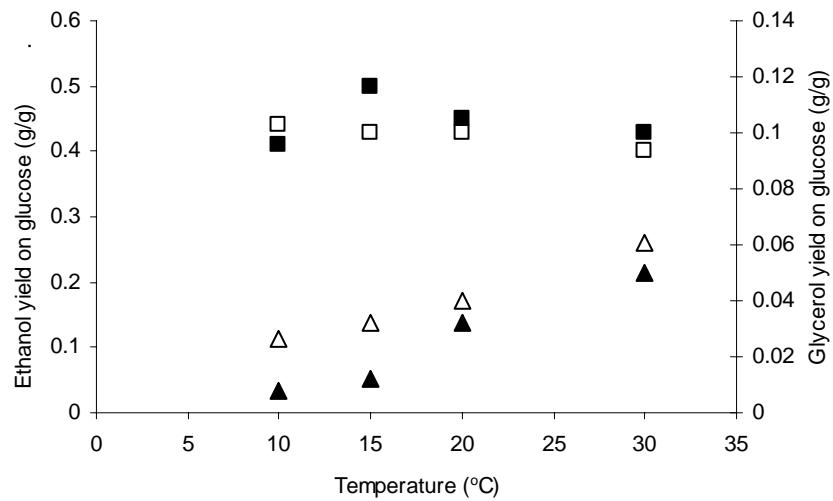


Figure 3.17 Effect of cultivation temperature on ethanol (square) and glycerol (triangle) yields on glucose. Closed symbols: experimental results, open symbols: model predictions

3.3.3. Model Studies Incorporating the Effect of Temperature

In order to incorporate the effect of temperature on activities of glycolytic enzymes and its branches to glycerol and ethanol to the model, an equation for each enzyme, which relates the rate at a certain temperature to the reference temperature (30°C in our case), was derived from Arrhenius relation by the use of an activation energies (equation 3.44).

$$v^T = v^* \cdot e^{\frac{-E_a}{R} \cdot \left(\frac{1}{T} - \frac{1}{T^*} \right)} \quad (3.44)$$

where v^T is the rate obtained at temperature T (in K), v^* is the rate obtained at temperature T^* (in K), E_a (in J mol⁻¹) is the activation energy of the respective enzyme, and R is the universal gas constant (in 8.314 J K⁻¹ mol⁻¹). Kinetic equation for each respective enzyme was multiplied by this factor, i.e. v_{\max} values were recalculated for each temperature, which is constant over time course of fermentation.

Activation energy of hexose transporter was calculated as 53.19 J mol⁻¹ from data of Reinhardt *et al.* (Reinhardt *et al.*, 1997). Since, while calculating the kinetic constants and then activation energies, they used two component model with one facilitated diffusion component and one first order component (pore diffusion), their data was reassessed according to one component Michaelis-Menten kinetics and E_a values were recalculated. Temperature changes for glycogen, trehalose, and succinate branches were assumed to be the same with the transporter.

One can note that, model was more successful at 30 and 20 °C than the lower temperatures for glucose consumption (Figure 3.15). Prediction for ethanol production at 20 °C was slightly lower than the experimental results. Except at 30 °C, glycerol productions were over estimated. Increase in glycerol yield with

increasing temperature was also reflected by the model, although not to the same degree (Figure 3.17). These differences are most probably due to the other physiological responses of yeast to low temperatures, which were not considered in the model. Organisms respond to cold by general reduction in transcriptional and translational efficiency (Al-Fageeh and Smales, 2006) and protein turnover (Somero, 2004). Enhanced trehalose synthesis were only observed at near freezing temperatures (<10 °C) or at the late phase of cold stress (10-20 °C) (Al-Fageeh and Smales, 2006; Tai *et al.*, 2007). Tai *et al.* (2007) observed similar glycolytic flux at 12 and 30 °C at a dilution rate of 0.03 h⁻¹ in anaerobic chemostat cultures of *S. cerevisiae*, although activities of glycolytic enzymes were up to 7.5 fold lower when assayed at 12°C than at 30 °C. They observed massive differences in the intracellular concentrations of glycolytic intermediates and nucleotides dictating a metabolic control on glycolytic enzyme activity rather than transcriptional control.

CHAPTER 4

CONCLUSIONS

Being at the center of most metabolic pathways and also one of the better known pathways, the glycolytic pathway has been of interest of modeling studies, although there are not many of them. The model in this study was based on that of Teusink *et al.* (2000) in which almost all kinetic parameters were obtained from the same organism under the same assay conditions. This model is unique in that sense among the models concentrated on glycolytic pathway of yeast. Firstly, MATLAB program was constructed for the model, so that I had more flexibility and have more power on model and its variables than the software packages. Secondly, some of the steps were modified and some are added to the model and some modifications were made on the parameters of the model.

As third step, I concentrated on some of the environmental factors that are known to be among the major effectors of metabolism and its products: ethanol concentration and temperature. While testing the effect of ethanol concentration and temperature on activities of enzymes, assay conditions were very similar to that of the previous work (Teusink *et al.*, 2000) to add up to what was done before. Results obtained from these experiments were incorporated into the model.

All enzymes tested were affected to some extent by increasing concentrations of ethanol in the assay medium, the least affected being the PYK and the most inhibited ones being GLYCPDH, GAPDH, PGK, and ADH (forward). In order to test the model, fermentations under non-growing conditions were performed with varying initial concentrations of ethanol. Glucose consumption and ethanol and

glycerol production rates decreased with increasing concentrations of ethanol. After incorporating the results obtained from enzyme assays with increasing ethanol concentrations along with the effect on transporters from literature, model was able to reflect the decrease in consumption and production rates obtained from fermentation experiments. However, exact fit couldn't be obtained. When the result of simulation in which the effect of ethanol on all steps was incorporated in to the model was compared with that in which just the effect on transporters was included, it was seen that inclusion of effect just on HXT was enough to reflect the decrease in rates. From this observation one may say that the rate determining step of glycolysis is the hexose transport step.

Temperature has a well known effect on enzymatic reactions, increasing the rate by increasing temperatures up to a point of protein denaturation. The effect of temperature on activities of glycolytic enzymes and its branches to ethanol and glycerol was determined. One important observation for the enzymes tested was the relatively higher activation energies of higher part of the glycolysis and glycerol branch (GLYCPDH) than that of lower part enzymes as well as ethanol branch (ADH). This observation is in accordance with the increased yields of glycerol productions at higher temperatures obtained in fermentations. This effect was also reflected by the model although not to same extend, the higher the temperature the higher the glycerol yield.

It must be noted that model could have been modified for the exact fit to experimentally observed concentrations. However, approach in this study was rather making as minimum modification as possible. Apart from that, being a stressor, low temperature or high ethanol levels may have given rise to some other response of cells which were not reflected in the enzyme kinetics. These were not taken into account in the scope of this thesis.

It is one more time proved that modeling is a powerful tool to understand the system, to test the knowledge, and to suggest points to work on it. This work was the first in our laboratory to construct a kinetic model to investigate the

metabolism. There will be other studies based on this work. Hexose transport step seems to be the first step that needs to be elucidated. The influence of environmental factors including the ones in the study should be tested on sugar uptake capacity of hexose transporters.

REFERENCES

- Al-Fageeh, M. B. and Smales, C. M. (2006). "Control and regulation of the cellular responses to cold shock: The responses in yeast and mammalian systems." Biochemical Journal 397: 247-259.
- Albertyn, J., Vantonder, A. and Prior, B. A. (1992). "Purification and characterization of glycerol-3-phosphate dehydrogenase of *Saccharomyces cerevisiae*." Febs Letters 308(2): 130-132.
- Alexandre, H., Ansanay-Galeote, V., Dequin, S. and Blondin, B. (2001). "Global gene expression during short-term ethanol stress in *Saccharomyces cerevisiae*." Febs Letters 498(1): 98-103.
- Andre, L., Hemming, A. and Adler, L. (1991). "Osmoregulation in *Saccharomyces cerevisiae* - studies on the osmotic induction of glycerol production and glycerol-3-phosphate dehydrogenase (NAD⁺)." Febs Letters 286(1-2): 13-17.
- Ansell, R., Granath, K., Hohmann, S., Thevelein, J. M. and Adler, L. (1997). "The two isoenzymes for yeast NAD⁺-dependent glycerol 3-phosphate dehydrogenase encoded by *gpd1* and *gpd2* have distinct roles in osmoadaptation and redox regulation." The EMBO Journal 16(9): 2179-2187.
- Birch, R. M. and Walker, G. M. (2000). "Influence of magnesium ions on heat shock and ethanol stress responses of *Saccharomyces cerevisiae*." Enzyme and Microbial Technology 26(9-10): 678-687.
- Bisson, L. F., Coons, D. M., Kruckeberg, A. L. and Lewis, D. A. (1993). "Yeast sugar transporters." Critical Reviews in Biochemistry and Molecular Biology 28(4): 259-308.

- Blazquez, M. A., Lagunas, R., Gancedo, C. and Gancedo, J. M. (1993). "Trehalose-6-phosphate, a new regulator of yeast glycolysis that inhibits hexokinases." Febs Letters 329(1-2): 51-54.
- Blomberg, A. and Adler, L. (1989). "Roles of glycerol and glycerol-3-phosphate dehydrogenase (NAD⁺) in acquired osmotolerance of *Saccharomyces cerevisiae*." Journal of Bacteriology 171(2): 1087-1092.
- Bosch, D., Johansson, M., Ferndahl, C., Franzen, C. J., Larsson, C. and Gustafsson, L. (2008). "Characterization of glucose transport mutants of *Saccharomyces cerevisiae* during a nutritional upshift reveals a correlation between metabolite levels and glycolytic flux." Fems Yeast Research 8(1): 10-25.
- Buziol, S., Becker, J., Baumeister, A., Jung, S., Mauch, K., Reuss, M. and Boles, E. (2002). "Determination of *in vivo* kinetics of the starvation-induced hxt5 glucose transporter of *Saccharomyces cerevisiae*." Fems Yeast Research 2(3): 283-291.
- Casey, G. P. and Ingledew, W. M. (1986). "Ethanol tolerance in yeasts." CRC Critical Reviews in Microbiology 13(3): 219-280.
- Ciriacy, M. (1997). Alcohol dehydrogenases. Yeast sugar metabolism : Biochemistry, genetics, biotechnology, and applications. Zimmermann, F. K. and Entian, K. D. Lancaster, PA, Technomic Pub.
- Ciriacy, M. and Reifenberger, E. (1997). Hexose transport. Yeast sugar metabolism : Biochemistry, genetics, biotechnology, and applications. Zimmermann, F. K. and Entian, K. D. Lancaster, PA, Technomic Pub.
- Crabtree, H. G. (1929). "Observations on the carbohydrate metabolism of tumours." Biochemical Journal 23(3): 536-545.
- Cronwright, G. R., Rohwer, J. M. and Prior, B. A. (2002). "Metabolic control analysis of glycerol synthesis in *Saccharomyces cerevisiae*." Applied and Environmental Microbiology 68(9): 4448-4456.
- Çalık, P. and Özdamar, T. H. (2002). "Bioreaction network flux analysis for industrial microorganisms: A review." Reviews in Chemical Engineering 18(6): 553-596.

- Dano, S., Madsen, M. F., Schmidt, H. and Cedersund, G. (2006). "Reduction of a biochemical model with preservation of its basic dynamic properties." Febs Journal 273(21): 4862-4877.
- Dasari, G., Worth, M. A., Connor, M. A. and Pamment, N. B. (1990). "Reasons for the apparent difference in the effects of produced and added ethanol on culture viability during rapid fermentations by *Saccharomyces cerevisiae*." Biotechnology and Bioengineering 35(2): 109-122.
- Davies, S. E. C. and Brindle, K. M. (1992). "Effects of overexpression of phosphofructokinase on glycolysis in the yeast *Saccharomyces cerevisiae*." Biochemistry 31(19): 4729-4735.
- de Smidt, O., du Preez, J. C. and Albertyn, J. (2008). "The alcohol dehydrogenases of *Saccharomyces cerevisiae*: A comprehensive review." Fems Yeast Research 8(7): 967-978.
- Dedeken, R. H. (1966). "Crabtree effect - a regulatory system in yeast." Journal of General Microbiology 44(2): 149-&.
- Diderich, J. A., Teusink, B., Valkier, J., Anjos, J., Spencer-Martins, I., van Dam, K. and Walsh, M. C. (1999). "Strategies to determine the extent of control exerted by glucose transport on glycolytic flux in the yeast *Saccharomyces bayanus*." Microbiology-Uk 145: 3447-3454.
- Dombek, K. M. and Ingram, L. O. (1986). "Determination of the intracellular concentration of ethanol in *Saccharomyces cerevisiae* during fermentation." Applied and Environmental Microbiology 51(1): 197-200.
- Dombek, K. M. and Ingram, L. O. (1986). "Magnesium limitation and its role in apparent toxicity of ethanol during yeast fermentation." Applied and Environmental Microbiology 52(5): 975-981.
- Drewke, C., Thielen, J. and Ciriacy, M. (1990). "Ethanol formation in adho mutants reveals the existence of a novel acetaldehyde-reducing activity in *Saccharomyces cerevisiae*." Journal of Bacteriology 172(7): 3909-3917.
- Elbing, K., Larsson, C., Bill, R. M., Albers, E., Snoep, J. L., Boles, E., Hohmann, S. and Gustafsson, L. (2004). "Role of hexose transport in control of glycolytic flux in *Saccharomyces cerevisiae*." Applied and Environmental Microbiology 70(9): 5323-5330.

- Ferreira, C., van Voorst, F., Martins, A., Neves, L., Oliveira, R., Kielland-Brandt, M. C., Lucas, C. and Brandt, A. (2005). "A member of the sugar transporter family, *stl1p* is the glycerol/h⁺ symporter in *Saccharomyces cerevisiae*." Molecular Biology of the Cell 16(4): 2068-2076.
- Flikweert, M. T., de Swaaf, M., van Dijken, J. P. and Pronk, J. T. (1999). "Growth requirements of pyruvate-decarboxylase-negative *Saccharomyces cerevisiae*." Fems Microbiology Letters 174(1): 73-79.
- Francois, J. and Parrou, J. L. (2001). "Reserve carbohydrates metabolism in the yeast *Saccharomyces cerevisiae*." Fems Microbiology Reviews 25(1): 125-145.
- François, J., Blazquez, M. A., Arino, J. and Gancedo, C. (1997). Storage carbohydrates in the yeast *Saccharomyces cerevisiae*. Yeast sugar metabolism: Biochemistry, genetics, biotechnology, and applications. Zimmermann, F. K., Entian, K. D. and Lancaster, PA, Technomic Pub.
- Giersch, C. (2000). "Mathematical modelling of metabolism." Current Opinion in Plant Biology 3(3): 249-253.
- Gombert, A. K. and Nielsen, J. (2000). "Mathematical modelling of metabolism." Current Opinion in Biotechnology 11(2): 180-186.
- Gray, W. D. and Sova, C. (1956). "Relation of molecule size and structure to alcohol inhibition of glucose utilization by yeast." Journal of Bacteriology 72(3): 349-356.
- Guijarro, J. M. and Lagunas, R. (1984). "*Saccharomyces cerevisiae* does not accumulate ethanol against a concentration gradient." Journal of Bacteriology 160(3): 874-878.
- Hallsworth, J. E. (1998). "Ethanol-induced water stress in yeast." Journal of Fermentation and Bioengineering 85(2): 125-137.
- Hallsworth, J. E., Prior, B. A., Nomura, Y., Iwahara, M. and Timmis, K. N. (2003). "Compatible solutes protect against chaotrope (ethanol)-induced, nonosmotic water stress." Applied and Environmental Microbiology 69(12): 7032-7034.

- Hansen, J. and Kielland-Brandt, M. C. (1997). Brewer's yeast. Yeast sugar metabolism: Biochemistry, genetics, biotechnology, and applications Zimmermann, F. K. and Entian, K. D. Lancaster, PA, Technomic Pub.
- Hartree, E. F. (1972). "Determination of protein: A modification of the lowry method that gives a linear photometric response." Analytical Biochemistry 48: 422-427.
- Hofmeyr, J. H. S., Kacser, H. and Vandermerwe, K. J. (1986). "Metabolic control analysis of moiety-conserved cycles." European Journal of Biochemistry 155(3): 631-641.
- Hynne, R., Dano, S. and Sorensen, P. G. (2001). "Full-scale model of glycolysis in *Saccharomyces cerevisiae*." Biophysical Chemistry 94(1-2): 121-163.
- Ingram, L. O. N. and Buttke, T. M. (1984). "Effects of alcohols on microorganisms." Advances in Microbial Physiology 25: 253-300.
- Jones, R. P. (1989). "Biological principles for the effects of ethanol." Enzyme and Microbial Technology 11(3): 130-153.
- Jonker, C. M., Snoep, J. L., Treur, J., Westerhoff, H. V. and Wijngaards, W. C. A. (2002). "Putting intentions into cell biochemistry: An artificial intelligence perspective." Journal of Theoretical Biology 214(1): 105-134.
- Kaino, T. and Takagi, H. (2008). "Gene expression profiles and intracellular contents of stress protectants in *Saccharomyces cerevisiae* under ethanol and sorbitol stresses." Applied Microbiology and Biotechnology 79(2): 273-283.
- Kovar, K. and Meyer, H. P. (2005). "What's in store for yeast biotechnology? The joint 3rd swiss-czech and biotech2005 symposium in retrospect." Chimia 59(10): 723-726.
- Leao, C. and van Uden, N. (1982). "Effects of ethanol and other alkanols on the glucose-transport system of *Saccharomyces cerevisiae*." Biotechnology and Bioengineering 24(11): 2601-2604.
- Leao, C. and van Uden, N. (1983). "Effects of ethanol and other alkanols on the ammonium transport-system of *Saccharomyces cerevisiae*." Biotechnology and Bioengineering 25(8): 2085-2090.

- Leao, C. and van Uden, N. (1984). "Effects of ethanol and other alkanols on the general amino-acid permease of *Saccharomyces cerevisiae*." Biotechnology and Bioengineering 26(4): 403-405.
- Lei, F. and Jorgensen, S. B. (2001). "Estimation of kinetic parameters in a structured yeast model using regularisation." Journal of Biotechnology 88(3): 223-237.
- Lentini, A., Rgers, P., Higgins, V., Daes, I., Chandler, M., Stanley, G. and Chambers, P. (2003). The impact of ethanol stress on yeast physiology. Brewing yeast fermentation performance. Smart, K. Oxford, UK; Malden, MA, Blackwell Science.
- Loureirodias, M. C. and Peinado, J. M. (1982). "Effect of ethanol and other alkanols on the maltose transport-system of *Saccharomyces cerevisiae*." Biotechnology Letters 4(11): 721-724.
- Lowry, O. H., Rosebrough, N. J., Farr, L. A. and Randall, R. J. (1951). "Protein measurement with the folin phenol reagent." Journal of Biological Chemistry 193: 265-275.
- Luong, J. H. T. (1985). "Kinetics of ethanol inhibition in alcohol fermentation." Biotechnology and Bioengineering 27(3): 280-285.
- Madigan, M. T., Martinko, J. M., Parker, J. and Brock, T. D. (1997). Brock biology of microorganisms. Needham Heights, Mass., Simon & Schuster Custom Pub.
- Maier, A., Volker, B., Boles, E. and Fuhrmann, G. F. (2002). "Characterisation of glucose transport in *Saccharomyces cerevisiae* with plasma membrane vesicles (countertransport) and intact cells (initial uptake) with single hxt1, hxt2, hxt3, hxt4, hxt6, hxt7 or gal2 transporters." Fems Yeast Research 2(4): 539-550.
- Marin, M. R. (1999). "Alcoholic fermentation modelling: Current state and perspectives." American Journal of Enology and Viticulture 50(2): 166-178.
- Mathews, C. K., Van Holde, K. E. and Ahern, K. G. (1999). Biochemistry. San Francisco, Calif., Benjamin Cummings.

- Medawar, W., Strehaiano, P. and Delia, M. L. (2003). "Yeast growth: Lag phase modelling in alcoholic media." Food Microbiology 20(5): 527-532.
- Mendes, P. (1993). "Gepasi - a software package for modeling the dynamics, steady-states and control of biochemical and other systems." Computer Applications in the Biosciences 9(5): 563-571.
- Michnick, S., Roustan, J. L., Remize, F., Barre, P. and Dequin, S. (1997). "Modulation of glycerol and ethanol yields during alcoholic fermentation in *Saccharomyces cerevisiae* strains overexpressed or disrupted for *gpd1* encoding glycerol 3-phosphate dehydrogenase." Yeast 13(9): 783-793.
- Millar, D. G., Griffithsmith, K., Algar, E. and Scopes, R. K. (1982). "Activity and stability of glycolytic-enzymes in the presence of ethanol." Biotechnology Letters 4(9): 601-606.
- Nader, W., Betz, A. and Becker, J. U. (1979). "Partial-purification, substrate-specificity and regulation of α -l-glycerolphosphate dehydrogenase from *Saccharomyces carlsbergensis*." Biochimica Et Biophysica Acta 571(2): 177-185.
- Nagodawithana, T. W. and Steinkraus, K. H. (1976). "Influence of rate of ethanol production and accumulation on viability of *Saccharomyces cerevisiae* in rapid fermentation." Applied and Environmental Microbiology 31(2): 158-162.
- Nagodawithana, T. W., Whitt, J. T. and Cutaia, J. (1977). "Study of the effect of ethanol on selected enzymes of the glycolytic pathway." ASBC Journal 35(4): 179-183.
- Nevoigt, E. and Stahl, U. (1997). "Osmoregulation and glycerol metabolism in the yeast *Saccharomyces cerevisiae*." Fems Microbiology Reviews 21(3): 231-241.
- Nissen, T. L., Schulze, U., Nielsen, J. and Villadsen, J. (1997). "Flux distributions in anaerobic, glucose-limited continuous cultures of *Saccharomyces cerevisiae*." Microbiology-Uk 143: 203-218.
- Olivier, B. G. and Snoep, J. L. (2004). "Web-based kinetic modelling using jws online." Bioinformatics 20(13): 2143-2144.

- Otterstedt, K., Larsson, C., Bill, R. M., Stahlberg, A., Boles, E., Hohmann, S. and Gustafsson, L. (2004). "Switching the mode of metabolism in the yeast *Saccharomyces cerevisiae*." Embo Reports 5(5): 532-537.
- Özcan, S. and Johnston, M. (1999). "Function and regulation of yeast hexose transporters." Microbiology and Molecular Biology Reviews 63(3): 554-+.
- Pascual, C., Alonso, A., Garcia, I., Romay, C. and Kotyk, A. (1988). "Effect of ethanol on glucose-transport, key glycolytic-enzymes, and proton extrusion in *Saccharomyces cerevisiae*." Biotechnology and Bioengineering 32(3): 374-378.
- Pizarro, F., Varela, C., Martabit, C., Bruno, C., Prez-Correa, J. R. and Agosin, E. (2007). "Coupling kinetic expressions and metabolic networks for predicting wine fermentations." Biotechnology and Bioengineering 98(5): 986-998.
- Postma, E., Verduyn, C., Scheffers, W. A. and Vandijken, J. P. (1989). "Enzymic analysis of the crabtree effect in glucose-limited chemostat cultures of *Saccharomyces cerevisiae*." Applied and Environmental Microbiology 55(2): 468-477.
- Postmus, J., Canelas, A. B., Bouwman, J., Bakker, B. M., van Gulik, W., de Mattos, M. J. T., Brul, S. and Smits, G. J. (2008). "Quantitative analysis of the high temperature-induced glycolytic flux increase in *Saccharomyces cerevisiae* reveals dominant metabolic regulation." Journal of Biological Chemistry 283(35): 23524-23532.
- Reijenga, K. A., Snoep, J. L., Diderich, J. A., van Verseveld, H. W., Westerhoff, H. V. and Teusink, B. (2001). "Control of glycolytic dynamics by hexose transport in *Saccharomyces cerevisiae*." Biophysical Journal 80(2): 626-634.
- Reinhardt, C., Volker, B., Martin, H. J., Kneiseler, J. and Fuhrmann, G. F. (1997). "Different activation energies in glucose uptake in *Saccharomyces cerevisiae* dfy1 suggest two transport systems." Biochimica Et Biophysica Acta-Biomembranes 1325(1): 126-134.
- Remize, F., Barnavon, L. and Dequin, S. (2001). "Glycerol export and glycerol-3-phosphate dehydrogenase, but not glycerol phosphatase, are rate limiting

- for glycerol production in *Saccharomyces cerevisiae*." Metabolic Engineering 3(4): 301-312.
- Ricci, M., Martini, S., Bonechi, C., Trabalzini, L., Santucci, A. and Rossi, C. (2004). "Inhibition effects of ethanol on the kinetics of glucose metabolism by *Saccharomyces cerevisiae*: NMR and modelling study." Chemical Physics Letters 387(4-6): 377-382.
- Rizzi, M., Baltes, M., Theobald, U. and Reuss, M. (1997). "*In vivo* analysis of metabolic dynamics in *Saccharomyces cerevisiae* .2. Mathematical model." Biotechnology and Bioengineering 55(4): 592-608.
- Ruijter, G. J. G., Panneman, H. and Visser, J. (1997). "Overexpression of phosphofructokinase and pyruvate kinase in citric acid-producing *aspergillus niger*." Biochimica Et Biophysica Acta-General Subjects 1334(2-3): 317-326.
- Sauro, H. M. (1993). "Scamp - a general-purpose simulator and metabolic control analysis program." Computer Applications in the Biosciences 9(4): 441-450.
- Schaaff, I., Heinisch, J. and Zimmermann, F. K. (1989). "Overproduction of glycolytic-enzymes in yeast." Yeast 5(4): 285-290.
- Sharma, S. C. (1997). "A possible role of trehalose in osmotolerance and ethanol tolerance in *Saccharomyces cerevisiae*." Fems Microbiology Letters 152(1): 11-15.
- Smith, M. G., Des Etages, S. G. and Snyder, M. (2004). "Microbial synergy via an ethanol-triggered pathway." Molecular and Cellular Biology 24(9): 3874-3884.
- Smits, H. P., Hauf, J., Muller, S., Hobbey, T. J., Zimmermann, F. K., Hahn-Hagerdal, B., Nielsen, J. and Olsson, L. (2000). "Simultaneous overexpression of enzymes of the lower part of glycolysis can enhance the fermentative capacity of *Saccharomyces cerevisiae*." Yeast 16(14): 1325-1334.
- Snoep, J. L. and Westerhoff, H. V. (2004). "The silicon cell initiative." Current Genomics 5(8): 687-697.

- Somero, G. N. (2004). "Adaptation of enzymes to temperature: Searching for basic "Strategies"." Comparative Biochemistry and Physiology, Part B 139: 321-333.
- Steinmeyer, D. E. and Shuler, M. L. (1989). "Structured model for *Saccharomyces cerevisiae*." Chemical Engineering Science 44(9): 2017-2030.
- Taherzadeh, M. J., Adler, L. and Liden, G. (2002). "Strategies for enhancing fermentative production of glycerol - a review." Enzyme and Microbial Technology 31(1-2): 53-66.
- Tai, S. L., Daran-Lapujade, P., Luttk, M. A. H., Walsh, M. C., Diderich, J. A., Krijger, G. C., van Gulik, W. M., Pronk, J. T. and Daran, J. M. (2007). "Control of the glycolytic flux in *Saccharomyces cerevisiae* grown at low temperature - a multi-level analysis in anaerobic chemostat cultures." Journal of Biological Chemistry 282(14): 10243-10251.
- Teusink, B., Diderich, J. A., Westerhoff, H. V., van Dam, K. and Walsh, M. C. (1998). "Intracellular glucose concentration in derepressed yeast cells consuming glucose is high enough to reduce the glucose transport rate by 50%." Journal of Bacteriology 180(3): 556-562.
- Teusink, B., Passarge, J., Reijenga, C. A., Esgalhado, E., van der Weijden, C. C., Schepper, M., Walsh, M. C., Bakker, B. M., van Dam, K., Westerhoff, H. V. and Snoep, J. L. (2000). "Can yeast glycolysis be understood in terms of in vitro kinetics of the constituent enzymes? Testing biochemistry." European Journal of Biochemistry 267(17): 5313-5329.
- Teusink, B., Walsh, M. C., van Dam, K. and Westerhoff, H. V. (1998). "The danger of metabolic pathways with turbo design." Trends in Biochemical Sciences 23(5): 162-169.
- Thevelein, J. M. and Hohmann, S. (1995). "Trehalose synthase - guard to the gate of glycolysis in yeast." Trends in Biochemical Sciences 20(1): 3-10.
- Visser, D., van der Heijden, R., Mauch, K., Reuss, M. and Heijnen, S. (2000). "Tendency modeling: A new approach to obtain simplified kinetic models of metabolism applied to *Saccharomyces cerevisiae*." Metabolic Engineering 2(3): 252-275.

- Walker, G. M. and Maynard, A. (1997). "Accumulation of magnesium ions during fermentative metabolism in *Saccharomyces cerevisiae*." Journal of Industrial Microbiology & Biotechnology 18(1): 1-3.
- Walsh, M. C., Smits, H. P., Scholte, M. and Vandam, K. (1994). "Affinity of glucose-transport in *Saccharomyces cerevisiae* is modulated during growth on glucose." Journal of Bacteriology 176(4): 953-958.
- Westhead, E. W. and Malmstrom, B. G. (1957). "The chemical kinetics of the enolase reaction with special reference to the use of mixed solvents." Journal of Biological Chemistry 228(2): 655-671.
- Wiechert, W. (2002). "Modeling and simulation: Tools for metabolic engineering." Journal of Biotechnology 94(1): 37-63.
- Wojda, I., Alonso-Monge, R., Bebelman, J. P., Mager, W. H. and Siderius, M. (2003). "Response to high osmotic conditions and elevated temperature in *Saccharomyces cerevisiae* is controlled by intracellular glycerol and involves coordinate activity of map kinase pathways." Microbiology-Sgm 149: 1193-1204.

APPENDIX A

GROWTH CURVE OF YEAST

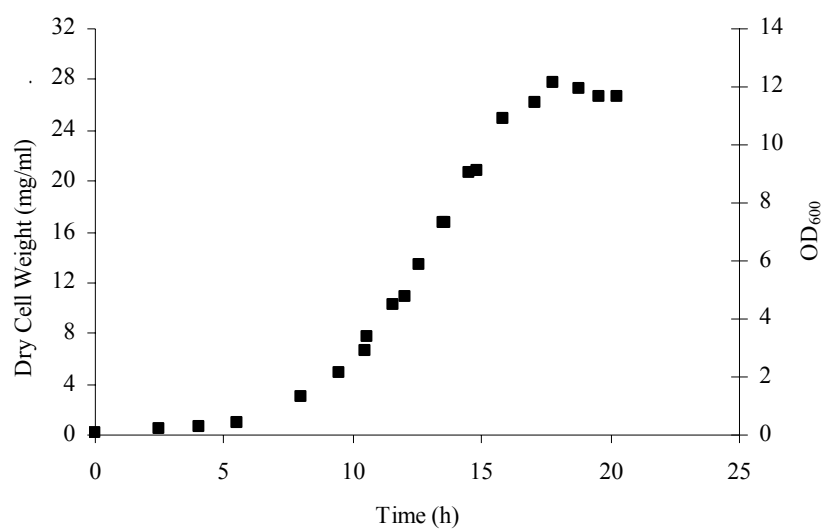


Figure A.1 Growth curve of brewer's yeast in YPD medium (Glucose: 5% w/v).

APPENDIX B

RATE EQUATIONS USED IN THE MODEL

Rate equations used in the model with their type are given below. All equations were taken from Teusink *et al.* (2000). Details of the kinetics of TPI, GLYCPDH and GLYCPASE are given in Chapter 3. Values of kinetic parameters are given in Table A.1 and A.2.

Hexose transport: Symmetrical carrier model

$$v_{HXT} = \frac{v_{m_{HXT}} \cdot \left(Glc_o - \frac{Glc_{in}}{K_{eq,hxt}} \right)}{K_{mGlc_o} \cdot \left(1 + \frac{Glc_o}{K_{mGlc_o}} + \frac{Glc_{in}}{K_{mGlc_{in}}} + K_{ihxt} \cdot \frac{Glc_o}{K_{mGlc_o}} \cdot \frac{Glc_{in}}{K_{mGlc_{in}}} \right)}$$

Hexokinase: Reversible Michaelis-Menten kinetics for two non-competing substrate-product couples

$$v_{HXX} = \frac{v_{m_{HXX}} \cdot \left(Glc_{in} \cdot ATP - \frac{G6P \cdot ATP}{K_{eq,HXX}} \right)}{K_{mGlc_{in}} \cdot K_{mATP} \left(1 + \frac{Glc_{in}}{K_{mGlc_{in}}} + \frac{G6P}{K_{mG6P}} \right) \cdot \left(1 + \frac{ATP}{K_{mATP}} + \frac{ADP}{K_{mADP}} \right)}$$

Phosphoglucose isomerase: One substrate, one product reversible Michaelis-Menten kinetics

$$v_{PGI} = \frac{v_{mPGI} \cdot \left(G6P - \frac{F6P}{K_{eq,PGI}} \right)}{K_{mG6P} \cdot \left(1 + \frac{G6P}{K_{mG6P}} + \frac{F6P}{K_{mF6P}} \right)}$$

Phosphofructo kinase: Two substrate Monod, Wyman, Changeux model for allosteric enzymes

$$v_{PFK} = \frac{v_{mPFK} (gr \cdot \lambda_1 \cdot \lambda_2 \cdot R)}{(R^2 + L \cdot T^2)} \quad \text{where}$$

$$\lambda_1 = \frac{F6P}{K_{R,F6P}}, \quad \lambda_2 = \frac{ATP}{K_{R,ATP}}, \quad R = 1 + \lambda_1 \cdot \lambda_2 + G_R \cdot \lambda_1 \cdot \lambda_2, \quad T = 1 + c_{ATP} \cdot \lambda_2$$

$$L = L_0 \cdot \left(\frac{1 + \frac{C_{i,ATP} \cdot ATP}{K_{ATP}}}{1 + \frac{ATP}{K_{ATP}}} \right)^2 \cdot \left(\frac{1 + \frac{C_{i,AMP} \cdot AMP}{K_{AMP}}}{1 + \frac{AMP}{K_{AMP}}} \right)^2 \cdot \left(\frac{1 + \frac{C_{i,F26bP} \cdot F26bP}{K_{F26bP}} + \frac{C_{i,F16bP} \cdot F16bP}{K_{F16bP}}}{1 + \frac{F26bP}{K_{F26bP}} + \frac{F16bP}{K_{F16bP}}} \right)$$

Aldolase: Ordered uni-bi kinetics (GAP dissociates first)

$$v_{ALD} = \frac{v_{mALD} \cdot \left(F16bP - \frac{DHAP \cdot GAP}{K_{eq,ALD}} \right)}{K_{mF16bP} \cdot \left(1 + \frac{F16bP}{K_{mF16bP}} + \frac{DHAP}{K_{mDHAP}} + \frac{GAP}{K_{mGAP}} + \frac{F16bP}{K_{mF16bP}} \cdot \frac{GAP}{K_{iGAP}} + \frac{DHAP}{K_{mDHAP}} \cdot \frac{GAP}{K_{mGAP}} \right)}$$

Glyceraldehyde-3-phosphatedehydrogenase: Reversible Michaelis-Menten kinetics for two non-competing substrate-product couples

$$v_{\text{GAPDH}} = \frac{\left(\frac{v_{m_{\text{GAPDH},f}} \cdot \text{NAD} \cdot \text{GAP}}{K_{m_{\text{NAD}}} \cdot K_{m_{\text{GAP}}}} - \frac{v_{m_{\text{GAPDH},r}} \cdot \text{BPG} \cdot \text{NADH}}{K_{m_{\text{BPG}}} \cdot K_{m_{\text{NADH}}}} \right)}{\left(1 + \frac{\text{NAD}}{K_{m_{\text{NAD}}}} + \frac{\text{NADH}}{K_{m_{\text{NADH}}}} \right) \cdot \left(1 + \frac{\text{BPG}}{K_{m_{\text{BPG}}}} + \frac{\text{GAP}}{K_{m_{\text{GAP}}}} \right)}$$

Phosphoglycerate kinase: Reversible Michaelis-Menten kinetics for two non-competing substrate-product couples

$$v_{\text{PGK}} = \frac{v_{m_{\text{PGK}}} \cdot (K_{eq,PGK} \cdot \text{BPG} \cdot \text{ADP} - \text{G3P} \cdot \text{ATP})}{K_{m_{\text{BPG}}} \cdot K_{m_{\text{G3P}}} \left(1 + \frac{\text{BPG}}{K_{m_{\text{BPG}}}} + \frac{\text{G3P}}{K_{m_{\text{G3P}}}} \right) \cdot \left(1 + \frac{\text{ADP}}{K_{m_{\text{ADP}}}} + \frac{\text{ATP}}{K_{m_{\text{ATP}}}} \right)}$$

Phosphoglycerate mutase: One substrate, one product reversible Michaelis-Menten kinetics

$$v_{\text{PGM}} = \frac{v_{m_{\text{PGM}}} \cdot \left(\text{G3P} - \frac{\text{G2P}}{K_{eq,PGM}} \right)}{K_{m_{\text{G3P}}} \cdot \left(1 + \frac{\text{G3P}}{K_{m_{\text{G3P}}}} + \frac{\text{G2P}}{K_{m_{\text{G2P}}}} \right)}$$

Enolase: One substrate, one product reversible Michaelis-Menten kinetics

$$v_{\text{PGM}} = \frac{v_{m_{\text{ENO}}} \cdot \left(\text{G2P} - \frac{\text{PEP}}{K_{eq,ENO}} \right)}{K_{m_{\text{G2P}}} \cdot \left(1 + \frac{\text{G2P}}{K_{m_{\text{G2P}}}} + \frac{\text{PEP}}{K_{m_{\text{PEP}}}} \right)}$$

Pyruvate kinase: Reversible Michaelis-Menten kinetics for two non-competing substrate-product couples

$$v_{PYK} = \frac{v_{mPYK} \cdot \left(PEP \cdot ADP - \frac{PYR \cdot ATP}{K_{eq,PYK}} \right)}{K_{PEP} \cdot K_{ADP} \left(1 + \frac{PEP}{K_{mPEP}} + \frac{PYR}{K_{mPYR}} \right) \cdot \left(1 + \frac{ADP}{K_{mADP}} + \frac{ATP}{K_{mATP}} \right)}$$

Pyruvate decarboxylase: Irreversible Hill kinetics

$$v_{PDC} = \frac{v_{mPDC} \cdot \left(\frac{PYR}{K_{mPYR}} \right)^{n_{hill}}}{1 + \left(\frac{PYR}{K_{mPYR}} \right)^{n_{hill}}}$$

Alcohol dehydrogenase: Ordered bi-bi kinetics with the cofactor binding first

$$v_{ADH} = \frac{-\frac{v_{mADH}}{K_{iNAD} \cdot K_{EtOH}} \cdot \left(ETOH \cdot NAD - \frac{ACE \cdot NADH}{K_{eq,ADH}} \right)}{\left[1 + \frac{ETOH \cdot K_{NAD}}{K_{iNAD} \cdot K_{EtOH}} + \frac{K_{NADH} \cdot ACE}{K_{iNADH} \cdot K_{ACE}} + \frac{NAD}{K_{iNAD}} + \frac{ETOH \cdot NAD}{K_{iNAD} \cdot K_{EtOH}} + \frac{ETOH \cdot ACE \cdot NAD}{K_{iACE} \cdot K_{iNAD} \cdot K_{EtOH}} + \frac{K_{NADH} \cdot ACE \cdot NAD}{K_{iNAD} \cdot K_{iNADH} \cdot K_{ACE}} + \frac{NADH}{K_{iNADH}} + \frac{ETOH \cdot K_{NAD} \cdot NADH}{K_{iNAD} \cdot K_{iNADH} \cdot K_{EtOH}} + \frac{ACE \cdot NADH}{K_{iNADH} \cdot K_{ACE}} + \frac{ETOH \cdot ACE \cdot NADH}{K_{iEtOH} \cdot K_{iNADH} \cdot K_{ACE}} \right]}$$

ATPase: $v_{ATPase} = K_{ATPase} \cdot ATP$

Glycogen branch: $v_{glyco} = K_{glycogen}$

Trehalose branch: $v_{trehalose} = K_{trehalose}$

Succinate branch: $v_{succ} = K_{succ} \cdot ACE$

Table A.1 Values of kinetic parameters used in the model (all values are taken from Teusink *et al.* (2000) except c: Cronwright *et al.* (2002), d: Nader *et al.* (1979), and e: Rizzi *et al.* (1997))

Enzyme	v_{\max} ($\text{mmol L}_{\text{cvt}}^{-1} \text{min}^{-1}$)	K_{eq}	K_a (mM)	K_b (mM)	K_p (mM)	K_q (mM)	K_i (mM)
HXT (high affinity)	97.264	1	1.1918 (Glc _{out})		1.1918 (Glc _{in})		0.91 ^a
HXK	226.452	3800	0.08 (Glc _{in})	0.15 (ATP)	30 (G6P)	0.23 (ADP)	
PGI	339.677	0.314	1.4 (G6P)		0.3 (F6P)		
PFK	182.903						
ALD	322.258	0.069	0.3 (F16bP)		2.4 (DHAP)	2.0 (GAP)	10 (GAP)
GAPDH	1184.52 (frwd) 6549.68 (bkwd)		0.21 (GAP)	0.09 (NAD)	0.0098 (BPG)	0.06 (NADH)	
PGK	1306.45	3200	0.003 (BPG)	0.2 (ADP)	0.53 (G3P)	0.3 (ATP)	
PGM	2525.81	0.19	1.2 (G3P)		0.08 (G2P)		
ENO	365.806	6.7	0.04 (G2P)		0.5 (PEP)		
PYK	1088.71	6500	0.14 (PEP)	0.53 (ADP)	21 (PYR)	1.5 (ATP)	
PDC	174.191		4.33 (PYR)				
Hill coefficient	1.9						
ADH	810	0.00001 ^b	17 (EtOH)	0.17 (NAD)	0.11 (NADH)	1.11 (AcAld)	90 (EtOH) 0.92 (NAD) 0.031 (NADH) 1.1 (AcAld)
GLYCPDH^c	67	10000	0.2 ^d (DHAP)	0.023 (NADH)	1.2 (Gly3P)	0.93 (NAD)	2 (ADP) 0.73 (ATP) 4.8 (F16bP)
GLYCPASE^c	104		3.5 (Gly3P)			1 (Gly)	
TPI^c	2268	0.045	0.38 (DHAP)		0.064 (GAP)		

^a “Interactive constant” K_i depends on the relative mobility of the unbound and bound carrier; ^b Adjusted, original value is 0.000069

Table A.2 Values of parameters of phosphofructokinase kinetics (Teusink *et al.* (2000))

	K_R (mM)	c	K (mM)	c_i
F6P	0.1	0		
ATP	0.71	3	0.65	100
AMP			0.0995	0.0845
F16bP			0.111	0.397
F26bP			6.82×10^{-4}	0.0174
Others	5.12 (G_R)	0.66 (L_o)		

APPENDIX C

STRUCTURE OF THE PROGRAM

Main program;

```
global vmhxt Keq_hxt Ka_hxt Kp_hxt Ki_hxt
...
Constants & fixed concentrations
vmhxt=97.264; Keq_hxt=1; Ka_hxt=1.1918; Kp_hxt=1.1918; Ki_hxt=0.91;
...

% initial conditions
Co=[0.087 1.39 0.28 0.1 5.17 0 0.1 0.1 0.1 3.36 0.04 50 0.15 1.2 0.39 5];

tspan=(0:0.001:5);
[nt,mt]=size(tspan);

options=odeset('RelTol',1e-5,'AbsTol',1e-5);
[t,C] = ode23s (@time_dependence,tspan,Co,options);

concentration = fopen('conc_data.xls','at');
fprintf(concentration,'Time\tGlu_out\tGlu_in\tG6P\tF6P\tF16P\tGAP\tDHAP\...\n');
for i = 1:increment:mt
fprintf(concentration,'%3.3f\t%+3.3f\t%+3.3f\t%+3.3f\t%+3.3f\t%+3.3f\t...\n', t(i),C(i,1:22));
end
fclose(concentration);

% Calculation of rates

rate(:,1)=ko_hxt.*((vmhxt.*(C(:,1)-(C(:,2)/Keq_hxt)))/(Ka_hxt.*(1+(C(:,1)/Ka_hxt)+...
(C(:,2)/Kp_hxt)+((Ki_hxt.*C(:,1)).*C(:,2))/(Kp_hxt*Ka_hxt))));
...

rate(:,1)=ko_hxt.*((vmhxt.*(C(:,1)-(C(:,2)/Keq_hxt)))/(Ka_hxt.*(1+(C(:,1)/Ka_hxt)+...
(C(:,2)/Kp_hxt)+((Ki_hxt.*C(:,1)).*C(:,2))/(Kp_hxt*Ka_hxt))));
```

Constants of the kinetic equation

Initial concentrations of metabolites (Co)
& interval of integration (tspan)

ODE solver (to solve the functions
defined in side_program)

Function to write calculated metabolite
concentrations to an excel file

Calculation of rate
of a reaction

Sub_program;

```
function dC = time_dependence(t,C)
```

Command defining the function to be called by main program

```
% Glucose_in  
dC(1) = V_hxt(C(1)) - V_hxk(C(1),C(2),C(16));  
dC(2)=.....  
:  
dC = dC';
```

ODE defining the time dependence of concentration of intracellular metabolite

```
% Kinetic eqns for each rxn
```

```
-----  
function rate_1= V_hxt(GLC_in)
```

Function for the kinetics of the enzyme (or transporter)

```
global vmhxt Glco Keq_hxt Ka_hxt Kp_hxt Ki_hxt
```

```
rate_1=(vmhxt*(Glco-GLC_in/Keq_hxt))/(Ka_hxt*(1+(Glco/Ka_hxt)+(GLC_in/Kp_hxt)+  
((Ki_hxt*Glco*GLC_in)/(Kp_hxt*Ka_hxt))));
```

```
-----  
function rate_2= V_hxk(GLC_in, Glu6P,ATP,ADP)
```

```
:  
:
```

APPENDIX D

MATLAB PROGRAM USED FOR THE MODEL

Main Program:

```
clear all

global vmhxt Keq_hxt Ka_hxt Kp_hxt Ki_hxt
global vmhxx Ka_hxx Kb_hxx Kp_hxx Kq_hxx Keq_hxx
global sumAXP Keq_ak
global vmpgi Ka_pgi Kp_pgi Keq_pgi
global vmpfk Gr Lo Kr_f6p Kr_ATP C_ATP K_AMP Ci_AMP K_ATP Ci_ATP
global K_f26bp Ci_f26bp K_f16bp Ci_f16bp
global F26BP
global vmald Keq_ald Ka_ald Kq_ald Kp_ald Kiq_ald Keq_tpi
global vmgapdh_f vmgapdh_r Ka_gapdh Kp_gapdh Kb_gapdh Kq_gapdh
global vmpgk Keq_pgk Ka_pgk Kp_pgk Kb_pgk Kq_pgk
global vmpgm Ka_pgm Kp_pgm Keq_pgm
global vmeno Ka_eno Kp_eno Keq_eno
global vmpyk Keq_pyk Ka_pyk Kp_pyk Kb_pyk Kq_pyk
global vmpdc Kpdc_pyr n_pdc
global vmaldh Keq_aldh Kp_aldh Ka_aldh Kq_aldh Kb_aldh
global Kip_aldh Kia_aldh Kiq_aldh Kib_aldh
global vmaadh Ka_aadh Kb_aadh Ko_aadh Kab_aadh
global vmpdh Kpdh_nad Kpdh_pyr Kipdh_pyr Kipdh_nadh
global vmglycpdh Keq_glycpdh Ka_glycpdh Kb_glycpdh
global vmglycpase Ka_glycpase Kpi_glycpase Pi
global Kq_glycpdh Kp_glycpdh
global Kglycogen Ktrehalose Ksucc K_ATPase
global Ksulf ko_aldh ko_tpi ko_glycpdh ko_ald ko_pdc ko_hxt ko_glycpase
global vmtpi Ka_tpi Kp_tpi Keq_tpi
global KADP_glycpdh KATP_glycpdh Kf16p_glycpdh
global mumax Ks VE ko_glycogen ko_trehal
global Kee_hxt
global vmhxt_1 Kmhxt_1 vmhxt_2 Kmhxt_2
global T Tref ko_pfk R ko_gapdh ko_hxx ko_succ Kglycerol
%% Kinetic constants:

%% VMAX VALUES FROM LITERATURE:
% vmhxt=97.264; % one carrier model with high affinity
vmhxt=163.7; % one carrier model with low affinity
% vmhxt_1= 45.96; vmhxt_2= 5.11; %two carrier model
```

% vmh_{xk}=226.452; vmp_{gi}=339.677; vmp_{fk}=182.903; vma_{ld}=322.258; vmg_{apdh_f} = 1184.52;
% vmg_{apdh_r} = 6549.68; vmp_{gk} = 1306.45; vmp_{gm}=2525.81; vme_{no}=365.806; vmp_{yk} = 1088.71;
% vmp_{dc}=174.194; vma_{ldh}=810; vmt_{pi}=2268; vmg_{lycpdh} = 67;
%% VMAX VALUES FROM THIS STUDY:

vmh_{xk}=452; vmp_{gi}=473.33; vmp_{fk}=184; vma_{ld}=334.67; vmt_{pi}=6898.13; vmg_{apdh_f} = 245.33;
vmg_{apdh_r} = 1681.33; vmp_{gk} = 1561.33; vmp_{gm}=2664; vme_{no}=502.67; vmp_{yk} = 409.6;
vmp_{dc}=293.33; vma_{ldh}=560; vmg_{lycpdh} = 41.6;

%% HXT

% Keq_{hxt}=1; Ka_{hxt}=1.1918; Kp_{hxt}=1.1918; Ki_{hxt}=0.91; % one carrier with HIGH affinity
Keq_{hxt}=1; Ka_{hxt}=55; Kp_{hxt}=55; Ki_{hxt}=0.91; % one carrier model with LOW affinity
% Km_{hxt_1}=43.4; Km_{hxt_2}= 2.15; %two carrier model

% HXK

Keq_{h_{xk}}=3800; Ka_{h_{xk}}=0.08; Kp_{h_{xk}}=30; Kb_{h_{xk}}=0.15; Kq_{h_{xk}}=0.23;

% PGI

Ka_{pgi}=1.4; Kp_{pgi}=0.3; Keq_{pgi}=0.314;

% PFK

Gr=5.12; Lo=0.66; Kr_{f6p}=0.1; Kr_{ATP}=0.71; C_{ATP}=3; K_{AMP}=0.0995; Ci_{AMP}=0.0845;
K_{ATP}=0.65; Ci_{ATP}=100; K_{f26bp}=0.000682; Ci_{f26bp}=0.0174; K_{f16bp}=0.111;
Ci_{f16bp}=0.397;

% ALD

Keq_{ald}=0.069; Ka_{ald}=0.3; Kq_{ald}=2; Kp_{ald}=2.4; Ki_{q_ald}=10;

% GAPDH

Ka_{gapdh} = 0.21; Kp_{gapdh} = 0.0098; Kb_{gapdh} = 0.09; Kq_{gapdh} = 0.06;

% PGK

Keq_{pgk} = 3200; Ka_{pgk} = 0.003; Kp_{pgk} = 0.53; Kb_{pgk} = 0.2; Kq_{pgk} = 0.3;

% PGM

Ka_{pgm}=1.2; Kp_{pgm}=0.08; Keq_{pgm}=0.19;

% ENO

Ka_{eno}=0.04; Kp_{eno}=0.5; Keq_{eno}=6.7;

% PYK

Keq_{pyk} = 6500; Ka_{pyk} = 0.14; Kp_{pyk} = 21; Kb_{pyk} = 0.53; Kq_{pyk} = 1.5;

% PDC

Kp_{dc_pyr}=4.33; n_{pdc}=1.9;

% ALDH

Keq_{aldh}=0.00001; Kp_{aldh}=0.11; Ka_{aldh}=17; Kq_{aldh}=1.11; Kb_{aldh}=0.17;
Kip_{aldh}=0.031; Kia_{aldh}=90; Ki_{q_aldh}=1.1; Kib_{aldh}=0.92;

% AADH & PDH

vma_{adh}=22; Ka_{aadh}=4.5; Kb_{aadh}=3.0; Ko_{aadh}=0.045; Kab_{aadh}=1260;
vmp_{dh}=6.32; Kp_{dh_nad}=160; Kp_{dh_pyr}=70; Kip_{dh_pyr}=20; Kip_{dh_nadh}=50;

%% GLYCPDH & GLYCPASE

Keq_glycpdh = 10000; Ka_glycpdh = 0.2; Kb_glycpdh = 0.023; Kq_glycpdh = 0.93;
Kp_glycpdh = 1.2; KADP_glycpdh=2; KATP_glycpdh=0.73; Kf16p_glycpdh=4.8;
vmglycpase=104; Ka_glycpase=3.5; Kpi_glycpase=1; Pi=1;

%% TPI

Keq_tpi = 0.045; Ka_tpi=0.38 ; Kp_tpi=0.064;

%% BRANCHES & OTHERS

Kglycogen=6; Ktrehalose=2.4; Ksucc=21.4; K_ATPase=39.5;
Kglycerol=1.9; %% value for transport of glycerol

%% Fixed concentrations:

F26BP = 0.02;

%% Activation energies of enzymes: 1> HXT; 2> HXK; 3> PGI; 4> PFK; 5> ALD;

%% 6> GAPDH(f); 22> GAPDH(r); 7> PGK; 8> PGM; 9> ENO; 10> PYK; 11> PDC; 12> ADH;
15> GLYCPDH; 20> TPI;

Ea=([1 30]); %% matrix for activation energies

Ea(1)=53187; Ea(2)=48256.53; Ea(3)=40269.62; Ea(4)=52949.23;
Ea(5)=65865.81; Ea(6)=28819.72; Ea(22)=32641.9;
Ea(7)=30433.56; Ea(8)=29381.78; Ea(9)=61546.42; Ea(10)=46528.773;
Ea(11)=37126.74; Ea(15)=58397.72; Ea(20)=55704.66;
Ea(12)=38423.85;

Tref=303.15; %% Reference temperature in kelvin (30C in our case)

T=283.15; %% fermentation temperature in kelvin

R=8.314; %% gas constant

%% New vmax values obtained by the use of activation energies (relative activities wrt 30C)

Q=(1/T-1/Tref)/R;

vmhxt=vmhxt*exp(-Ea(1)*Q); vmhxc=vmhxc*exp(-Ea(2)*Q);
vmpgi=vmpgi*exp(-Ea(3)*Q); vmpfk=vmpfk*exp(-Ea(4)*Q);
vmald=vmald*exp(-Ea(5)*Q); vmtpi=vmtpi*exp(-Ea(20)*Q);
vmglycpdh=vmglycpdh*exp(-Ea(15)*Q); vmgapdh_f=vmgapdh_f*exp(-Ea(6)*Q);
vmgapdh_r=vmgapdh_r*exp(-Ea(22)*Q); vmpgk=vmpgk*exp(-Ea(7)*Q);
vmpgm=vmpgm*exp(-Ea(8)*Q); vmeno=vmeno*exp(-Ea(9)*Q);
vmpyk=vmpyk*exp(-Ea(10)*Q); vmpdc=vmpdc*exp(-Ea(11)*Q);
vmaldh=vmaldh*exp(-Ea(12)*Q);
Kglycogen=Kglycogen*exp(-Ea(1)*Q); Ktrehalose=Ktrehalose*exp(-Ea(1)*Q);
Ksucc=Ksucc*exp(-Ea(1)*Q);

vmaxes = fopen('vmax_values.xls','at');

fprintf(vmaxes,'T\tvmhxt\tvmhxc\tvmpgi\tvmpfk\tvmald\tvmtpi\tvmglycpdh\tvmgapdh_f\tvmgapd
h_r\tvmpgk\tvmpgm\tvmeno\tvmpyk\tvmpdc\tvmaldh\n');

fprintf(vmaxes,'%3f\t%3.5f\t%+3.5f\t%+3.5f\t%+3.5f\t%+3.5f\t%+3.5f\t%+3.5f\t%+3.7f\t
%+3.5f\t%+3.5f\t%+3.5f\t%+3.5f\t%+3.5f\t%+3.5f\n',...)

T,vmhxt,vmhxc,vmpgi,vmpfk,vmald,vmtpi,vmglycpdh,vmgapdh_f,vmgapdh_r,vmpgk,vmpgm,vm
eno,vmpyk,vmpdc,vmaldh);
fclose(vmaxes);

%% values for the adjustment of enzyme capacities


```

% figure(1)
% plot(t,C)
% xlabel('time(min)', 'Color', 'r')
% ylabel('concentration(mM)', 'Color', 'r')
% title('concentration vs time', 'Color', 'r')

%% KINETIC EQUATIONS FOR THE CALCULATION OF RATES
%-----
% ETOH_1=1;
% ETOH_1=1./(1+(C(:,21)/Kee_hxt)); %% noncompetitive type effect
ETOH_1=(exp(-Kee_hxt*C(:,21))); %% exponential effect
rate(:,1)=ETOH_1.*(ko_hxt.*((vmhxt.*(C(:,1)-
(C(:,2)/Keq_hxt))./(Ka_hxt.*(1+(C(:,1)/Ka_hxt)+...
(C(:,2)/Kp_hxt)+(Ki_hxt.*C(:,1).*C(:,2))./(Kp_hxt*Ka_hxt)))))); % one carrier model
%rate(:,1)=ETOH_1.*ko_hxt.*((vmhxt_1.*C(:,1)./(Kmhxt_1+C(:,1)))+(vmhxt_2.*C(:,1)./(Kmhxt_
2+C(:,1)))); % two carrier model
%-----
% ETOH_2=1;
ETOH_2=1-(33.29E-6*exp(36.29E-4*C(:,21)));
rate(:,2)=ko_hxk.*ETOH_2.*(vmhxk.*(C(:,2).*C(:,16))-((C(:,3).*C(:,16))./Keq_hxk))./...
(Kb_hxk.*Ka_hxk.*(1+(C(:,3)/Kp_hxk)+...
(C(:,2)/Ka_hxk)).*(1+(C(:,17)/Kq_hxk)+(C(:,16)/Kb_hxk))));
%-----
% ETOH_3=1;
ETOH_3=1.16-(0.1597*exp(43.65E-5*C(:,21)));
rate(:,3)=ETOH_3.*(vmpgi.*(C(:,3)-(C(:,4)/Keq_pgi)))./...
(Ka_pgi.*(1+(C(:,3)/Ka_pgi)+(C(:,4)/Kp_pgi)));
%-----
% ETOH_4=1;
ETOH_4=1.06-(0.05763*exp(82.93E-5*C(:,21)));
L=Lo.*(((1+((Ci_ATP/K_ATP).*C(:,16)))./(1+((1/K_ATP).*C(:,16))))).^2).*...
(((1+((Ci_AMP/K_AMP).*C(:,18)))./(1+((1/K_AMP).*C(:,18))))).^2).*...
(((1+((Ci_f26bp/K_f26bp).*F26BP)+((Ci_f16bp/K_f16bp).*C(:,5)))./...
(1+((1/K_f26bp).*F26BP)+((1/K_f16bp).*C(:,5))));
Lambda_1=(C(:,4)/Kr_f6p);
Lambda_2=(C(:,16)/Kr_ATP);
R=1+(Lambda_1.*Lambda_2)+(Gr.*Lambda_1.*Lambda_2);
T=1+(C_ATP.*Lambda_2);
rate(:,4)=ETOH_4.*ko_pfk.*vmpfk.*(Gr.*Lambda_1.*Lambda_2.*R)./(R.^2+(L.*T.^2));
%-----
% ETOH_5=1;
ETOH_5=1-(32.03E-5*exp(28.19E-4*C(:,21)));
rate(:,5)=ETOH_5.*ko_ald.*(vmald.*(C(:,5))-((C(:,7).*C(:,6))./Keq_ald)))./...
(Ka_ald.*(1+(C(:,5)/Ka_ald)+(C(:,7)/Kp_ald)+(C(:,6)/Kq_ald)+...
((C(:,6).*C(:,5))./(Ka_ald*Kiq_ald))+((C(:,7).*C(:,6))./(Kp_ald*Kq_ald))));
%-----
% ETOH_6= 1;
ETOH_6=(1.0*exp(-53.65E-5*C(:,21)));
rate(:,6)=ETOH_6.*ko_gapdh.*(-(vmgapdh_r.*C(:,8).*C(:,15))./(Kp_gapdh*Kq_gapdh))+...
((vmgapdh_f.*C(:,6).*C(:,14))./(Ka_gapdh*Kb_gapdh))./...
(((1+(C(:,14)/Kb_gapdh)+(C(:,15)/Kq_gapdh)).*(1+(C(:,8)/Kp_gapdh)+(C(:,6)/Ka_gapdh))));
%-----
% ETOH_7= 1;
ETOH_7=1.0*exp(-48.57E-5*C(:,21));
rate(:,7)=ETOH_7.*(vmpgk.*(Keq_pgk.*C(:,8).*C(:,17)-
(C(:,9).*C(:,16))))./((Kq_pgk*Kp_pgk).*...
(1+(C(:,17)/Kb_pgk)+(C(:,16)/Kq_pgk)).*(1+(C(:,8)/Ka_pgk)+(C(:,9)/Kp_pgk)));

```



```

%-----
% ETOH_8= 1;
ETOH_8= 1.33-0.3323*exp(30.25E-5*C(:,21));
rate(:,8)=ETOH_8.*(vmpgm.*(C(:,9)-(C(:,10)/Keq_pgm)))/(Ka_pgm.*(1+...
(C(:,9)/Ka_pgm)+(C(:,10)/Kp_pgm)));
%-----
% ETOH_9= 1;
ETOH_9= 1.3-(0.301*exp(31.21E-5*C(:,21)));
rate(:,9)=ETOH_9.*(vmeno.*(C(:,10)-(C(:,11)/Keq_eno)))/...
(Ka_eno.*(1+(C(:,10)/Ka_eno)+(C(:,11)/Kp_eno)));
%-----
% ETOH_10= 1;
ETOH_10= 1.02-(19.27E-3*exp(66.64E-5*C(:,21)));
rate(:,10)=ETOH_10.*(vmpyk.*(C(:,11).*C(:,17)-
((C(:,12).*C(:,16))/Keq_pyk)))/(Ka_pyk*Kb_pyk).*...
(1+(C(:,11)/Ka_pyk)+(C(:,12)/Kp_pyk)).*(1+(C(:,17)/Kb_pyk)+(C(:,16)/Kq_pyk)));
%-----
% ETOH_11= 1;
ETOH_11= 1.997-0.9941*exp(9.92E-5*C(:,21));
rate(:,11)=ETOH_11.*ko_pdc.*((vmpdc.*((C(:,12)/Kpdc_pyr).^n_pdc))/...
(1+((C(:,12)/Kpdc_pyr).^n_pdc)));
%-----
% ETOH_12= 1;
ETOH_12= 1.02-(0.01739*exp(10.52E-4*C(:,21)));
rate(:,12)=ETOH_12.*ko_aldh.*(-(vmaldh.*((C(:,21).*C(:,14))-
((C(:,13).*C(:,15))/Keq_aldh)))/...
((Kib_aldh*Ka_aldh).*(1+((C(:,21).*Kb_aldh)/(Kib_aldh*Ka_aldh))+...
(Kp_aldh.*C(:,13))/(Kip_aldh*Kq_aldh)+(C(:,14)/Kib_aldh)+...
((C(:,21).*C(:,14))/(Kib_aldh*Ka_aldh)+(C(:,21).*C(:,13).*C(:,14))/...
(Kiq_aldh*Kib_aldh*Ka_aldh)+(Kp_aldh.*C(:,13).*C(:,14))/...
(Kib_aldh*Kip_aldh*Kq_aldh)+(C(:,15)/Kip_aldh)+...
((C(:,21).*Kb_aldh.*C(:,15))/(Kib_aldh*Kip_aldh*Ka_aldh))+...
((C(:,13).*C(:,15))/(Kip_aldh*Kq_aldh)+(C(:,21).*C(:,13).*C(:,15))/...
(Kia_aldh*Kip_aldh*Kq_aldh)));
%-----
rate(:,13)=0;
% rate(:,13)=vmaadh.*(C(:,13).*C(:,14))/(C(:,13).*C(:,14))+((Ka_aadh/Ko_aadh).*C(:,14))+...
% ((Kb_aadh/Ko_aadh).*C(:,13))+((Kab_aadh/Ko_aadh)));
%-----
rate(:,14)=0;
% rate(:,14)=vmpdh.*(C(:,12).*C(:,14))/(Kpdh_nad.*C(:,12))+Kpdh_pyr.*C(:,14))+...
% (((Kipdh_pyr*Kpdh_nad)/Kipdh_nadh).*C(:,15))+...
% (C(:,12).*C(:,14))+((Kpdh_nad/Kipdh_nadh).*C(:,13).*C(:,15)));
%-----
% ETOH_15= 1;
ETOH_15= (1.0*exp(-38.5E-5*C(:,21)));

%% GLYCPDH kinetic eqn. not containing F16bP, ATP, ADP as effectors
rate(:,15)=ETOH_15.*ko_glycpdh.*(vmglycpdh.*(-(C(:,19).*C(:,14))/Keq_glycpdh))+...
(C(:,15).*C(:,7)))/(Ka_glycpdh*Kb_glycpdh).*(1+(C(:,14)/Kq_glycpdh)+...
(C(:,15)/Kb_glycpdh)).*(1+(C(:,19)/Kp_glycpdh)+(C(:,7)/Ka_glycpdh)));

%% GLYCPDH kinetic eqn. containing F16bP, ATP, ADP as effectors
% rate(:,15)=ETOH_15.*ko_glycpdh.*(vmglycpdh.*(-(C(:,19).*C(:,14))/Keq_glycpdh))+...
% (C(:,15).*C(:,7)))/(Ka_glycpdh*Kb_glycpdh).*(1+(C(:,5)/Kf16p_glycpdh)+...
% (C(:,17)/KADP_glycpdh)+(C(:,16)/KATP_glycpdh)).*(1+(C(:,14)/Kq_glycpdh)+...
% (C(:,15)/Kb_glycpdh)).*(1+(C(:,19)/Kp_glycpdh)+(C(:,7)/Ka_glycpdh)));

```


%% DIFFERENTIAL EQUATIONS FOR CONCENTRATION CHANGES OF METABOLITES

global VE

% Glucose-out

% dC(1)=0;

dC(1)=(hxt_etoh(C(21))*(-V_hxt(C(1),C(2))))/VE; % one carrier model

% dC(1)=(hxt_etoh(C(21))*(-V_hxt(C(1))))/VE; % two carrier model

% Glucose_in

% dC(2) = V_hxt(C(1),C(2)) - V_hxk(C(2),C(3),C(16),C(17))-mu(C(1))*C(2);

dC(2) = ((hxt_etoh(C(21)))*V_hxt(C(1),C(2))) - ...

((hxk_etoh(C(21)))*(V_hxk(C(2),C(3),C(16),C(17))))-mu(C(1))*C(2); % one carrier model

% dC(2) = ((hxt_etoh(C(21)))*V_hxt(C(1))) - ...

% ((hxk_etoh(C(21)))*(V_hxk(C(2),C(3),C(16),C(17))))-mu(C(1))*C(2); % two carrier model

% Glucose-6P

dC(3) = ((hxk_etoh(C(21)))*(V_hxk(C(2),C(3),C(16),C(17)))) -...

(pgi_etoh(C(21)))*V_pgi(C(3),C(4)) - (hxt_etoh(C(21)))*V_glyco -
2*(hxt_etoh(C(21)))*V_trehal - mu(C(1))*C(3);

% Fructose-6P

dC(4) = (pgi_etoh(C(21)))*V_pgi(C(3),C(4)) -...

(pfk_etoh(C(21)))*V_pfk(C(4),C(5),C(16),C(18)) - mu(C(1))*C(4);

% Fructose-1,6P

dC(5) = (pfk_etoh(C(21)))*V_pfk(C(4),C(5),C(16),C(18)) - ...

(ald_etoh(C(21)))*V_ald(C(5),C(7),C(6)) - mu(C(1))*C(5);

% GAP

dC(6) = (ald_etoh(C(21)))*V_ald(C(5),C(7),C(6)) -

(gapdh_etoh(C(21)))*V_gapdh(C(6),C(8),C(14),C(15)) +...

(tpi_etoh(C(21)))*V_tpi(C(7),C(6)) - mu(C(1))*C(6);

% DHAP

dC(7) = (ald_etoh(C(21)))*V_ald(C(5),C(7),C(6)) -

(gpd_etoh(C(21)))*V_glycpdh(C(7),C(19),C(14),C(15)) -...

(tpi_etoh(C(21)))*V_tpi(C(7),C(6)) - mu(C(1))*C(7);

% dC(7) = (ald_etoh(C(21)))*V_ald(C(5),C(7),C(6)) -

(gpd_etoh(C(21)))*V_glycpdh(C(7),C(19),C(14),C(15),C(5),C(16),C(17)) -...

% (tpi_etoh(C(21)))*V_tpi(C(7),C(6)) - mu(C(1))*C(7);

% 1,3-bPglycerate

dC(8) = (gapdh_etoh(C(21)))*V_gapdh(C(6),C(8),C(14),C(15)) -...

(pgk_etoh(C(21)))*V_pgk(C(8),C(9),C(16),C(17)) - mu(C(1))*C(8);

% 3-Pglycerate

dC(9) = (pgk_etoh(C(21)))*V_pgk(C(8),C(9),C(16),C(17)) -

(pgm_etoh(C(21)))*V_pgm(C(9),C(10)) - mu(C(1))*C(9);

% 2-Pglycerate

dC(10) = (pgm_etoh(C(21)))*V_pgm(C(9),C(10)) - (eno_etoh(C(21)))*V_eno(C(10),C(11)) -

mu(C(1))*C(10);

% PEP

dC(11) = (eno_etoh(C(21)))*V_eno(C(10),C(11))-

(pyk_etoh(C(21)))*V_pyk(C(11),C(12),C(16),C(17)) - mu(C(1))*C(11);

```

% PYR
dC(12) = (pyk_etoh(C(21)))*V_pyk(C(11),C(12),C(16),C(17)) - (pdc_etoh(C(21)))*V_pdc(C(12))
-...
  V_pdh(C(12),C(14),C(15)) - mu(C(1))*C(12);

% Acetaldehyde
dC(13) = (pdc_etoh(C(21)))*V_pdc(C(12)) -
(aldh_etoh(C(21)))*V_aldh(C(13),C(21),C(14),C(15)) -...
  V_aadh(C(13),C(14))-2*(hxt_etoh(C(21)))*V_succ(C(13))-V_sulf(C(13)) - mu(C(1))*C(13);

% NAD
%% for GLYCPDH kinetic eqn. not containing F16bP, ATP, ADP as effectors
dC(14)= (aldh_etoh(C(21)))*V_aldh(C(13),C(21),C(14),C(15)) -
(gapdh_etoh(C(21)))*V_gapdh(C(6),C(8),C(14),C(15)) +...
  ((gpd_etoh(C(21)))*(V_glycpdh(C(7),C(19),C(14),C(15)))) - ...
  V_aadh(C(13),C(14)) + V_pdh(C(12),C(14),C(15)) - 3*(hxt_etoh(C(21)))*V_succ(C(13)) -
mu(C(1))*C(15);
%% for GLYCPDH kinetic eqn. containing F16bP, ATP, ADP as effectors
% dC(14)= (aldh_etoh(C(21)))*V_aldh(C(13),C(21),C(14),C(15)) -
(gapdh_etoh(C(21)))*V_gapdh(C(6),C(8),C(14),C(15)) +...
% ((gpd_etoh(C(21)))*(V_glycpdh(C(7),C(19),C(14),C(15),C(5),C(16),C(17)))) -...
% V_aadh(C(13),C(14)) + V_pdh(C(12),C(14),C(15))-3*(hxt_etoh(C(21)))*V_succ(C(13)) -
mu(C(1))*C(14);

% NADH
%% for GLYCPDH kinetic eqn. not containing F16bP, ATP, ADP as effectors
dC(15)= -(aldh_etoh(C(21)))*V_aldh(C(13),C(21),C(14),C(15)) +
(gapdh_etoh(C(21)))*V_gapdh(C(6),C(8),C(14),C(15)) -...
  ((gpd_etoh(C(21)))*(V_glycpdh(C(7),C(19),C(14),C(15)))) + ...
  V_aadh(C(13),C(14)) - V_pdh(C(12),C(14),C(15)) + 3*(hxt_etoh(C(21)))*V_succ(C(13)) -
mu(C(1))*C(15);

%% for GLYCPDH kinetic eqn. containing F16bP, ATP, ADP as effectors
% dC(15)= -(aldh_etoh(C(21)))*V_aldh(C(13),C(21),C(14),C(15)) +
(gapdh_etoh(C(21)))*V_gapdh(C(6),C(8),C(14),C(15)) -...
% ((gpd_etoh(C(21)))*(V_glycpdh(C(7),C(19),C(14),C(15),C(5),C(16),C(17)))) + ...
% V_aadh(C(13),C(14)) - V_pdh(C(12),C(14),C(15)) + 3*(hxt_etoh(C(21)))*V_succ(C(13)) -
mu(C(1))*C(15);

% ATP
% dC(16)= -(hxt_etoh(C(21)))*(V_hxk(C(2),C(3),C(16),C(17)))) - (hxt_etoh(C(21)))*V_glyco -
(hxt_etoh(C(21)))*V_trehal -...
% (pfk_etoh(C(21)))*V_pfk(C(4),C(5),C(16),C(18)) +
(pgk_etoh(C(21)))*V_pgk(C(8),C(9),C(16),C(17)) +...
% (pyk_etoh(C(21)))*V_pyk(C(11),C(12),C(16),C(17)) - V_ATPase(C(16)) -
4*(hxt_etoh(C(21)))*V_succ(C(13)) - mu(C(1))*C(16);
dC(16)=0;

% % ADP
% dC(17)= ((hxt_etoh(C(21)))*(V_hxk(C(2),C(3),C(16),C(17)))) + (hxt_etoh(C(21)))*V_glyco +
(hxt_etoh(C(21)))*V_trehal +...
% (pfk_etoh(C(21)))*V_pfk(C(4),C(5),C(16),C(18)) -
(pgk_etoh(C(21)))*V_pgk(C(8),C(9),C(16),C(17)) -...
% (pyk_etoh(C(21)))*V_pyk(C(11),C(12),C(16),C(17)) + V_ATPase(C(16)) +
4*(hxt_etoh(C(21)))*V_succ(C(13)) -mu(C(1))*C(17);
dC(17)=0;

```

```

% AMP
dC(18)=0;

% Glycerol-3P
%% for GLYCPDH kinetic eqn. not containing F16bP, ATP, ADP as effectors
dC(19) = ((gpd_etoh(C(21)))*V_glycpdh(C(7),C(19),C(14),C(15))) -...
  ((gpd_etoh(C(21)))*V_glycpase(C(19))) - mu(C(1))*C(19);
%% for GLYCPDH kinetic eqn. containing F16bP, ATP, ADP as effectors
% dC(19) = ((gpd_etoh(C(21)))*(V_glycpdh(C(7),C(19),C(14),C(15),C(5),C(16),C(17)))) -...
%   ((gpd_etoh(C(21)))*V_glycpase(C(19))) - mu(C(1))*C(19);
% dC(19) =0;

% Glycerol_in
% dC(20)= V_glycpase(C(19))/VE; % without transport step
dC(20)= ((gpd_etoh(C(21)))*V_glycpase(C(19)))- hxt_etoh(C(21))*V_glyc_trans(C(20),C(23));

% Ethanol
dC(21) = (aldh_etoh(C(21)))*V_aldh(C(13),C(21),C(14),C(15))/VE;
% dC(21)=0;

% ACE-Sulfite
dC(22)=V_sulf(C(13));

% Glycerol_out
% dC(23)= V_glycpase(C(19))/VE; % without transport step
dC(23)= (hxt_etoh(C(21))*V_glyc_trans(C(20),C(23)))/VE;

dC = dC';

function growth=mu(Glco)

global mumax Ks

% growth=(mumax*Glco)/(Ks+Glco);
growth=0;

%% KINETIC EQUATIONS FOR EACH ENZYME
% -----
function rate_1= V_hxt(Glco,GLC_in)
% function rate_1= V_hxt(Glco)

global vmhxt Keq_hxt Ka_hxt Kp_hxt Ki_hxt ko_hxt
global vmhxt_1 Kmhxt_1 vmhxt_2 Kmhxt_2

% rate_1=0;
rate_1=ko_hxt*(vmhxt*(Glco-(GLC_in/Keq_hxt)))/(Ka_hxt*(1+(Glco/Ka_hxt)+...
  (GLC_in/Kp_hxt)+((Ki_hxt*Glco*GLC_in)/(Kp_hxt*Ka_hxt))); % one carrier model
% rate_1=ko_hxt*((vmhxt_1*Glco/(Kmhxt_1+Glco))+(vmhxt_2*Glco/(Kmhxt_2+Glco))); % two
carrier model
% -----
function rate_2= V_hxk(GLC_in, Glu6P,ATP,ADP)

global vmhxk Ka_hxk Kb_hxk Kp_hxk Kq_hxk Keq_hxk ko_hxk

% rate_2=0;

```

```

rate_2=ko_hxk*(vmhxk*(GLC_in*ATP-
((Glu6P*ATP)/Keq_hxk))/(Kb_hxk*Ka_hxk*(1+(Glu6P/Kp_hxk)+...
(GLC_in/Ka_hxk))*(1+(ADP/Kq_hxk)+(ATP/Kb_hxk)));
% -----
function rate_3= V_pgi(Glu6P,F6P)

global vmpgi Ka_pgi Kp_pgi Keq_pgi

% rate_3=0;
rate_3=(vmpgi*(Glu6P-(F6P/Keq_pgi)))/(Ka_pgi*(1+(Glu6P/Ka_pgi)+(F6P/Kp_pgi)));
% -----
function rate_4= V_pfk(F6P, F16P,ATP,AMP)

global vmpfk Gr Lo Kr_f6p Kr_ATP C_ATP K_AMP Ci_AMP K_ATP Ci_ATP
global K_f26bp Ci_f26bp K_f16bp Ci_f16bp F26BP ko_pfk

% rate_4=0;
L=Lo*(((1+((Ci_ATP/K_ATP)*ATP))/(1+(ATP/K_ATP)))^2)*...
(((1+((Ci_AMP/K_AMP)*AMP))/(1+(AMP/K_AMP)))^2)*...
((1+((Ci_f26bp/K_f26bp)*F26BP)+((Ci_f16bp/K_f16bp)*F16P))/...
(1+((1/K_f26bp)*F26BP)+((1/K_f16bp)*F16P)));

Lambda_1=(F6P/Kr_f6p);
Lambda_2=(ATP/Kr_ATP);
R=1+(Lambda_1*Lambda_2)+(Gr*Lambda_1*Lambda_2);
T=1+(C_ATP*Lambda_2);

rate_4=ko_pfk*vmpfk*(Gr*Lambda_1*Lambda_2*R)/(R^2+(L*T^2));
% -----
function rate_5= V_ald(F16P, DHAP,GAP)

global vmald Keq_ald Ka_ald Kq_ald Kp_ald Kiq_ald ko_ald

% rate_5=0;
rate_5=ko_ald*(vmald*(F16P-((DHAP*GAP)/Keq_ald)))/...
(Ka_ald*(1+(F16P/Ka_ald)+(DHAP/Kp_ald)+(GAP/Kq_ald)+...
((GAP*F16P)/(Ka_ald*Kiq_ald))+((DHAP*GAP)/(Kp_ald*Kq_ald)));
% -----
function rate_6= V_gapdh(GAP, BPG,NAD,NADH)

global vmgapdh_f vmgapdh_r Ka_gapdh Kp_gapdh Kb_gapdh Kq_gapdh ko_gapdh

% rate_6=0;
rate_6=ko_gapdh*(((vmgapdh_r*BPG*NADH)/(Kp_gapdh*Kq_gapdh))+((vmgapdh_f*GAP*...
NAD)/(Ka_gapdh*Kb_gapdh)))/((1+(NAD/Kb_gapdh)+(NADH/...
Kq_gapdh))*(1+(BPG/Kp_gapdh)+(GAP/Ka_gapdh)));
% -----
function rate_7= V_pgk(BPG,G3P,ATP,ADP)
global vmpgk Keq_pgk Ka_pgk Kp_pgk Kb_pgk Kq_pgk

% rate_7=0;
rate_7=(vmpgk*(Keq_pgk*BPG*ADP-(G3P*ATP)))/((Kq_pgk*Kp_pgk)*...
(1+(ADP/Kb_pgk)+(ATP/Kq_pgk))*(1+(BPG/Ka_pgk)+(G3P/Kp_pgk)));
% -----

```

```

function rate_8= V_pgm(G3P,G2P)

global vmpgm Ka_pgm Kp_pgm Keq_pgm

% rate_8=0;
rate_8=(vmpgm*(G3P-(G2P/Keq_pgm)))/(Ka_pgm*(1+(G3P/Ka_pgm)+ (G2P/Kp_pgm)));
% -----
function rate_9= V_eno(G2P,PEP)

global vmeno Ka_eno Kp_eno Keq_eno

% rate_9=0;
rate_9=(vmeno*(G2P-(PEP/Keq_eno)))/(Ka_eno*(1+(G2P/Ka_eno)+ (PEP/Kp_eno)));
% -----
function rate_10= V_pyk(PEP,PYR,ATP,ADP)

global vmpyk Keq_pyk Ka_pyk Kp_pyk Kb_pyk Kq_pyk

% rate_10=0;
rate_10=(vmpyk*(PEP*ADP-((PYR*ATP)/Keq_pyk)))/((Ka_pyk*Kb_pyk)*...
(1+PEP/Ka_pyk+PYR/Kp_pyk)*(1+(ADP/Kb_pyk)+(ATP/Kq_pyk)));
% -----
function rate_11= V_pdc(PYR)

global vmpdc Kpdc_pyr n_pdc
global ko_pdc

% rate_11=0;
rate_11=ko_pdc*((vmpdc*((PYR/Kpdc_pyr)^n_pdc))/(1+((PYR/Kpdc_pyr)^n_pdc)));
% -----
function rate_12= V_aldh(ACE,ETOH,NAD,NADH)

global vmaldh Keq_aldh Kp_aldh Ka_aldh Kq_aldh Kb_aldh
global Kip_aldh Kia_aldh Kiq_aldh Kib_aldh
global ko_aldh

% rate_12=0;
rate_12=(ko_aldh*(-(vmaldh*((ETOH*NAD)-((ACE*NADH)/Keq_aldh))))/...
((Kib_aldh*Ka_aldh)*(1+((ETOH*Kb_aldh)/(Kib_aldh*Ka_aldh))+...
((Kp_aldh*ACE)/(Kip_aldh*Kq_aldh))+NAD/Kib_aldh)+((ETOH*NAD)/...
(Kib_aldh*Ka_aldh))+((ETOH*ACE*NAD)/(Kiq_aldh*Kib_aldh*Ka_aldh))+...
((Kp_aldh*ACE*NAD)/(Kib_aldh*Kip_aldh*Kq_aldh))+NADH/Kip_aldh)+...
((ETOH*Kb_aldh*NADH)/(Kib_aldh*Kip_aldh*Ka_aldh))+((ACE*NADH)/...
(Kip_aldh*Kq_aldh))+((ETOH*ACE*NADH)/(Kia_aldh*Kip_aldh*Kq_aldh)));
% -----
function rate_13= V_aadh(ACE,NAD)

global vmaadh Ka_aadh Kb_aadh Ko_aadh Kab_aadh

rate_13=0;
% rate_13=vmaadh*(ACE*NAD)/((ACE*NAD)+((Ka_aadh/Ko_aadh)*NAD)+...
% ((Kb_aadh/Ko_aadh)*ACE)+(Kab_aadh/Ko_aadh));
% -----
function rate_14= V_pdh(PYR,NAD,NADH)

global vmpdh Kpdh_nad Kpdh_pyr Kipdh_pyr Kipdh_nadh

```

```

rate_14=0;
% rate_14=vmpdh*(PYR*NAD)/((Kpdh_nad*PYR)+(Kpdh_pyr*NAD)+...
%   (((Kipdh_pyr*Kpdh_nad)/Kipdh_nadh)*NADH)+(PYR*NAD)+...
%   ((Kpdh_nad/Kipdh_nadh)*PYR*NADH));
% -----
% function rate_15= V_glycpdh(DHAP,GLY,NAD,NADH,F16P,ATP,ADP)
function rate_15= V_glycpdh(DHAP,GLY,NAD,NADH)

global vmglycpdh Keq_glycpdh Ka_glycpdh Kb_glycpdh
global Kq_glycpdh Kp_glycpdh
global KADP_glycpdh KATP_glycpdh Kf16p_glycpdh ko_glycpdh

% rate_15=0;
%% GLYCPDH kinetic eqn. not containing F16bP, ATP, ADP as effectors
rate_15=ko_glycpdh*(vmglycpdh*(-((GLY*NAD)/Keq_glycpdh)+(NADH*DHAP))/...
  ((Ka_glycpdh*Kb_glycpdh)*(1+(NAD/Kq_glycpdh)+(NADH/Kb_glycpdh))*...
  (1+(GLY/Kp_glycpdh)+(DHAP/Ka_glycpdh))));

%% GLYCPDH kinetic eqn. containing F16bP, ATP, ADP as effectors
% rate_15=ko_glycpdh*((vmglycpdh*(-((GLY*NAD)/Keq_glycpdh)+(NADH*DHAP))/...
%   ((Ka_glycpdh*Kb_glycpdh)*(1+(F16P/Kf16p_glycpdh)+...
%   (ADP/KADP_glycpdh)+(ATP/KATP_glycpdh))*...
%   (1+(NAD/Kq_glycpdh)+(NADH/Kb_glycpdh))*...
%   (1+(GLY/Kp_glycpdh)+(DHAP/Ka_glycpdh))));
% -----
function rate_16= V_glyco

global Kglycogen ko_glycogen

% rate_16=0;
rate_16=ko_glycogen*Kglycogen;
% -----
function rate_17= V_trehal

global Ktrehalose ko_trehal

% rate_17=0;
rate_17=ko_trehal*Ktrehalose;
% -----
function rate_18= V_succ(ACE)

global Ksucc ko_succ

% rate_18=0;
rate_18=ko_succ*Ksucc*ACE;
% -----
function rate_19= V_ATPase(ATP)

global K_ATPase

% rate_19=0;
rate_19=K_ATPase*ATP;
% -----
function rate_20= V_tpi(DHAP,GAP)

global vmtpi Ka_tpi Kp_tpi Keq_tpi
global ko_tpi

```



```

% rate_20=0;
rate_20=ko_tpi*(vmtpi*(DHAP-(GAP/Keq_tpi)))/((Ka_tpi*(1+(GAP/Kp_tpi)))+DHAP);
% -----

function rate_21= V_glycpase(GLY)

global vmglycpase Ka_glycpase Kpi_glycpase Pi ko_glycpase

% rate_21=0;
rate_21=ko_glycpase*(vmglycpase*GLY)/(Ka_glycpase*(1+(Pi/Kpi_glycpase))*...
(1+(GLY/Ka_glycpase)));
% -----
function rate_22= V_sulf(ACE)

global Ksulf

% rate_22=0;
rate_22=Ksulf*ACE;
% -----
function rate_23= V_glyc_trans(Glycin,Glycout)

global Kglycerol

% rate_23=0;
rate_23=Kglycerol*(Glycin-Glycout);

%% FUNCTIONS FOR THE EFFECT OF ETHANOL ON ENZYMES
% -----
function ETOH_1= hxt_etoh(ETOH)

global Kee_hxt

% ETOH_1=1;
% ETOH_1=1/(1+(ETOH/Kee_hxt)); %% noncompetitive type effect
ETOH_1=(exp(-Kee_hxt*ETOH)); %% exponential effect
% -----
function ETOH_2= hxk_etoh(ETOH)

global Kee_hxk

% ETOH_2=1;
ETOH_2= 1-(33.29E-6*exp(36.29E-4*ETOH));
% -----
function ETOH_3= pgi_etoh(ETOH)

% ETOH_3=1;
ETOH_3= 1.16-(0.1597*exp(43.65E-5*ETOH));
% -----
function ETOH_4= pfk_etoh(ETOH)

% ETOH_4=1;
ETOH_4= 1.06-(0.05763*exp(82.93E-5*ETOH));
% -----

```

```

function ETOH_5= ald_etoh(ETOH)

% ETOH_5=1;
ETOH_5= 1-(32.03E-5*exp(28.19E-4*ETOH));
% -----
function ETOH_6= gapdh_etoh(ETOH)

% ETOH_6=1;
ETOH_6= (1.0*exp(-53.65E-5*ETOH));
% -----
function ETOH_7= pgk_etoh(ETOH)

% ETOH_7=1;
ETOH_7= 1.0*exp(-48.57E-5*ETOH);
% -----
function ETOH_8= pgm_etoh(ETOH)

% ETOH_8=1;
ETOH_8= 1.33-0.3323*exp(30.25E-5*ETOH);
% -----
function ETOH_9= eno_etoh(ETOH)

% ETOH_9=1;
ETOH_9= 1.3-(0.301*exp(31.21E-5*ETOH));
% -----
function ETOH_10= pyk_etoh(ETOH)
% ETOH_10=1;
ETOH_10= 1.02-(19.27E-3*exp(66.64E-5*ETOH));
% -----
function ETOH_11= pdc_etoh(ETOH)

% ETOH_11=1;
ETOH_11= 1.997-0.9941*exp(9.92E-5*ETOH);
% -----
function ETOH_12= aldh_etoh(ETOH)

% ETOH_12=1;
ETOH_12= 1.02-(0.01739*exp(10.52E-4*ETOH));
% -----
function ETOH_20= tpi_etoh(ETOH)

% ETOH_20=1;
ETOH_20= 1.01-(10.78E-3*exp(12.33E-4*ETOH));
% -----
function ETOH_15= gpd_etoh(ETOH)

global Kee_gpd

% ETOH_15=1;
ETOH_15= (1.0*exp(-38.5E-5*ETOH));
% -----

```

APPENDIX E

SAMPLES FOR FITS FOR THE EFFECT OF ETHANOL ON ACTIVITIES OF ENZYMES

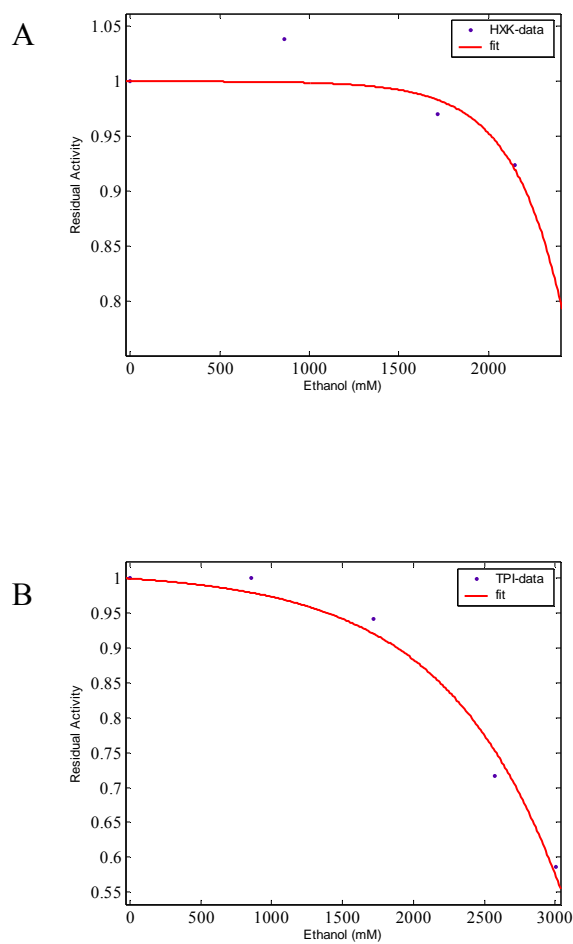


Figure A.2 Fits for the effect of ethanol on activity of hexokinase (A) and of triosephosphate isomerase (B)

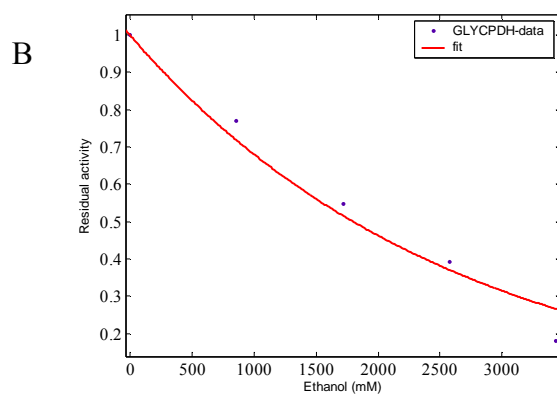
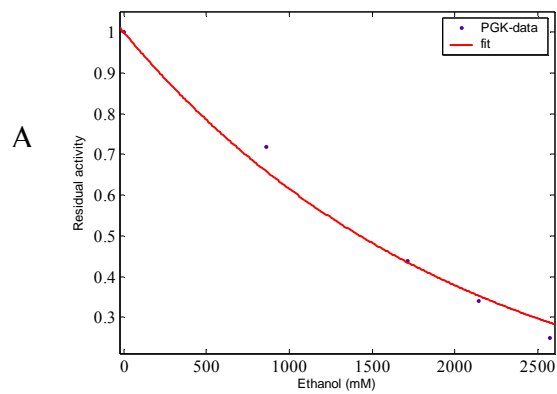


Figure A.3 Fit for the effect of ethanol on activity of phosphoglycerate kinase (A) and of glycerol-3-phosphate dehydrogenase (B)

CURRICULUM VITAE

PERSONAL INFORMATION

Surname, Name: Şahin, Ceylan
Nationality: Turkish (TC)
Date and Place of Birth: 19 July 1977, İslahiye
Marital Status: Single
Phone: +90 312 210 5622
Fax: +90 312 210 2767
e-mail: ceyslansah@gmail.com

EDUCATION

Degree	Institution	Year of Graduation
MS	Middle East Technical University, Food Engineering, Ankara	2002
BS	Middle East Technical University, Food Engineering, Ankara	1999
High School	Mersin Fen Lisesi, Mersin	1994

WORK EXPERIENCE

Year	Place	Enrollment
2006- Present	Ministry of Agriculture and Rural Affairs- General Directorate of Protection and Control	Technical Expert (Engineer)
2000-2006	METU Department of Food Engineering	Research Assistant
1998 July	Ödesan-Öderoğlu Dairy Factory, Mersin	Intern Engineering Student
1997 July- August	Etap Inc, Fruit Juice Factory (Cappy), Mersin	Intern Engineering Student

FOREIGN LANGUAGES

Advanced English, Elementary level Italian, Entry level German

PUBLICATIONS

Sahin C., Hamamci H., Autolytic and Proteolytic Yeast Biomass Degradation, 11th European Congress on Biotechnology, Book of Abstracts, Basel, Switzerland, p. 107, 2003

HOBBIES

Music, swimming